The 1993 IGTI Scholar Lecture

# Loss Mechanisms in Turbomachines

**J. D. Denton**
Whittle Laboratory,
Cambridge University
Engineering Department,
Cambridge, United Kingdom

*The origins and effects of loss in turbomachines are discussed with the emphasis on trying to understand the physical origins of loss rather than on reviewing the available prediction methods. Loss is defined in terms of entropy increase and the relationship of this to the more familiar loss coefficients is derived and discussed. The sources of entropy are, in general: viscous effects in boundary layers, viscous effects in mixing processes, shock waves, and heat transfer across temperature differences. These are first discussed in general and then the results are applied to turbomachinery flows. Understanding of the loss due to heat transfer requires some discussion of cycle thermodynamics. Sections are devoted to discussing blade boundary layer and trailing edge loss, tip leakage loss, endwall loss, effects of heat transfer, and miscellaneous losses. The loss arising from boundary layer separation is particularly difficult to quantify. Most of the discussion is based on axial flow machines, but a separate section is devoted to the special problems of radial flow machines. In some cases, e.g., attached blade boundary layers, the loss mechanisms are well understood, but even so the loss can seldom be predicted with great accuracy. In many other cases, e.g., endwall loss, the loss mechanisms are still not clearly understood and prediction methods remain very dependent on correlations. The paper emphasizes that the use of correlations should not be a substitute for trying to understand the origins of loss, and suggests that a good physical understanding of the latter may be more valuable than a quantitative prediction.*

## 1 Introduction

Efficiency is probably the most important performance parameter for most turbomachines. This is especially true for gas turbine engines, whether used for aircraft propulsion or for land-based power plants, because their net power output is the difference between the turbine work and the compressor work. These are roughly in the ratio 2:1 so a small change in the efficiency of either component causes a much larger proportional change in the power output.

Over the years enormous effects have been expended in trying to improve the efficiency of all types of turbomachines, and for many large machines the total-to-total efficiency is now over 90 percent. This makes further improvements ever more difficult to obtain; however, advances are still possible, not only in the efficiency itself but also in the amount, and hence cost, of the development work needed to achieve the required performance. Present levels of efficiency have been achieved by an ever-improving understanding of the fluid mechanics and thermodynamics of the flow, which in turn has been obtained by a combination of improved experimental and theoretical methods applied both to whole machines and to individual components. In particular the advent of modern numerical methods of flow calculation has greatly improved our ability to model the flow through a machine.

The factors influencing efficiency are extremely complex. Before the advent of the aircraft gas turbine they were scarcely recognized and the development of turbomachines such as steam and hydraulic turbines, pumps, and fans proceeded largely on a trial and error basis. The explosion of research on aircraft engines in the 1940s and 50s led to a great improvement in our understanding and several performance prediction methods were developed, e.g., Howell (1945), and Ainley and Mathieson (1951), some of which are still in use today. These methods categorized the sources of loss in the machine, typically as profile loss, secondary (or endwall) loss, and tip leakage loss, and attempted to predict each independently of the others. The predictions were usually based on correlations of experimental data obtained either from cascade tests or from the performance of actual machines. In some cases analytical models of the loss production mechanisms were formulated, e.g., Carter (1948), but these were usually highly idealized.

These performance prediction methods were widely used in the 60s and 70s with comparatively little development. Although the predictions of the individual loss components were sometimes shown to be of very limited accuracy (Denton, 1973; Dunham, 1970), the overall methods were empirically tuned by each manufacturer to obtain agreement with his existing machines and were then extrapolated to predict the performance of new designs. In this way the efficiency could usually be predicted to an accuracy of about $\pm 2$ percent. This success sometimes led to a view that the predictions were based on a sound understanding of the flow physics. It is the author's

Contributed by the International Gas Turbine Institute and presented at the International Gas Turbine and Aeroengine Congress and Exposition, Cincinnati, Ohio May 24-27, 1993. Manuscript received at ASME Headquarters April 1993. Paper No. 93-GT-435. Associate Technical Editor: H. Lukas.

view that this is seldom the case and that the success of these methods has led to an excessive reliance upon them and a reluctance to query their basic principles and assumptions. There have been many instances where a designer was unwilling to try out a new idea because a 30-year-old loss correlation predicted that it would give no improvement.

In the late 1970s and 1980s the advent of new instrumentation, e.g., laser anemometer measurements and ensemble-averaged hot-wire data, led to a greatly improved understanding of the flow, both in cascades and in actual machines. Better numerical predictions of the flow also contributed to this understanding, especially as regards three-dimensional effects. These new measurements and calculations showed that the real flow in a turbomachine is extremely complicated due to both three-dimensional effects and unsteadiness. In particular boundary layer transition was found to be a much more complex phenomenon than previously imagined (Mayle, 1992). Although the simple models used for performance prediction were shown to be grossly oversimplified, it was not apparent how they could be extended to include the new physics. The latter was too complex to be described by a simple model while numerical solutions were (and are) not yet accurate enough to give *quantitative* predictions of unsteady turbulent flow.

The result of these developments is currently that, while the improved understanding of the flow has been assimilated by many research workers and designers, most practical performance prediction methods continue to be based on correlations. Such correlations can tell us nothing about new design features that were not available at the time the correlation was developed. For example, such features as three-dimensional blade stacking for turbines or end-bending for compressors are not included in any published performance prediction method. Although the effects of such geometric changes on the inviscid flow can now be predicted numerically, their effects upon the loss can still not be quantified. In these circumstances a designer can only use his judgment and understanding of the flow physics in deciding on desirable changes. It is the author's view that a good physical understanding of the flow, and particularly of the origins of loss, is more important to the designer than is the availability of a good but oversimplified loss correlation. The objectives of this paper are to try to help young engineers to develop this understanding and to make more experienced engineers see things in a new light.

Most publications are concerned with emphasizing how well their authors understand the problem they are addressing. In contrast this paper will emphasize our lack of understanding of many loss generating mechanisms in the hope that if we realize our limitations we will more easily be able to overcome them.

## 2 Loss Components and Loss Coefficients

The historical breakdown of loss into "profile loss," "endwall loss," and "leakage loss" continues to be widely used although it is now clearly recognized that the loss mechanisms are seldom really independent.

Profile loss is usually taken to be the loss generated in the blade boundary layers well away from the end walls. It is often assumed that the flow here is two dimensional so the loss may be based on two-dimensional cascade tests or boundary layer calculations. The extra loss arising at a trailing edge is usually included as profile loss.

Endwall loss is still sometimes referred to as "secondary" loss because it arises partly from the secondary flows generated when the annulus boundary layers pass through a blade row. However, it will become clear that the loss does not arise directly from the secondary flow but is due to a combination of many factors. It is often difficult to separate endwall loss from profile loss and leakage loss and the title "secondary loss" is sometimes taken to include all the losses that cannot otherwise be accounted for.

Tip leakage loss arises from the leakage of flow over the

## Nomenclature

$A$ = area
$A_r$ = aspect ratio
$C$ = chord
$C_d$ = dissipation coefficient
$C_p$, $C_v$ = specific heat capacities
$C_{pb}$ = base pressure coefficient
$C_s$ = blade surface length
$C_f$ = skin friction factor
$C_o$ = velocity based on stage isentropic enthalpy change
$C_x$ = blade axial chord
$D$ = drag force
$f$ = frictional force per unit mass
$F$ = total frictional force
$g$ = tip clearance
$H$ = boundary layer or wake shape factor
$h$ = static enthalpy, blade height
$h_o$ = stagnation enthalpy
$I$ = momentum flux = $PA + mV$
M = Mach number
$m$ = mass flow rate
$m_{fc}$ = mass fraction of coolant
$p$ = blade pitch
$P$ = static pressure
$P_o$ = stagnation pressure
$Q$, $q$ = heat flow
$R$ = gas constant
Re = Reynolds number based on blade chord
$Re_\theta$ = Reynolds number based on momentum thickness
$r$ = radius
$S$ = total entropy
$s$ = specific entropy
$s_\delta$ = specific entropy at edge of boundary layer
$\dot{S}_a$ = entropy creation rate per unit surface area
$\dot{S}_v$ = entropy creation rate per unit volume
$T$ = static temperature
$T_o$ = stagnation temperature
$T_q$ = blade row torque
$t$ = trailing edge thickness
$U$ = blade rotational speed
$V$ = flow velocity
$V_o$, $V_\delta$ = blade surface velocity, at edge of boundary layer
$w$ = throat width
$x$, $y$, $z$ = Cartesian coordinates
$Y$ = stagnation pressure loss coefficient
$z$ = distance along streamline
$\alpha$ = flow angle measured from the axial direction
$\gamma$ = specific heat ratio
$\delta$ = boundary layer overall thickness
$\delta^*$ = boundary layer displacement thickness
$\delta_e$ = boundary layer energy thickness
$\eta$, $\eta_c$ = efficiency, cycle efficiency
$\phi$ = flow coefficient = $V_x/U$
$\rho$ = fluid density
$\psi$ = stage loading coefficient = $\Delta h_o/U^2$
$\tau$ = shear stress
$\theta$ = boundary layer momentum thickness
$\zeta_s$, $\zeta$ = entropy and energy loss coefficient

### Subscripts

1 = at inlet to blade row or stage
2 = at exit from blade row or stage
$\delta$ = at the edge of the boundary layer
$c$ = coolant flow
$is$ = isentropic
$m$ = mainstream flow
$o$ = stagnation conditions
$te$ = just before the trailing edge

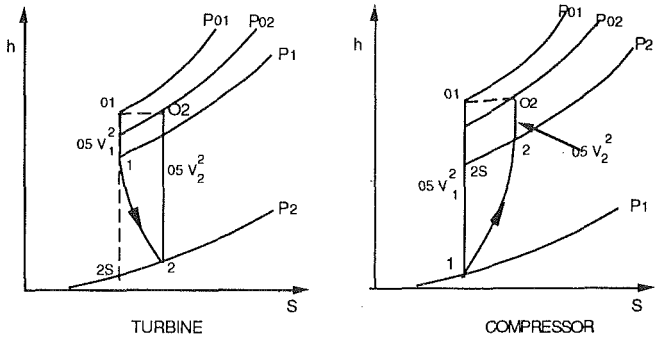


**Fig. 1 Enthalpy-entropy diagram for cascade flow**

tips of rotor blades and the hub clearance of stator blades. The detailed loss mechanisms clearly depend on whether the blades are shrouded or unshrouded. The interaction between the leakage loss and the endwall loss may be very strong, especially for unshrouded compressor blades, and some methods do not distinguish between endwall loss and leakage loss.

The relative magnitudes of the above three categories of loss are dependent on the type of machine and on such details as blade aspect ratio and tip clearance. However, in many machines the three are comparable in magnitude, each accounting for about 1/3 of the total loss.

So far we have used the word "loss" without defining what we really mean by it. In general any flow feature that reduces the efficiency of a turbomachine will be called loss, but this does not include factors that affect the cycle efficiency as opposed to the turbine or compressor efficiency.

**2.1 Definitions of Loss Coefficient.** There are many different definitions of loss coefficient in regular use for individual blade rows. Perhaps the most common is the stagnation pressure loss coefficient; referring to Fig. 1 this is defined by

$$Y=(P_{o1}-P_{o2})/(P_{o1}-P_1) \quad \text{for a compressor blade} \qquad (1a)$$

and

$$Y=(P_{o1}-P_{o2})/(P_{o2}-P_2) \quad \text{for a turbine blade} \qquad (1b)$$

The reason that this definition of loss coefficient is so common is that it is easy to calculate it from cascade test data and not because it is the most convenient to use in design.

A more useful loss coefficient for design purposes is the energy or enthalpy loss coefficient; again referring to Fig. 1 this is defined by

$$\zeta=\frac{h_2-h_{2s}}{h_{o2}-h_2} \quad \text{for a turbine blade} \qquad (2a)$$

and

$$\zeta=\frac{h_2-h_{2s}}{h_{o1}-h_1} \quad \text{for a compressor blade} \qquad (2b)$$

where the isentropic final enthalpy, $h_{2s}$, is the value obtained in an isentropic expansion or compression to the same final static pressure as the actual process. There are many other definitions of blade row loss coefficient in use; these are compared by Brown (1972) who shows that the energy loss coefficient is most likely to be independent of Mach number.

These blade row loss coefficients are perfectly satisfactory for cascade tests but are not directly applicable in machines where, in a rotating blade row, the relative stagnation pressure and the relative stagnation enthalpy can change as a result of changes in radius without there being any implied loss of efficiency. In a machine we define the isentropic efficiency as the ratio of the actual work to the isentropic work and so the only factors that change this efficiency are departures from isentropic flow. These may be due to either heat transfer or to thermodynamic irreversibility. For most machines the flow is closely adiabatic and so only entropy creation by irreversibilities contributes significantly to the loss of efficiency.

From the above we can conclude that the only rational measure of loss in an adiabatic machine is entropy creation. Any irreversible flow process creates entropy and so inevitably reduces the isentropic efficiency. It follows that individual blade row loss coefficients should really be defined in terms of entropy increase rather than stagnation pressure or kinetic energy loss. Entropy is a particularly convenient measure because, unlike stagnation pressure, stagnation enthalpy, or kinetic energy, its value does not depend on whether it is viewed from a rotating or a stationary blade row. Once the entropy increase in every blade row has been calculated the results may be summed to find the entropy increase for the whole machine. If we know one other thermodynamic property of the flow at exit from the machine, e.g., pressure or enthalpy, the state of the fluid leaving it is completely determined and hence the machine efficiency can be calculated.

Entropy is an unfamiliar quantity because it cannot be seen or measured directly, its value can only be inferred by measuring other properties. Basic thermodynamics tells us that for a single phase fluid entropy is a function of any two other thermodynamic properties such as temperature and pressure. For a perfect gas two of the relationships between specific entropy and more familiar quantities are

$$s-s_{\text{ref}}=C_p\ln(T/T_{\text{ref}})-R\ln(P/P_{\text{ref}}) \qquad (3a)$$

and

$$s-s_{\text{ref}}=C_v\ln(T/T_{\text{ref}})-R\ln(\rho/\rho_{\text{ref}}) \qquad (3b)$$

The temperatures, pressures, and densities used in these equations may be either all static values or all stagnation values because by definition the change from static to stagnation conditions is isentropic. Note that these equations only give *changes* of entropy, but this is also what determines turbomachine performance. The absolute value of entropy is always arbitrary.

For adiabatic flow through a stationary blade row stagnation temperature is constant and so entropy changes depend only on stagnation pressure changes via

$$\Delta s=-R\ln(P_{o2}/P_{o1}) \qquad (4a)$$

or, for small changes in stagnation pressure

$$\Delta s=-R\,\Delta P_o/P_o \qquad (4b)$$

Hence for stator blades and cascade flows loss of stagnation pressure can be taken to be synonymous with increase of entropy.

We must always be careful to distinguish between specific and total entropy. When we calculate entropy increases in the future we will usually obtain the total rate of entropy creation and must then divide it by the mass flow rate to obtain the change of specific entropy.

Because great use will be made of entropy throughout this paper it may be useful to introduce an analogy to help to understand it. Entropy may be considered to be like "smoke" that is created within the flow whenever something deleterious to machine efficiency is taking place. For example, "smoke" is continually being created in blade boundary layers and in shock waves. Once created the "smoke" cannot be destroyed and it is convected downstream through the machine and diffuses into the surrounding flow. The concentration of "smoke" at the exit from the machine includes a contribution from every source within the machine and the loss of machine efficiency is proportional to the average concentration of "smoke" at its exit.

We can define an entropy loss coefficient by

$$\zeta_s=\frac{T_2\Delta s}{h_{o2}-h_2} \quad \text{for turbine blades} \qquad (5a)$$

and

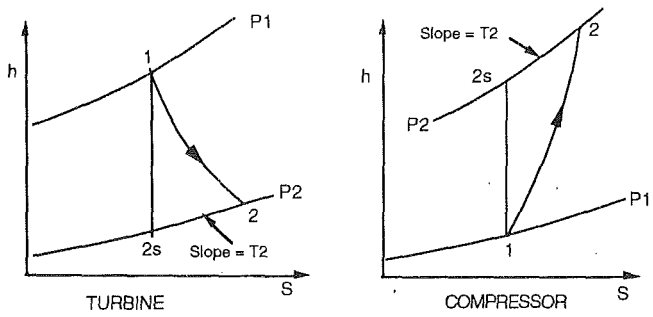


**Fig. 2 Expansion and compression processes on the *h-s* chart**

$$\zeta_s = \frac{T_2 \Delta s}{h_{o1} - h_1} \quad \text{for compressor blades} \tag{5b}$$

Using the fact that the slope of the constant pressure lines on the $h-s$ chart is equal to the local static temperature, it can be shown that the difference between the energy and entropy loss coefficients is

$$\zeta_s - \zeta \approx 0.25(\gamma - 1) M^2 \zeta \zeta_s \tag{5c}$$

which is of order $10^{-3}$ and so is always negligible. Throughout the remainder of this paper no distribution will be made between energy and entropy loss coefficients.

The entropy loss coefficients defined by Eq. (5) may be used directly as a measure of entropy production both in a cascade flow with constant stagnation temperature and also in the flow through the rotating blade rows of a machine where the relative stagnation temperature and pressure change due to change of radius.

At low speeds all definitions of loss coefficient approach the same value. The differences between them are only significant at relative Mach numbers greater than about 0.3. When deriving theoretical results for incompressible flow later in this paper no distinction will be made between the various definitions of loss coefficient.

**2.2 Relation of Loss to Drag.** In external aerodynamics the ultimate measure of lost performance is the drag on the aircraft or other object under consideration. It is not surprising, therefore, that the concept of drag has been carried over into turbomachinery flows. However, in order to define a drag we must first define a direction in which it acts. The choice of this direction is obvious for external flows but is not at all obvious in turbomachinery where a force acting in the direction of blade motion is essential for work transfer and a force acting in the meridional direction is essential for pressure changes. For example, the skin friction force acting on a highly staggered compressor blade has a large component in the opposite direction to rotation and so contributes to the work input. It is not immediately clear whether or not this work input contributes to the pressure rise.

In incompressible two-dimensional cascade flow it is possible to relate the component of blade force in the vector mean flow direction to the loss of stagnation pressure and hence to the entropy rise. This analysis is given in most textbooks, e.g., Horlock (1958). However, no such simple relationship exists for compressible flow or for flows that are not strictly two dimensional. Even when the relationship is valid it does not help us to understand the origins of loss. For example, does it imply that skin friction on parts of the blade surface that are highly inclined to the vector mean direction do little harm while that on parts of the surface aligned with the vector mean direction do most harm? Again the answer is not apparent.

It is the author's view that the concept of drag is of little use in turbomachinery and should be replaced by the concept of entropy generation. However, there are relationships between the two that can sometimes be useful. It is shown in Appendix 1 that in any flow with constant stagnation enthalpy the rate of entropy increase along a streamline is related to the viscous force per unit mass $F_x$ acting on the fluid in the direction of the streamline by

$$T\frac{ds}{dx} = -F_x \tag{6}$$

For one-dimensional flow in a duct of cross-sectional area $A$ Eq. (6) can be integrated over the duct to give the change in specific entropy $\Delta s$ along a short length of the duct as

$$T\Delta s = -\frac{\Delta F}{\rho A} \tag{7}$$

where $\Delta F$ is the streamwise component of the viscous force exerted by the boundaries on the fluid and may arise either from skin friction or from pressure drag. However, application of the equation in this form is difficult and may be misleading because it is only valid for uniform flow, i.e., with no gradients in the cross-stream direction. Nonuniform flow, even if there are no frictional forces on the walls, can cause the entropy to increase. For example, the mixing of two parallel streams with different velocities is considered in Appendix 2 and is shown to be irreversible even when there is no force acting.

Turning Eq. (6) into one for the total rate of entropy creation in the duct we get

$$\dot{S} = m\dot{s} = -\int \frac{1}{T} \mathbf{V} \cdot \mathbf{F}_v dVol \tag{8}$$

where $\mathbf{V}$ is the local flow velocity vector, $\mathbf{F}_v$ is the vector representing the local viscous force per unit volume, and the integral is over the volume of the duct. This relationship between the viscous forces and entropy creation is always valid for adiabatic flow but it is not generally useful because we need to know the viscous force acting on every particle of fluid, not only the drag on the solid boundaries. It does, however, show that the entropy creation rate is likely to be high in regions where high velocities coincide with high viscous forces.

**2.3 Relation of Entropy Change to Machine Efficiency.** The relationship between entropy creation and machine isentropic efficiency can be clearly seen by considering the expansion or compression process on an enthalpy–entropy diagram, Fig. 2.

Neglecting any difference between static and stagnation conditions and assuming no external heat transfer, the efficiency is closely given by

$$\eta_t \approx \frac{h_1 - h_2}{h_1 - h_2 + T_2(s_2 - s_1)} \quad \text{for a turbine} \tag{9a}$$

and by

$$\eta_c \approx 1 - \frac{T_2(s_2 - s_1)}{(h_2 - h_1)} \quad \text{for a compressor} \tag{9b}$$

The approximation only arises because we have assumed that the static temperature is constant along the line $2-2s$ in Fig. 2. This is unlikely to produce a significant error in most practical cases.

We see (Eq. (9*b*)) that the loss of efficiency of a compressor is directly proportional to the increase in specific entropy through the machine and also to its exit temperature. The same is very closely true for a turbine (Eq. (9*a*)) provided that the efficiency is high.

When entropy is created by a fluid dynamic process, the magnitude of entropy creation is usually inversely proportional to the *local* temperature, e.g., $T\Delta s = \zeta \times 1/2\, V^2$ is a common result. The loss coefficient $\zeta$ is unlikely to depend on temperature and so a flow process with fixed values of loss coefficient and flow velocity creates less entropy at a high temperature than does the same process taking place at a lower temperature.

The enthalpy change through a stage is always proportional to $V^2$ so the changes in enthalpy and entropy as fluid passes through a machine are related by

$$\Delta s \propto \zeta \Delta h/T \tag{10}$$

i.e., for constant values of loss coefficient, the magnitude of the slope $dh/ds$ of the expansion or compression line on the $h-s$ chart is proportional to temperature. This is reflected in the slopes of the compression and expansion processes illustrated in Fig. 2.

Since the loss of *overall* isentropic efficiency is proportional to the *total* entropy creation for both compressors and turbines, an irreversible flow process taking place at high temperatures produces a lower loss of *overall* efficiency than does the same process at low temperatures. This is the origin of the well-known "reheat effect," which causes the polytropic efficiency of a machine to be different from the isentropic efficiency. The result is that irreversibilities in the flow through the high-pressure stages of turbines and compressors tend to be less deleterious to the overall isentropic efficiency than those in the low-pressure stages. An estimate of the contribution of individual stage efficiencies to the overall isentropic efficiency may be obtained by summing the stage entropy increases, giving

$$\frac{1-\eta_{\text{overall}}}{\eta_{\text{overall}}} = \frac{T_{\text{exit}}}{\Delta h_{\text{overall}}} \sum_{\text{all stages}} \frac{(1-\eta_{\text{stage}})\Delta h_{\text{stage}}}{\eta_{\text{stage}} T_{2\,\text{stage}}} \tag{11}$$

The importance of this "reheat effect" increases with the overall temperature ratio of the machine. It is of approximately equal magnitude in high-pressure-ratio steam turbines and in aircraft engine compressors and turbines and is negligible for low-speed machines.

**2.4 Mechanisms for Entropy Creation.** Basic thermodynamics tells us that entropy creation occurs due to the following fluid dynamic processes:

1 Viscous friction in either boundary layers or free shear layers. The latter include the mixing processes in, for example, a leakage jet.
2 Heat transfer across finite temperature differences, e.g., from the mainstream flow to a flow of coolant gas.
3 Nonequilibrium processes such as occur in very rapid expansions or in shock waves.

The remainder of this paper will examine the entropy creation by each of these mechanisms in detail and will show how it can be quantified or approximated in practical situations.

## 3 Entropy Generation in Boundary Layers

Appendix 1 derives an expression for the rate of change of entropy flux in a two-dimensional boundary layer as

$$\dot{S}_a = \frac{d}{dx}\int_0^\delta (\rho V_x (s - s_\delta))\, dy = \int_0^\delta \frac{1}{T}\tau_{yx} dV_x \tag{12}$$

$\dot{S}_a$ may be thought of the rate of entropy production per unit surface area. Note that this is the *total* rate of entropy creation not the change in specific entropy.

Locally, within the boundary layer, the rate of entropy creation *per unit volume* is

$$\dot{S}_v = \frac{1}{T}\tau \frac{dV}{dy} \tag{13}$$

This may be interpreted as the viscous shear work, $\tau\, dV/dy$, being converted to heat at temperature $T$.

Typical variations of shear stress with velocity through turbulent boundary layers with $\text{Re}_\theta \approx 1000$ are given in Fig. 3. These were obtained from calculations using the Cebeci and Carr (1978) boundary layer code. Equation (12) shows that the area under the $\tau - V$ curve is proportional to the rate of

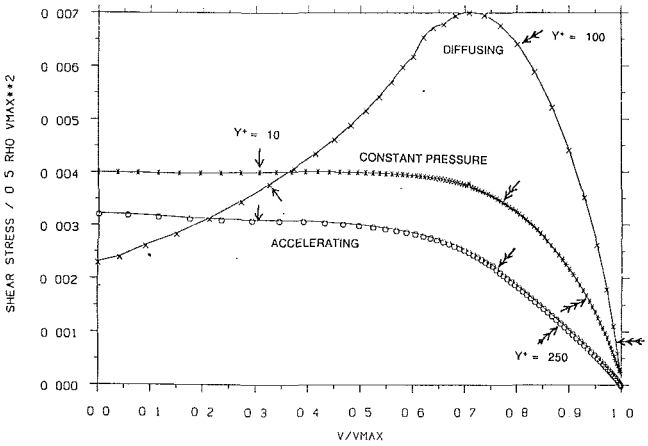


**Fig. 3 Variation of shear stress with velocity through boundary layers with $\text{Re}_\theta = 1000$**

entropy creation per unit surface area. It is noteworthy that for most boundary layers the velocity changes most rapidly near the surface and so most of the entropy generation is concentrated in the inner part of the layer. This is especially the case for turbulent boundary layers where much of the entropy creation occurs within the laminar sublayer and the logarithmic region. The well-known "universal velocity profile" of the boundary layer shows that only the outer part of the layer ($Y^+ > 500$) is greatly affected by the streamwise pressure gradient. Since this part generates little of the entropy, this result suggests that the entropy generation may be relatively insensitive to the detailed state of the boundary layer. Dawes (1990) gives a more detailed breakdown of the entropy generation in a boundary layer showing that about 90 percent of the entropy generation occurs within the inner part of the layer.

For practical use it is convenient to turn the entropy production rate into a dimensionless dissipation coefficient, which is defined by

$$C_d = T\dot{S}_a/\rho V_\delta^3 \tag{14}$$

where $V_\delta$ is the velocity at the edge of the boundary layer.

The exact magnitude of the dissipation coefficient cannot be calculated without knowing full details of the state of the boundary layer. However, correlation of much experimental work has led to some general results. These are described by Schlichting (1966). The most striking feature is that for turbulent boundary layers the dissipation coefficient is much less dependent on the state of the boundary layer, i.e., on the shape factor, than is the more familiar skin friction coefficient. Schlichting gives the following equation for turbulent boundary layers with $1.2 < H < 2.0$ and with $10^3 < \text{Re}_\theta < 10^5$:

$$C_d = 0.0056\, \text{Re}_\theta^{-1/6} \tag{15}$$

This equation is compared with results from the Cebeci calculation for three different boundary layers in Fig. 4. The boundary layer code gives similar results to Eq. (15) for a constant pressure boundary layer but the accelerated boundary layer has a significantly lower rate of entropy generation. The diffusing boundary layer represents a compressor blade suction surface at a Reynolds number of $5 \times 10^5$ where the boundary layer is near separation and the dissipation coefficient is predicted to be about 45 percent greater than that suggested by Eq. (15).

This comparison suggests that for $\text{Re}_\theta > 500$ the dissipation coefficient is relatively insensitive to the boundary layer thickness (i.e., proportional to $\theta^{-1/6}$). In the range $500 < \text{Re}_\theta < 1000$ it is also relatively insensitive to the shape factor of the boundary layer. Denton and Cumpsty (1987) suggest that for many turbomachine blades where the average $\text{Re}_\theta$ is of order 1000, a reasonable approximation is simply to take

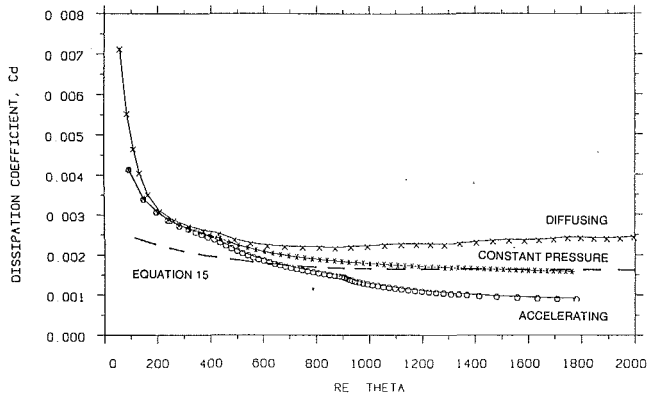


**Fig. 4 Calculated dissipation coefficients for turbulent boundary layers**

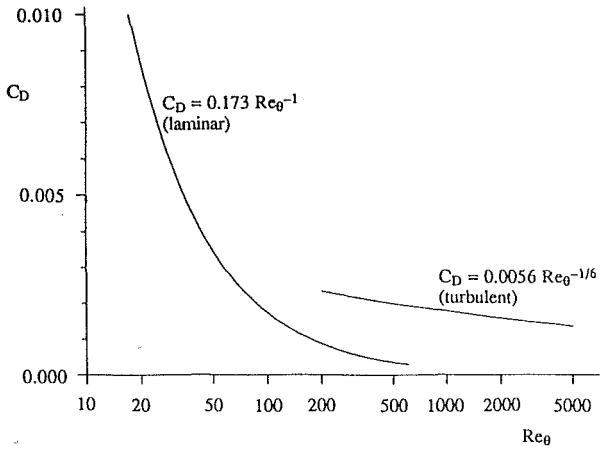


**Fig. 5 Dissipation coefficient for laminar and turbulent boundary layers**

$$C_d = 0.002 = \text{const} \tag{16}$$

for turbulent boundary layers. Moore and Moore (1983) found a similar value of $C_d = 0.0024$ for one particular boundary layer. However, Eq. (15) and the results from Fig. 4 suggest that a value of $C_d = 0.0018$ may be more appropriate.

For laminar boundary layers, the dissipation coefficient is more dependent on boundary layer thickness. Truckenbrodt (1952) quotes results showing

$$C_d = \beta\, \mathrm{Re}_\theta^{-1} \tag{17}$$

where the value of $\beta$ varies only slightly with shape factor, being about 0.17 for typical laminar boundary layers. The same author also quotes an analytical result giving $\beta = 0.173$ for a laminar boundary layer with no pressure gradient.

An analytical result can be derived for laminar boundary layers by integrating the well-known Pohlhausen family of velocity profiles (Schlichting, 1978, p. 206) to give

$$C_d = \mathrm{Re}_\theta^{-1}\,(0.1746 + 0.0029\lambda + 0.000076\lambda^2) \tag{18}$$

where terms with higher powers of $\lambda$ have been neglected. $\lambda$ is the Pohlausen pressure gradient parameter whose value ranges from $+12$ for a highly accelerated boundary layer to $-12$ at separation. The corresponding range of $\beta$ is 0.220 to 0.151. Hence Eq. (18) confirms that the dissipation coefficient is relatively insensitive to the state of the boundary layer, the dissipation being slightly increased in an accelerating boundary layer and reduced in one near separation. Since laminar boundary layers are much more likely to exist on turbomachinery blades with favorable pressure gradients, i.e., with $\lambda$ positive, a typical value of $\beta = 0.2$ as suggested by Denton and Cumpsty is realistic.

The variation of $C_d$ with $\mathrm{Re}_\theta$ obtained from Eqs. (15) and (17) is shown in Fig. 5. It is noteworthy that in the $\mathrm{Re}_\theta$ range where either a laminar or a turbulent boundary layer could exist, i.e., $300 < \mathrm{Re}_\theta < 1000$, the dissipation in the laminar boundary layer is much less (by a factor of between 2 and 5) than that in the turbulent one. This large difference highlights the importance of predicting boundary layer transition on turbomachine blades.

There are no known results for the effects of Mach number on the dissipation coefficient. However, over the Mach number range prevalent in turbomachines, $0 < M < 2$, the effects of Mach number on skin friction are generally considered to be small. The effects on entropy generation, as shown by Eq. (12), should be similar. However, the increase in temperature near the surface, where most of the entropy generation is taking place, implies that the surface temperature rather than the free-stream static temperature should be used in Eq. (12). For adiabatic surfaces this will not be significantly different from the stagnation temperature of the flow.

The entropy increase of fluid in the boundary layer may be used to define an entropy thickness of the boundary layer by

$$\delta_s = \frac{T_\delta}{\rho_\delta V_\delta^3} \int_0^\delta \rho V (s - s_\delta)\, dy \tag{19}$$

When defined in this way the entropy thickness becomes identical to the more familiar energy thickness $\delta_e$ of the boundary layer at low speeds.

Since all the entropy produced upstream of a point on the surface is contained in the boundary layer at that point, we can write an equation relating the total entropy generation to the local entropy thickness as

$$\dot{S} = \frac{\rho V_\delta^3 \delta_s}{T_\delta} = \int_0^x \frac{\rho V_\delta^3 C_d}{T_\delta}\, dx \tag{20}$$

The terms in this equation represent all of the entropy produced up in the boundary layer up to the point in question; in particular, at the trailing edge they represent all the entropy produced on the blade surface.

## 4 Entropy Generation in Mixing Processes

Entropy creation due to viscous shear occurs whenever a fluid is subject to a rate of shear strain. The rate of shear strain is not the same as the vorticity and so viscous dissipation is not confined to boundary layers. Even in the mainstream of an irrotational flow the fluid is being sheared and so entropy is being created (e.g., a free vortex flow will gradually change to a forced vortex, which has no shearing) but the rate of creation is usually negligible compared to that in shear layers.

Relatively high rates of shearing occur in wakes, at the edges of separated regions, in vortices, and in leakage jets. Since these are usually associated with turbulent flow the effective viscosity may be large, typically over 100 times the laminar viscosity, and the local entropy creation rates are considerable. The flow processes involved are extremely complex and often unsteady so it is seldom possible to quantify the *local* entropy creation rates. However, in many such processes the *overall* entropy creation can be calculated from a control volume analysis, which applies the equations for the conservation of mass, energy, and momentum between an upstream boundary, at which the flow is assumed known, and a far downstream boundary where the mixing processes are assumed to have restored the flow to a completely uniform condition. They key feature that makes such an approach possible is that we know that mixing will continue until the flow has become uniform, even although we do not know how long this will take. For example, the velocity deficit in a wake decays continually with distance downstream; we do not need to know the exact rate of decay to predict the overall result. As long as the mixing is effectively complete by the time the flow leaves the region of

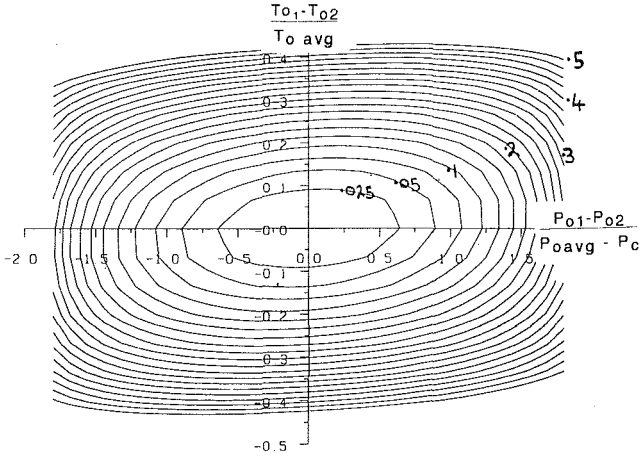


**Fig. 6 Entropy loss coefficient for the mixing of two streams at different stagnation pressures and temperatures. See Fig. A2.1 for notation.**

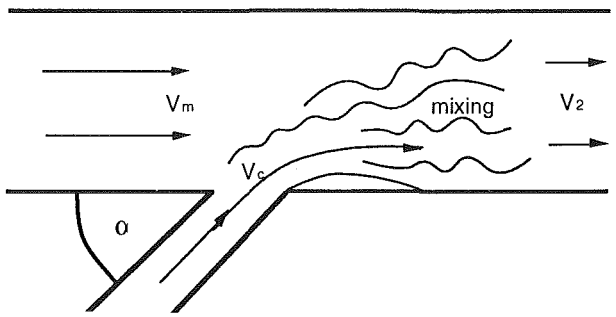


**Fig. 7 Mixing of injected flow with a mainstream flow at a different velocity and temperature**

interest we can calculate the total entropy created without knowing the details of how or where the mixing takes place.

As an example of such a mixing process Appendix 2 gives the theory for the mixing of two streams of fluid, which initially have different stagnation temperatures and pressures, in a constant area duct. Results for the entropy loss coefficient are presented in Fig. 6 for the case when the two streams initially occupy equal areas, and it can be seen that the total entropy creation depends on the difference in both the stagnation temperature and the stagnation pressure of the flows.

A great simplification of the theory is possible for the case when the flow rate of one of the steams is small. The theory for this case is presented by Shapiro (1953). For the case illustrated in Fig. 7 when a *small* flow of fluid, mass flow rate, $m_c$, is injected at an angle $\alpha$ and with velocity $V_c$ and stagnation temperature $T_{oc}$ into a mainstream flow, which has mass flow rate $m_m$, velocity $V_m$, Mach number $M_m$, and stagnation temperature $T_{om}$, the result is

$$\Delta s = C_p \frac{m_c}{m_m}\left\{\left(1+\frac{\gamma-1}{2}M_m^2\right)\frac{T_{oc}-T_{om}}{T_{om}} + (\gamma-1)M_m^2\left(1-\frac{V_c\cos\alpha}{V_m}\right)\right\} \quad (21)$$

If the two streams have the same stagnation temperature, this gives the rate of entropy creation as

$$Tm_m\Delta s = T\dot{S} = m_c(V_m^2 - V_m V_c\cos\alpha) \quad (22)$$

This result is for the entropy change of the main flow and does not include the entropy change of the injected flow. It will be extensively used later in this paper. Equations (21) and (22) are valid for both constant pressure and constant area mixing provided that the pressure and area changes are small.

In practice we cannot usually say exactly where mixing takes place and so we may not be able to assume that the pressure and area changes during mixing are small. It is therefore of interest to see how the total entropy production depends on the area in which the mixing takes place. Consider the situation sketched in Fig. 7 where, for simplicity the angle $\alpha$ is chosen to be 90 deg, the flow is assumed incompressible, and the stagnation temperature and pressure of the injected fluid are the same as that of the mainstream. A continuity and momentum balance gives the following result for the *total* entropy creation:

$$T\dot{S} = -(m_m+m_c)\frac{\Delta P_o}{\rho} = 0.5\,V_m^2 m_c\left(2+3\frac{m_c}{m_m}+\left(\frac{m_c}{m_m}\right)^2\right) \quad (23)$$

We imagine that the flow rate of the injected fluid $m_c$ is held constant while the height of the duct is changed with $V_m$ constant. Then $m_m$ changes in proportion to the area of the duct and Eq. (23) shows that, provided $m_c/m_m$ is small, the *total* entropy creation does not depend greatly on $m_m$, i.e., on the area in which the mixing takes place. A similar result is obtained if the mixing is assumed to be at constant pressure rather than at constant area. This helps to justify a common assumption that the mixing (of say a coolant or a tip leakage jet) takes place with the whole mainstream flow rather than just with the adjacent fluid. Eq. (23) shows that most of the entropy creation will have taken place by the time the jet has mixed with about 5 times its own flow rate of the mainstream (i.e., $m_c/m_m = 0.2$) and this will occur within a few diameters of the jet. The remaining entropy generation as the diluted jet mixes with the whole mainstream is much less significant.

Some workers calculate the loss due to mixing of a primary flow with a much smaller secondary flow by simply assuming that all the *relative* kinetic energy of the secondary flow is lost. For the case predicted by Eq. (22) this gives

$$T\dot{S} = 0.5\,m_c(V_m - V_c\cos\alpha)^2 + (V_c\sin\alpha)^2 \quad (24)$$

Comparing Eqs. (22) and (24) show that they give exactly the same result when $V_m = V_c$, but the first equation gives a lower loss when $V_c > V_m$. This is because the lost kinetic energy argument does not account for the static pressure recovery that arises from the momentum of the jet. In most applications the two approaches will give very similar results but the mixing calculation, Eq. (22), is felt to be more correct.

A further important example of a mixing process is the mixing out of a wake behind a trailing edge. Appendix 3 gives the theory for entropy creation due to the mixing out of a wake behind a blunt trailing edge in a constant area passage with (for simplicity only) incompressible flow. The analysis includes the boundary layers on the blade surface immediately upstream of the trailing edge and also the base pressure acting on the trailing edge. The latter is usually below the free-stream pressure by an amount that may be defined in terms of a base pressure coefficient, $C_{pb}$, by

$$C_{pb} = (P_b - P_{\text{ref}})/(0.5\,\rho\,V_{\text{ref}}^2) \quad (25)$$

where $P_{\text{ref}}$ and $V_{\text{ref}}$ may be either the far downstream pressure and velocity or the values on the blade surfaces immediately before the trailing edge. The latter definition is used in the following analysis. Typical values of $C_{pb}$ defined on this basis are in the range $-0.1$ to $-0.2$, although the value varies greatly with the state of the boundary layer, the shape of the trailing edge, and the ratio of trailing edge thickness to boundary layer thickness.

The resulting expression for the stagnation pressure loss coefficient (which in incompressible flow is identical to the entropy loss coefficient) is derived in Appendix 3 as

$$\zeta = \frac{\Delta P_o}{0.5\,\rho V_{te}^2} = -\frac{C_{pb}t}{w} + \frac{2\theta}{w} + \left(\frac{\delta^* + t}{w}\right)^2 \quad (26)$$

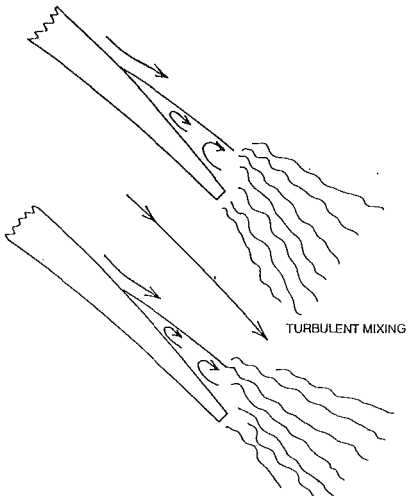


**Fig. 8 Trailing edge with a separated boundary layer**

Note how this result is independent of the details of the mixing process, which is likely to be unsteady with the formation of a Karman vortex street and with much of the entropy creation due to the viscous decay of the vortices. The details of this process cannot yet be predicted accurately by even the most sophisticated viscous flow calculations, but as we see the overall result is predictable using simple theory.

The theory of Appendix 3 requires an assumption for the average pressure acting on the suction surface downstream of the throat (see Fig. A3.1). Equation (26) assumes that this is the same as the far downstream pressure, $P_2$. A more common assumption, e.g., Stewart (1955), is that the pressure is the same as the throat pressure $P_1$. The actual suction surface pressure is likely to lie somewhere between these two assumptions. The author prefers to use the first assumption because it implies that the loss is not affected by the blade stagger, i.e., by the presence of adjacent blades. Since most of the dissipation takes place within a few trailing edge thicknesses this is felt to be realistic. The value assumed for the suction surface pressure has a large effect on the last term of Eq. (26) but not much effect on the other two terms. Fortunately the last term is usually comparatively small.

The major difficulty in applying this and similar theories to real blade rows is knowing the value of the base pressure coefficient. Much early work on this subject, e.g., Stewart et al. (1960), neglected the base pressure completely and so greatly underestimated the importance of trailing edge loss. Typically the value of $C_{pb}$ is about $-0.15$ and a typical turbine blade trailing edge blockage is 0.05 so the base pressure term contributes about 0.0075 to the loss coefficient while the last term of Eq. (26) contributes about 0.0025. For modern turbine blades the profile loss coefficient is of the order 0.03 and so the trailing edge contributes about 1/3 of the total profile loss. For compressor blades the trailing edge blockage is usually small but the boundary layers are thicker so the last term of Eq. (26) may be more important than the base pressure term.

Physically it is difficult to decide if the low base pressure produces the dissipation in the wake or if the dissipation causes the low base pressure. In fact the two are directly connected via Eq. (26) and anything that changes one must change the other. For example it is well known that for isolated blunt trailing edges the vortex shedding can be suppressed by attaching a splitter plate to the trailing edge; this therefore reduces the dissipation and so increases the base pressure. Similarly, the use of an elliptical rather than a square or semicircular trailing edge delays the separation of the boundary layers and this increases the average base pressure and reduces the dissipation and loss.

When considering base pressure, it would be more meaningful to measure it relative to the average pressure around the trailing edge in an inviscid flow. Since the latter has no loss and no boundary layers, Eq. (26) shows that for incompressible flow this pressure, $P_{bo}$, is given by

$$\frac{(P_{bo}-P_{te})}{(0.5\,\rho V_{te}^2)}=C_{pbo}=t/w \tag{27}$$

This is a positive base pressure, relative to the pressure $P_{te}$ just upstream of the trailing edge, and any value of base pressure below this value must be associated with a loss.

The fact that the mixed out loss depends on the momentum thickness of the boundary layers at the trailing edge, i.e., the middle term of Eq. (26), is an interesting result. The entropy that has been created in the boundary layers upstream of the trailing edge is measured by their entropy thickness, which, in incompressible flow, is identical to their energy thickness, so the entropy present just before the trailing edge would be

$$T\Delta S_{te}=0.5\,\rho V_{te}^3\delta_e \tag{28}$$

Hence, for a blade with zero trailing edge thickness, an amount of entropy given by

$$T\Delta S_w=0.5\,\rho V_{te}^3(2\theta-\delta_e) \tag{29}$$

is being created behind the trailing edge as a direct result of the mixing out of the boundary layers on the blade. This is entropy created by the viscous dissipation in the wake but is an inevitable consequence of the boundary layers on the blade surfaces. For the case of negligible trailing edge thickness the amount of dissipation in the wake depends on the difference between $2\theta$ and $\delta_e$ of the boundary layers just upstream of the trailing edge.

The ratio $\delta_e/\theta$ is a type of shape factor whose value depends on the state of the boundary layer. For a typical turbulent boundary layer its value is about 1.7 (Schlichting, 1978, p. 675) and so, *for thin trailing edges*, the ratio of the entropy present just before the trailing edge to that present far downstream is typically 0.85, i.e., about 15 percent of the total entropy is created behind the trailing edge. For boundary layers near separation this proportion rises to about 22 percent. For separated boundary layers and thick trailing edges an even greater proportion of the entropy is generated downstream and in the limit for a bluff body with very thin boundary layers all the entropy is generated in the wake.

The theory of Appendix 3 also applies to the case where the boundary layers are separated at the trailing edge, as illustrated in Fig. 8, provided that the static pressure just upstream of the trailing edge can still be assumed to be uniform. In this case the value of $\delta^*$ is likely to be greater than the trailing edge thickness and Eq. (26) suggests that there will be an extra loss due to the separation given by

$$\zeta_{\text{sep}}=\left(\frac{\delta^{*2}+2t\delta^*}{w^2}\right). \tag{30}$$

This implies that only large separations will cause significant loss, e.g., for a thin trailing edge a separation causing 10 percent blockage produces only 1 percent loss. However, this result makes the dubious assumption that a uniform pressure continues to act over the whole of the trailing edge plane. It is probable that in reality a low pressure extends over much of the separated region giving an increased contribution to the base pressure term in Eq. (26). Physically the separated region will give rise to larger vortices and so greater dissipation in the wake than would the trailing edge alone. On this basis it can be argued that the total dissipation will be roughly proportional to the combined thickness of the trailing edge and separation rather than to the square of the blockage as suggested by Eq. (26). A crude approximation that is compatible with this suggestion is to apply a low base pressure over the combined thickness of the trailing edge plus separation, i.e., to use $(t+\delta^*)$

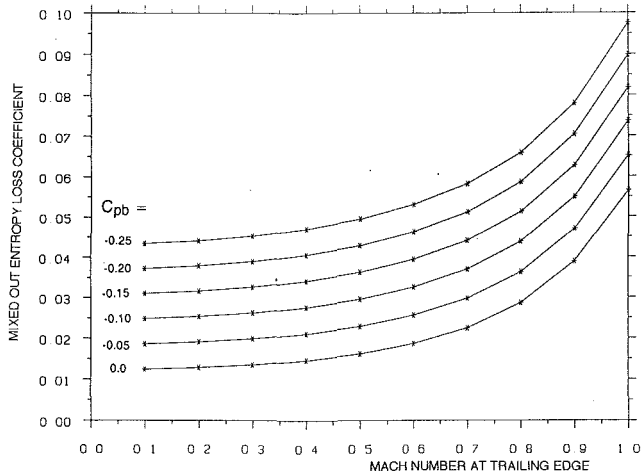


**Fig. 9 Variation of trailing edge loss with base pressure coefficient and Mach number for 10 percent throat blockage**

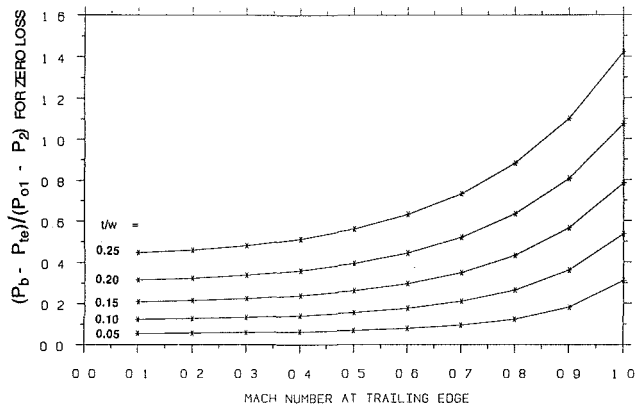


**Fig. 10 Base pressure coefficient for zero loss as a function of Mach number and trailing edge blockage**

instead of $t$ in the base pressure term of Eq. (26). However, with this assumption the value of the base pressure that should be used remains very uncertain.

From the preceding discussion it can be seen that the influence of a separated boundary layer at the trailing edge remains a major unknown when calculating loss. It is clear from test data (and from Lieblein's correlation of loss versus diffusion factor) that separated boundary layers do give rise to high loss and this can only be reconciled with Eq. (26) by applying a low base pressure over the whole separated region. The author is not aware of any method of predicting this pressure. As discussed in section 7.2 this is likely to be especially important for compressor blades.

A very similar type of calculation can be applied to the mixing of coolant flow injected through the blade surfaces, (e.g., Hartsel, 1972) and also to the mixing of a tip leakage jet emerging into the mainstream from the tip gap (Denton and Cumpsty, 1987). In these cases the uncertainty about the magnitude of the base pressure does not arise, and so the results are more directly usable to quantify loss.

All the above theory assumes incompressible flow with mixing taking place at a constant area. For compressible flow the same equations may be solved numerically. Figure 9 shows the variation of trailing edge loss coefficient with downstream Mach number for a trailing edge with 10 percent blockage at various values of base pressure coefficient. For other values of blockage the loss may be taken as being proportional to blockage. Although the base pressure itself can only be found by experiment, the base pressure for zero loss can be found exactly from the conservation equations and it is interesting

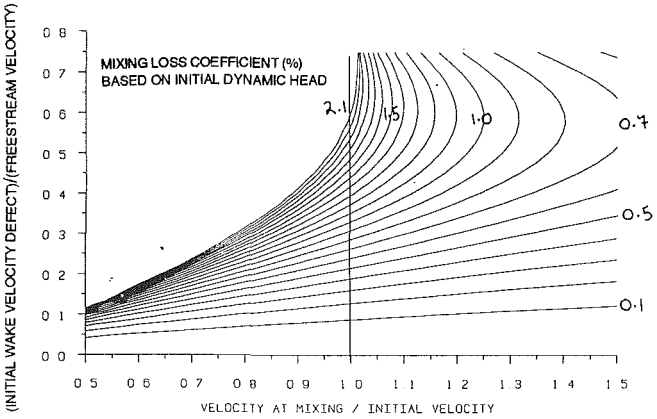


**Fig. 11 Effect of wake acceleration or deceleration on the mixing loss. Calculations for $t/w = 0.1$, $M_1 = 0.5$.**

to see how it varies with Mach number. Figure 10 shows the result from numerical solutions of the equations for varying trailing edge blockage and varying downstream Mach number with the assumption that $P_s = P_2$ (Appendix 3). It is significant that as the Mach number is increased the base pressure for zero loss becomes significantly greater than the pressure on the blade surface immediately before the trailing edge. Since experiments (e.g., Sieverding et al., 1983) usually show that the base pressure is lower than the latter pressure, this helps to explain why trailing edge loss increases rapidly as the downstream Mach number approaches unity.

The assumption of constant area mixing, which was made in the preceding theory, will not always be valid. Wakes in turbomachines mix out in a complex environment, which will be unsteady if the mixing is not complete before the next blade row. Neglecting unsteadiness for the moment, we can illustrate the effects of a change of area by means of simple physical arguments and numerical calculations.

Physically, when a shear layer is subjected to a favorable streamwise pressure gradient the transverse velocity gradient, $dV/dy$, is reduced because the slower moving fluid speeds up by more than the faster moving fluid. Hence the rate of shear strain is decreased and the rate of entropy generation, which is proportional to $\mu_{\text{eff}}\,(dV/dy)^2$, will be reduced. From this argument we would expect acceleration of a wake to reduce the dissipation and hence the mixing loss. Conversely deceleration should amplify the velocity gradient and increase the loss. A simple illustration of this is possible for two-dimensional incompressible flow. Using the momentum integral equation and the continuity equation for a wake it can be shown that

$$\frac{d\Delta P_o}{dx} = \Delta P_o(1-H)\frac{1}{V}\frac{dV}{dx} \tag{31}$$

where $\Delta P_o$ is the stagnation pressure loss that would be obtained from a mixing calculation at the local flow area; $x$ is the distance along the wake and $H$ is its local shape factor. Since $H$ is always greater than unity Eq. (31) shows that acceleration will decrease the mixed out loss and deceleration increase it. Large values of $H$, such as occur close to the trailing edge, increase the magnitude of the effect. Only when the wake is nearly mixed out so that $H \to 1$ does a change in velocity cease to have any effect on the mixed out loss.

As a numerical example of the same phenomenon, Fig. 11 shows the mixing loss coefficient for a "square" wake that is (hypothetically) accelerated or decelerated isentropically to the mixing velocity and then allowed to mix out at constant area. This is a very idealized model since in reality mixing continues while the wake is being accelerated or decelerated, but its does serve to illustrate the magnitude of the effect. Deceleration is seen to cause a very significant increase in loss while acceleration causes a slight reduction.

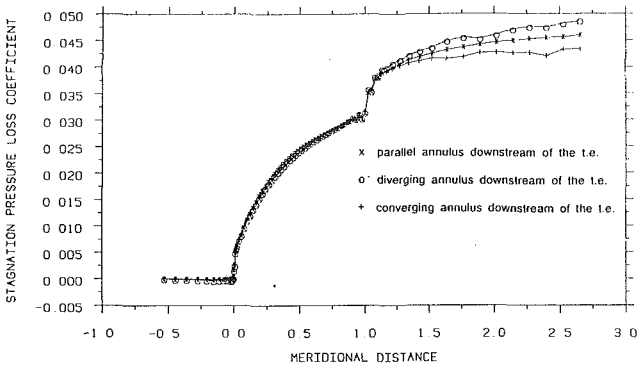


**Fig. 12 Computed growth of stagnation pressure loss within and downstream of a compressor cascade**

The importance of this effect in a turbomachine is difficult to establish since mixing is a continuous process and cannot be said to take place at one location or one velocity. In a wake mixing is initially very rapid and the velocity on the wake centerline may reach 90 percent of free-stream velocity within a few trailing edge thicknesses. However, as shown by Prato and Lakshimarayana (1993) mixing continues for up to one chord downstream of the blade row, by which time the free-stream velocity may have changed considerably.

An important consequence of the control volume approach to mixing is that numerical calculations do not have to predict the details of the mixing processes exactly in order to compute the correct loss. As long as conditions at the trailing edge are predicted correctly then the mixed out loss should also be correct. As an illustration of the ideas presented in this section, Fig. 12 shows results from a viscous calculation on a compressor cascade. The flow is just subsonic and the suction surface boundary layer is very nearly separated at the trailing edge. The change of mass-averaged stagnation pressure through and downstream of the cascade is plotted and shows that in this case about 1/3 of the total loss is generated behind the trailing edge. The calculation was repeated with the change of stream surface thickness downstream of the trailing edge varied by ±25 percent, while keeping the flow on the blade surface constant. Figure 12 shows that this has only a small effect on the overall loss, changing it by about ±5 percent. This is a consequence of most of the mixing occurring close to the trailing edge before the area has changed significantly.

## 5 Entropy Production in Shock Waves

It is well known that shock waves are irreversible and hence are sources of entropy. The entropy creation occurs due to heat conduction and high viscous normal stresses within the shock wave, which is only a few molecular free paths in thickness. Text books, e.g., Shapiro (1953), often derive the equation for the entropy increase across a *plane normal* shock wave. Expanding this in powers of $(M^2-1)$, where M is the upstream Mach number, leads to the following approximate result for weak shocks:

$$\Delta s \approx C_v \frac{2\gamma(\gamma-1)}{3(\gamma+1)^2}(M^2-1)^3 + O(M^2-1)^4 \qquad (32)$$

This shows that the entropy creation varies roughly as the cube of $(M^2-1)$.

The above result is for normal shock waves. Oblique shocks will always produce less entropy than a normal one with the same upstream Mach number. In fact Eq. (32) is equally applicable to oblique shock waves provided M is interpreted as the component of Mach number perpendicular to the shock front.

The pressure rise across a weak shock wave is also proportional to $(M^2-1)$ and Eq. (32) can be rewritten as

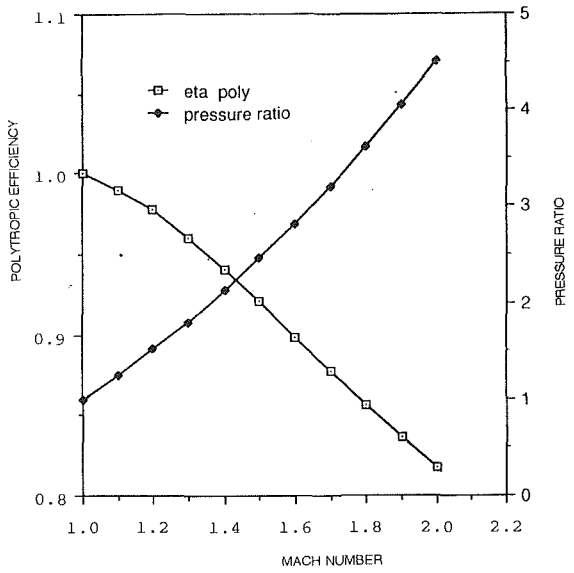


**Fig. 13 Compression in a normal shock wave expressed as a polytropic efficiency**

$$\Delta s \approx R\frac{\gamma+1}{12\gamma^2}\left(\frac{\Delta P}{P_1}\right)^3 + O\left(\frac{\Delta P}{P_1}\right)^4 \qquad (33)$$

which applies to both normal and oblique shocks.

The efficiency of a compression process in a weak shock may be defined by

$$\eta = 1 - \frac{T\Delta s}{\Delta h} \approx 1 - \frac{\Delta s}{R\,\Delta P/P} \approx 1 - \frac{\gamma+1}{12\gamma^2}\left(\frac{\Delta P}{P}\right)^2 \qquad (34)$$

For $\Delta P/P = 0.5$, $\gamma = 1.4$ (which corresponds to a normal shock with an upstream Mach number of about 1.2) this gives $\eta \approx 0.97$, which suggests that weak shock waves are a relatively efficient compression process. This is further illustrated in Fig. 13, which shows the polytropic efficiency of the compression process through a shock where the efficiency has been defined as

$$\eta_p = \frac{(\gamma-1)}{\gamma}\frac{\ln(P_2/P_1)}{\ln(T_2/T_1)} \qquad (35)$$

and has been calculated using exact theory for a gas with $\gamma = 1.4$.

It is clear that a shock is actually a comparatively efficient compression mechanism if the component of upstream Mach number perpendicular to the shock front is less than 1.5. This helps to explain the development of efficient transonic compressors with inlet Mach numbers typically in the range 1.5–1.7.

**5.1 Shock Waves in Compressors.** For a single shock wave, the entropy generation is a unique function of the static pressure rise. However, Eq. (34) shows that this function is highly nonlinear so that if the same pressure rise can be accomplished by two shock waves instead of by a single one then the shock loss will be greatly reduced (by a factor of 4 if both shocks have the same pressure rise). On this argument it is hard to explain why the fans of most civil aero-engines seem to operate most efficiently with a single normal shock wave near the leading edge (e.g., Pierzga and Wood, 1985). It is also hard to explain the claimed reduction of shock loss by sweep for transonic compressor blading (Wennerstrom and Puterbaugh, 1984). Shock sweep will reduce the shock strength for a given upstream Mach number but not for a given pressure ratio. Possibe explanations are that a second shock is formed as a result of the sweep or that, since the sweep is usually produced by a change in radius, some of the pressure rise takes place by centrifugal effects, thereby reducing the pressure rise required from the shock and increasing its efficiency.

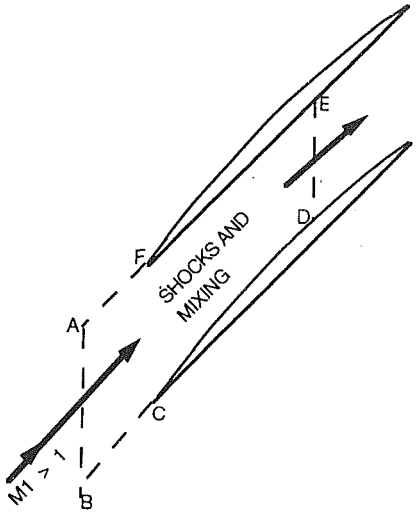


Fig. 14 Control volume used for the shock loss of transonic compressor blades

A recent paper by Freeman and Cumpsty (1989) shows that the performance of transonic compressors can be remarkably well predicted by applying conservation of mass, energy, and momentum between the upstream flow and the flow downstream of the shock system. The equation are applied to the control volume shown in Fig. 14. The flow is assumed to be uniform both upstream of the blade row, i.e., across $AB$, and at plane $DE$ downstream of the leading edge shock system. As in the case of mixing loss the control volume formulation predicts the overall changes without needing to consider the details of the flow within the control volume. In this case the loss occurs through the complex shock system within the control volume and so the method only applies to the loss generated by the leading edge shock system and not to any passage or trailing edge shocks.

Only the continuity equation and the streamwise momentum equation are solved and the streamwise force exerted on the flow by the blade is approximated by assuming that the average pressure on the blade surfaces $CD$ and $FE$, including the leading edge itself, is the same as the downstream pressure on $DE$. This assumption is very approximate and only gives realistic answers because transonic compressor blades are so thin. The assumption that the flow leaving the control volume through $DE$ is uniform is also dubious. Despite these approximations the method gives remarkably good predictions of the behavior of transonic compressors between peak efficiency and stall when the shock is near the leading edge. The fact that much of the performance can be predicted by a control volume analysis also explains why the performance of such compressors can be well predicted by modern three-dimensional flow calculations (e.g., Adamczyk et al., 1993), which do satisfy conservation of mass, energy, and momentum even when the details of the shock system are not captured accurately.

**5.2 Shock Waves in Turbines.** Compression is seldom a desirable feature of turbines, however, transonic turbines are commonly used to obtain high-stage pressure ratios and so shock waves do occur. Although local Mach numbers may be high, the shocks within the blade passage are usually oblique so that $\Delta P/P$ is small and they generate little direct loss (Eq. (33)). The most serious consequence of transonic flow in turbines is the shock system at the trailing edge, as illustrated in Fig. 15. The low base pressure formed immediately behind the trailing edge can generate a very large trailing edge loss. The flow expands around the trailing edge to this low pressure and is then recompressed by a strong shock wave at the point where the suction and pressure side flows meet. The entropy generation comes from the intense viscous dissipation at the edges

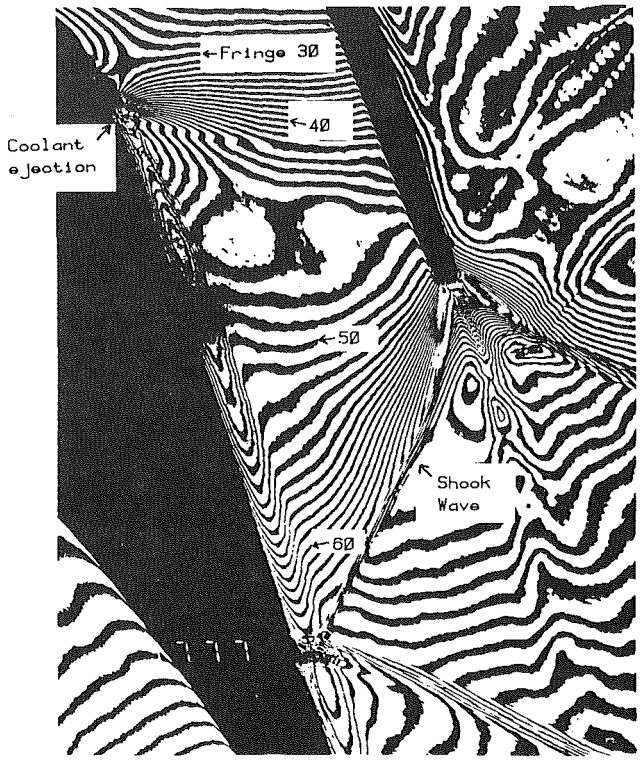


Fig. 15 Trailing edge shock system for a turbine blade, with suction surface coolant ejection

of the separated region immediately behind the trailing edge and from the strong shock formed at the close of this region. For cooled turbine blades with thick trailing edges this may be the largest single source of loss in the machine.

Denton and Xu (1990) apply a control volume argument very similar to that of Freeman and Cumpsty, to the trailing edge of choked turbine blades. Their model uses both of the momentum equations and uses the assumption that the flow is choked at the throat of the blade to determine the mass flow rate; it does not assume that the blade is thin. The method is therefore rigorous and based on reasonable assumptions. It shows that even in this case the loss can be calculated from conservation of mass, momentum, and energy provided the average pressure acting on the blade suction surface downstream of the throat can be predicted. Low values of this pressure are shown to reduce the loss. In practice the suction surface pressure must be obtained from a separate calculation of the flow field. However, the predicted loss is extremely sensitive to the value of this pressure and it is unlikely that it will be known accurately enough for the method to give a useful prediction.

**5.3 Shock Wave–Boundary Layer Interaction.** There are indirect sources of loss associated with shock waves in both compressors and turbines because of the interaction of the shock wave with the boundary layer. A boundary layer separation bubble will usually be formed at the foot of a weak shock and extra dissipation is likely to occur within and downstream of the bubble. If the boundary layer was laminar the bubble will almost certainly cause transition. Strong shock waves, which are especially likely to arise in transonic compressors, may cause complete boundary layer separation. For a normal shock wave this is likely if the upstream Mach number is greater than about 1.4 (Atkin and Squire, 1992). Hence, increases in the boundary layer loss are likely to occur from shock wave–boundary layer interaction in both turbines and compressors. In view of the high pressure rise obtainable via

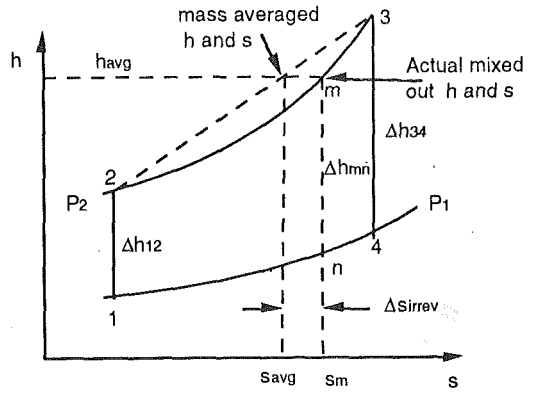

Fig. 16 Mixing of two flows at constant pressure

the shock wave, these may be perfectly acceptable in transonic compressors even when the shock separates the boundary layer.

## 6 Entropy Creation by Heat Transfer

Heat transfer from a turbomachine to its surroundings is usually small and the flow is almost invariably regarded as being adiabatic. Small machines with a large surface area to volume ratio (e.g., small turbochargers) are most likely to violate this assumption. For a compressor the work input to achieve a required pressure ratio is reduced by heat loss from the fluid to its surroundings and it is well known that isothermal compressors, with interstage cooling, are preferable to adiabatic ones for many applications. This does not apply to the compressors of gas turbines where any heat loss from the compressor has to be made up by burning extra fuel in the combustion chamber and results in a loss of cycle efficiency. For a turbine, heat loss to the environment will always decrease the work output and so should be avoided, e.g., by lagging the turbine if necessary.

The main effect of heat transfer is felt in cooled turbines where a separate stream of cool fluid is used to maintain the blades and disks at an acceptable temperature. The coolant flow is subsequently mixed with the main flow and expanded with it through the remaining stages of the turbine. Heat transfer from the main flow to the coolant flow takes place in three stages: first from the hot gas of the main flow to the cooled metal, second from the metal to the coolant flow within the internal passages of the blade, and finally from the mainstream flow to the coolant flow as the two flows are mixed. As a result of this heat transfer the main flow will do less work than if it were expanded adiabatically from its supply pressure and temperature to the exhaust pressure whilst the coolant flow will do more work than if it were expanded from its supply conditions to the same exhaust pressure. We will examine the effect of the heat transfer and mixing on the turbine performance.

**6.1 Thermodynamics of a Gas Turbine Cycle With Blade Cooling.** It is difficult to consider the entropy changes due to coolant flows without considering the whole thermodynamic cycle. The problem is highlighted by Fig. 16, which shows that when two flows of perfect gas at the same pressure but different temperatures are mixed at constant pressure there is an increase of entropy but no loss of potential work, i.e.,

$$(1-m_{fc})\Delta h_{34}+m_{fc}\Delta h_{12}=\Delta h_{mn} \tag{36}$$

where $m_{fc}$ is the mass fraction of cooling flow bled off at point 2.

Appendix 4 gives an analysis of a simple cycle. The cycle pressure ratio is assumed fixed and its efficiency is influenced by the turbine entry temperature $T_3$, by $m_{fc}$, and by the efficiency of the cooled part of the turbine $\eta_t$. The analysis shows that the change in overall cycle efficiency due to cooling can be written as

$$\Delta\eta_o=\left\{\frac{\partial\eta_c}{\partial T_3}\frac{dT_3}{dm_{fc}}+\left[\frac{\partial\eta_c}{\partial m_{fc}}+\frac{\partial\eta_c}{\partial\eta_t}\frac{d\eta_t}{dm_{fc}}\right]\right\}\Delta m_{fc} \tag{37}$$

The first term on the right-hand side of this equation represents the change of cycle efficiency due to a change in turbine entry temperature, which can be increased by increasing $m_{fc}$. This will be a positive term and represents the main objective of using cooling flows to increase cycle efficiency.

The second term represents the rate of change of cycle efficiency with cooling flow for constant values of turbine entry temperature and turbine efficiency. This will be a negative term because the net cycle efficiency can be thought of as a weighted average of the efficiency of the main cycle and of the lower efficiency cycle undergone by the cooling flow. This term includes the loss of work due to the heat transfer from the mainstream flow.

The third term will also be negative because it represents the change of cycle efficiency due to a change in the efficiency of the cooled part of the turbine. As described in Appendix 4, this efficiency is defined to include only viscous effects within the turbine which in turn are assumed to depend on the amount of coolant added. It is only this term that we will consider in detail in this paper.

Figure A 4.1 shows an idealized cycle in which coolant is assumed to be added at a uniform rate along the cooled part of the turbine expansion. Analyzing this cycle numerically for an overall pressure ratio 25:1, cooled turbine pressure ratio 4:1 and turbine entry temperature 1500 K, gives for the terms in Eq. (37):

$$\Delta\eta_o=\left\{1.03\times10^{-4}\frac{dT_3}{dm_{fc}}-0.18+0.38\frac{d\eta_t}{dm_{fc}}\right\}\Delta m_{fc} \tag{38}$$

The value of $dT_3/dm_{fc}$ is likely to be about $10^4$ (100°C per 1 percent cooling flow) and the value of $d\eta_t/dm_{fc}$ is likely to be about $-1$ (1 percent loss of efficiency per 1 percent cooling flow) and so Eq. (38) shows that the rate of loss of turbine efficiency with cooling flow has a large effect on the overall efficiency. The second term is also significant and emphasizes the importance of making the best possible use of the cooling flow, i.e., by making it do useful work and avoiding pressure drops due to throttling in the cooling passages.

**6.2 Thermodynamics of a Cooled Turbine.** The thermodynamics of a cooled turbine are also considered in Appendix 4, where it is shown that the loss of output from the mainstream flow is due mainly to the entropy creation by viscous effects rather than that caused by heat transfer. Using Shapiro's (1953) influence coefficients, it is shown that, for the situation shown in Figs. 7 and 15, when a mass flow $m_c$ of coolant is injected at velocity $V_c$ and angle $\alpha$ to a main flow with Mach number M and velocity $V_m$ the change of effective turbine efficiency is

$$\Delta\eta_t=-\frac{T_4}{\Delta T_{\text{ois}}}(\gamma-1)\text{M}^2\left(1-\frac{V_c\cos\alpha}{V_m}\right)\frac{m_c}{m_m} \tag{39}$$

From this it is clear that coolant addition to a mainstream flow at high Mach number is much more harmful than at low Mach numbers and also that coolant should be injected as nearly parallel to the main flow as is possible. If the coolant has a higher stagnation pressure than the main flow, so that $V_c > V_m$, and is injected almost parallel to it, then the stagnation pressure of the main flow and the efficiency of the turbine (which is defined in terms of the mainstream flow properties) may even be increased by the mixing. Interestingly, if the coolant is injected perpendicular to the main stream ($\alpha = 90$ deg) then its temperature and pressure, which determine $V_c$, have no effect on the turbine efficiency, which depends only on the mass fraction of coolant injected.

The entropy creation by irreversible mixing of cooling flows can also be calculated by applying conservation of mass, mo-

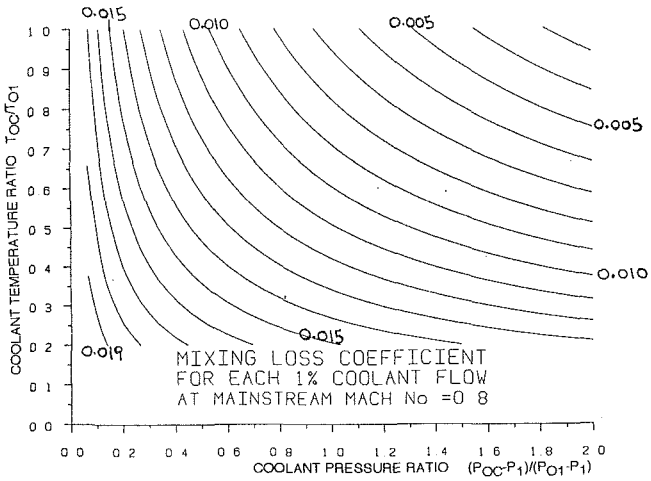


**Fig. 17 Entropy loss coefficient as a function of temperature ratio and pressure ratio for 1 percent of coolant flow injected at 45 deg to a main flow with Mach number = 0.8**

mentum, and energy in a very similar way to the method of Appendix 2. Such a method is described by Hartsel (1972). The analysis is complicated by the need to assume compressible flow, even at low Mach numbers, because of the large changes in temperature. Appendix 4 shows that only the entropy creation due to viscous effects, not that due to heat transfer, should be considered as a loss of turbine efficiency.

Results from a numerical calculation applied to cooling flow ejected through a slot with a velocity inclined at 45 deg to the mainstream direction ($\alpha = 45$ deg) are illustrated in Fig. 17 where the loss is presented as the loss coefficient of the mainstream flow per percent of coolant addition. Appendix 4 shows that only the entropy change due to viscous dissipation, and not that due to heat transfer, influences the turbine efficiency. Hence the loss coefficient plotted in Fig. 17 is defined using

$$\zeta_s = To_{\text{mix}} \frac{\Delta s_{\text{tot}} - dq/T_{\text{avg}}}{0.5\, V_{\text{mix}}^2} \tag{40}$$

where the heat $dq$ removed from the mainstream flow is assumed to have been transferred at a temperature $T_{\text{avg}} = 0.5\,(T_1 + T_{\text{mix}})$. This definition is consistent with Eq. (A4.9) of Appendix 4.

Figure 17 shows that the aerodynamic loss on mixing is almost equally influenced by the stagnation pressure and the stagnation temperature of the coolant. Low coolant temperatures and pressures cause a high loss because they produce a low value of $V_c$ in Eq. (39). Numerical calculations show that the loss coefficient as defined by Eq. (40) is not greatly affected by the value of free-stream Mach number.

The addition of coolant flow may cause other losses by disturbing the boundary layers on the blade or endwall surfaces, as shown in Fig. 15. These are not considered in the above analysis.

## 7 Two-Dimensional Losses in Turbomachinery

**7.1 Blade Boundary Layer Loss.** Application of the ideas presented above to real turbomachinery is complicated by the complexity of the geometry and flow. In particular the real flow is usually three-dimensional so that simplified one-dimensional and two-dimensional results should be used as guidelines and as an aid to understanding the physics of the flow rather than to obtain quantitative results.

Using Eq. (20), the total entropy generation in the blade boundary layers can be evaluated from

$$\dot{S} = \sum C_s \int_0^1 \frac{C_d \rho\, V_o^3}{T}\, d(x/C_s) \tag{41}$$

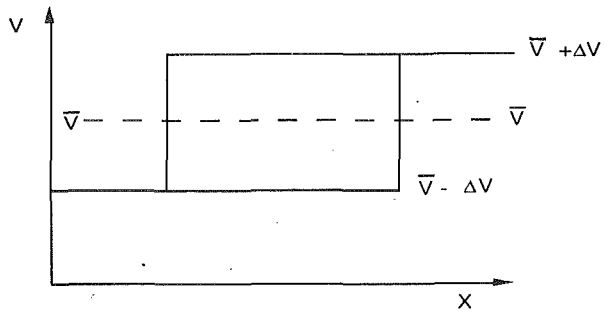


**Fig. 18 Idealized blade surface velocity distribution**

where the summation is for both blade surfaces, $x$ is the surface distance, and $C_s$ is the total length of the surface. To turn this into an entropy loss coefficient for the blade we must divide the total entropy produced by the mass flow rate and by a reference dynamic head, which would usually be based on $V_1$ for a compressor blade and on $V_2$ for a turbine blade, e.g.,

$$\zeta_s = \frac{T\dot{S}}{m\, 0.5\, V_{\text{ref}}^2} \tag{42}$$

Combining these two equations gives, for low-speed flow,

$$\zeta_s = 2 \sum \frac{C_s}{p \cos \alpha_{\text{ref}}} \int_0^1 C_d \left(\frac{V_o}{V_{\text{ref}}}\right)^3 d(x/C_s) \tag{43}$$

If the blade surface velocity distribution and the variation of $C_d$ are known this equation can be used to estimate the loss coefficient. The occurrence of the blade surface velocity in the form $(V/V_{\text{ref}})^3$ is very important. It shows that the suction surface is dominant in producing loss and that regions of high surface velocity contribute proportionally much higher amounts of loss.

The value of loss coefficient obtained from Eq. (43) is dominated by the location of the transition point where $C_d$ undergoes a rapid change, as shown in Fig. 5. In order to minimize the loss the boundary layers should be kept laminar for as long as possible. The extent of the laminar boundary layer will depend mainly on the Reynolds number, turbulence level, and on the detailed surface velocity distribution. At the high turbulence levels prevalent in turbomachines transition is likely to occur in the $\text{Re}_\theta$ range 200–500 while $\text{Re}_\theta$ at the trailing edge is usually in the range 500–2000 (although it will be greater than this for large high-pressure steam turbines and large hydraulic turbines). Figure 4 shows that over much of this range the dissipation coefficient is of the order of 0.002, as suggested by Denton and Cumpsty. Although one cannot expect this crude approximation to give accurate results for any one blade it can be used to predict *systematic* trends for the variation of loss with blade and stage design.

These equations also show clearly why for any specified combination of inlet and outlet flow angles there is an optimum pitch to chord ratio ($p/c$). We assume a rectangular velocity distribution as illustrated in Fig. 18, and that $C_d$ is constant.

Equation (41) gives

$$\dot{S} = C_d \rho\, C(2\overline{V}^3 + 6\overline{V}\Delta V^2) \tag{44}$$

Using the definition of blade circulation to obtain $V_x$ we get

$$m = \rho V_x p = \frac{2C\Delta V \rho}{(\tan\alpha_2 - \tan\alpha_1)} \tag{45}$$

and so the loss coefficient, based on mean velocity, becomes

$$\zeta_s = \frac{\dot{S}}{0.5 m \overline{V}^2} = C_d \left(2\frac{\overline{V}}{\Delta V} + 6\frac{\Delta V}{\overline{V}}\right)(\tan\alpha_2 - \tan\alpha_1) \tag{46}$$

which has a minimum value, corresponding to an optimum pitch-chord ratio, when $\Delta V/\overline{V} = 1/\sqrt{3}$. If $C_d$ is taken as 0.002 this simple method gives quite realistic loss coefficients.

If $C_d$ is assumed constant the value of loss obtained from

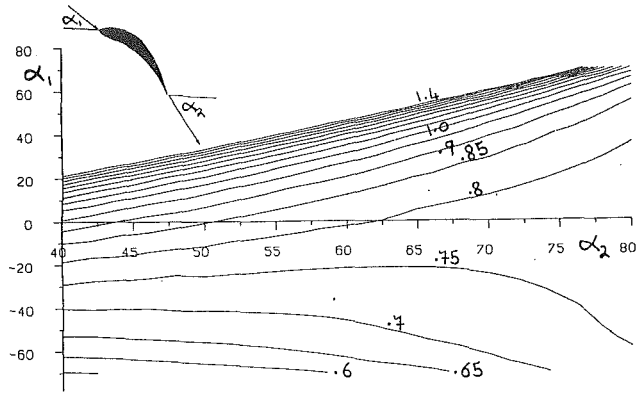


Fig. 19 Predicted optimum pitch-chord ratio of turbine blades

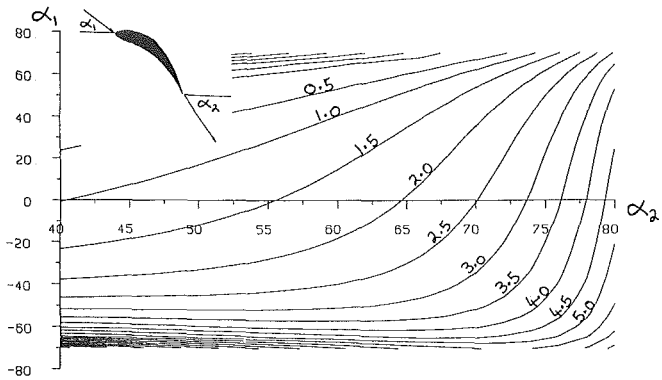


Fig. 20 Predicted profile loss coefficient (percent) of turbine blades at their optimum pitch-chord ratio

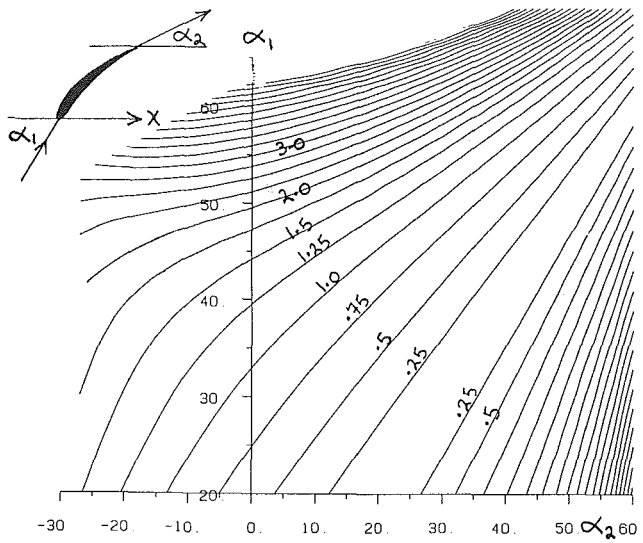


Fig. 21 Profile loss coefficient of compressor blades (percent) predicted by Eq. (43)

Eq. (43) is not greatly dependent on the surface velocity distribution and this permits a simple method of estimating the loss coefficients. If the inlet and outlet flow angles are specified and a plausible surface velocity distribution, more realistic than that of Fig. 18, is guessed then the pitch to chord ratio can be calculated from the tangential momentum change and an estimate of loss can be obtained from Eq. (43). By systematically varying the guessed velocity distribution one can then estimate the optimum $p/c$ ratio and minimum loss. Figure 19 shows the resulting optimum $p/c$ ratio and Fig. 20 the minimum loss calculated in this way for turbine blades. The results agree well with the predictions of Zweifel's rule for optimum $p/c$ ratio and with cascade measurements of loss coefficient.

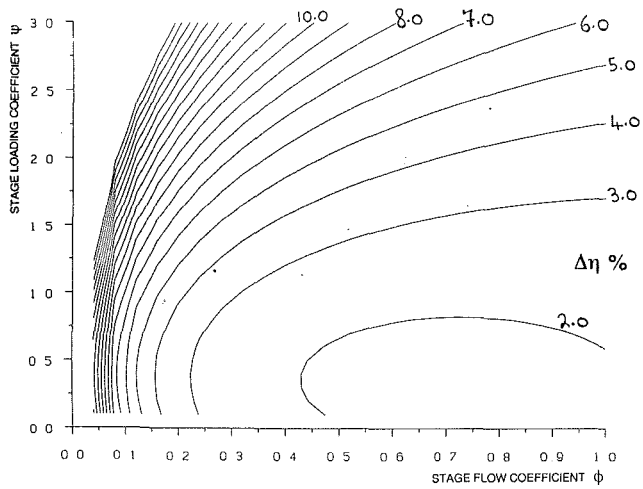


Fig. 22 Loss of efficiency (percent) due to profile loss alone for turbines with zero interstage swirl angle

For compressor blades the predictions, using exactly the same method, are not realistic. The calculated value of optimum pitch-chord ratio is too high, giving a diffusion factor well over 0.6. Consequently the predicted minimum loss is too low. The reason is that the method takes no account of boundary layer separation and one must conclude that this is a dominant feature in the design of compressor blades. The minimum loss will occur when the boundary layer is on the verge of separation; this can be simulated in the method by causing the predicted loss to rise very rapidly with diffusion factor when this is greater than about 0.55. The optimum pitch-chord ratio then occurs just above that which gives a diffusion factor of 0.55. The results from such a prediction are shown in Fig. 21.

When considering the design of a complete stage the entropy creation should be considered relative to the stage enthalpy change. If we define an isentropic velocity $C_o$, based on the stage isentropic enthalpy change, by

$$\Delta h_{is} = 0.5 C_o^2 \tag{47}$$

then the overall increase in specific entropy due to the blade surface boundary layers on both rows may be estimated from

$$\Delta s \approx \Delta h_{is} 2 \frac{C_o}{V_x} \sum \frac{C_s}{p} \int_0^1 \frac{C_d}{T} \left( \frac{V_o}{C_o} \right)^3 d(x/C_s) \tag{48}$$

where the summation is over all the blade surfaces. This result is easily converted into the stage efficiency via Eq. (9) and shows that it is the blade surface velocity relative to the isentropic velocity $C_o$ that is most important as regards stage efficiency. For high reaction stages $V/C_o$ will be greater in the rotor, which is then likely to contribute most to the loss of efficiency and conversely for low reaction stages. Again, by guessing likely surface velocity distributions, assuming that $C_d$ is constant, and calculating the optimum $p/c$ ratio for each blade row the integrals and summations of Eq. (48) can be performed and the stage efficiency estimated for any specified stage velocity triangles. Figure 22 shows the result for axial turbine stages with zero interstage swirl angle. It must be emphasized that this gives the loss of efficiency due to blade boundary layer losses alone. Given that a typical turbine stage efficiency is about 90 percent we can conclude that these are only responsible for about 1/3 of the total loss in most turbines.

The blade surface boundary layer loss varies significantly with Reynolds number and surface roughness. The variation with Re is as suggested by Fig. 5 with the loss increasing rapidly at very low Re ($\mathrm{Re} < 10^5$) due to the high dissipation in laminar boundary layers and possibly to laminar separation of the boundary layer. Within the transition region, $2 \times 10^5 < \mathrm{Re} < 6 \times 10^5$; the variation is complex and depends on the

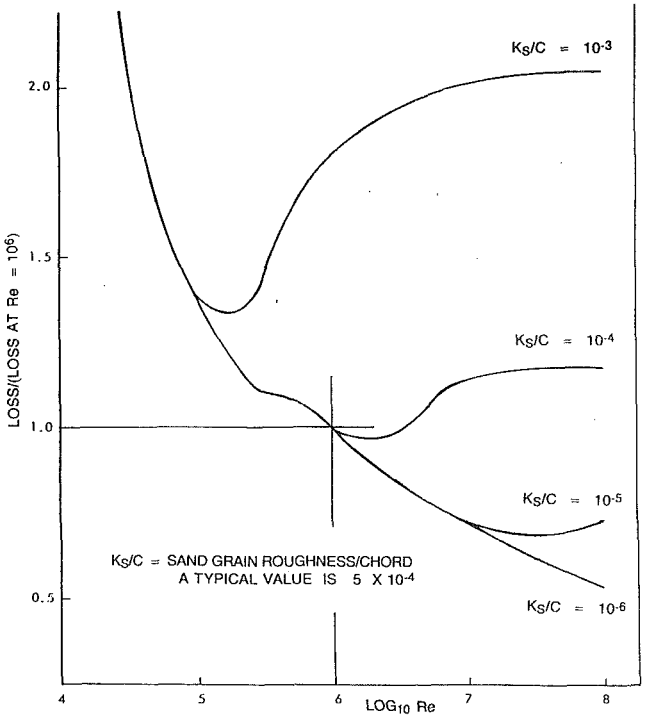


**Fig. 23 Variation of profile loss with Reynolds number and surface roughness**

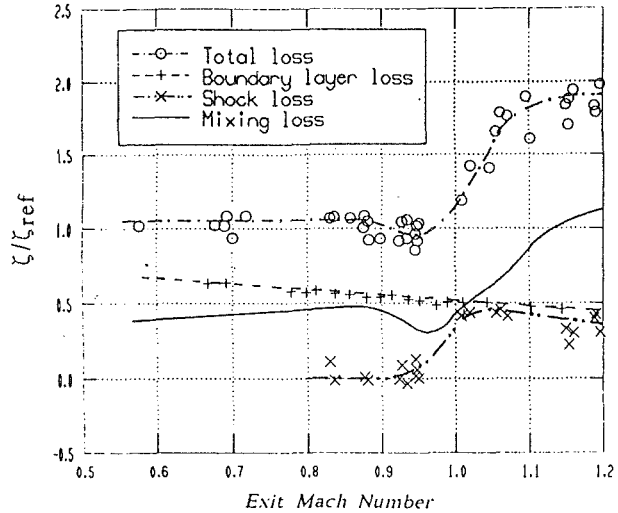


**Fig. 24 Variation of the two-dimensional components with Mach number for a turbine cascade (from Mee et al., 1992)**

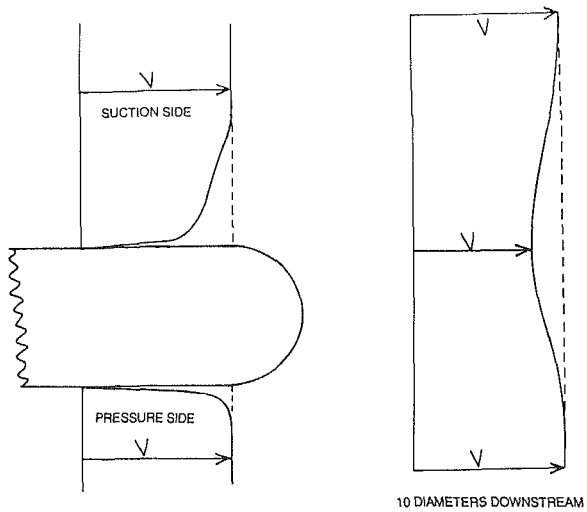


**Fig. 25 Velocity profiles at and downstream of a simulated turbine blade trailing edge**

details of the surface velocity distribution. The net result is a combination of the general decrease in loss with increasing Re and an increase in loss as the transition point moves upstream. At $Re > 6 \times 10^5$ the loss varies approximately as $Re^{-1/6}$ for very smooth blades. However, in this regime the turbulent boundary layer is significantly influenced by the surface roughness so that for machines that operate at very high Re the surface finish of the blades is very important. Curves for the variation of profile loss with Re and with roughness have been given by Koch and Smith (1976) for compressors and by Denton and Hoadley (1972) for turbines. Both sets of curves show similar trends although the latter, reproduced in Fig. 23, predicts an increase of loss with Re in the transition region at high values of roughness.

All the preceding analysis assumes two-dimensional flow in the blade surface boundary layers. The same approach can be applied to three-dimensional boundary layers where the convergence or divergence of the surface streamlines may thicken or thin the layer. Although this can have a considerable effect on the boundary layer thickness, it should not have a great effect on the entropy creation per unit surface area, unless convergence of the surface streamlines causes the boundary layer to separate. Hence it is suggested that Eq. (41) can be modified to estimate the entropy production over the whole blade surface, even in three-dimensional flow.

**7.2 Trailing Edge Loss.** The other major contribution to two-dimensional blade loss comes from the trailing edge. The magnitude of trailing edge loss has been seriously underestimated in the past, especially for turbine blades, due to the neglect of the base pressure term in Eq. (26). Figure 24 from Mee et al. (1992) shows that for a blade with a trailing edge blockage of 6.3 percent about 1/3 of the total two-dimensional loss is mixing loss behind the trailing edge in subsonic flow. The same figure shows that in supersonic flow this proportion rises to about 50 percent. Figure 25 (Roberts, 1992) shows the measured velocity profiles before and after the trailing edge of a simulated low-speed turbine blade with representative boundary layer to trailing edge thickness ratios, again about 1/3 of the total loss was found to be generated behind the trailing edge. Figure 25 serves to illustrate how thin the boundary layers are relative to the trailing edge and it is not surprising that the trailing edge itself can cause such a large proportion of the loss.

As explained previously the entropy can be expected to increase by about 18 percent behind a *thin* trailing edge due to the mixing out of the surface boundary layers. In the two cases just quoted it increases by about 50 percent so the loss attributable to trailing edge thickness is about 32 percent of the boundary layer loss or 21 percent of the total loss. The value of base pressure coefficient necessary to explain this increase is about $-0.075$, which is typical of the values found by Sutton (1990) for a wide range of trailing edge shapes.

An alternative means of estimating the base pressure coefficient is to compare measured losses with losses calculated from boundary layer loss alone and to attribute the difference to trailing edge loss. This has been done by Hart et al. (1991) for a total of 180 turbine cascade measurements. Hart used an inviscid calculation to find the base pressure for no loss and a boundary layer calculation to obtain the boundary layer parameters at the trailing edge. He then correlated his results to find the average value of $C_{pb}$ necessary to make the calculations agree with the measured loss. He found the average value of $C_{pb}$ to be $-0.13$ and that it did not correlate with either trailing edge thickness or boundary layer thickness. It

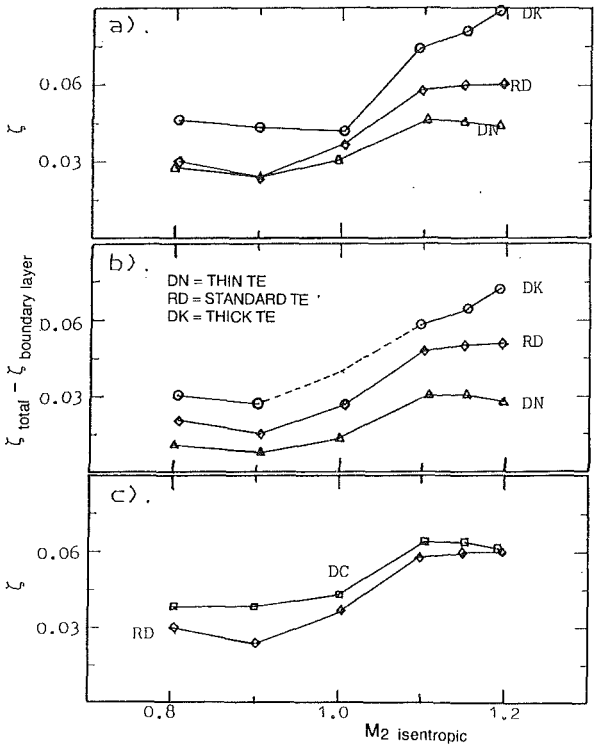


Fig. 26 The variation of loss with Mach number for turbine blades with varying trailing edge thickness, from Xu and Denton (1988)

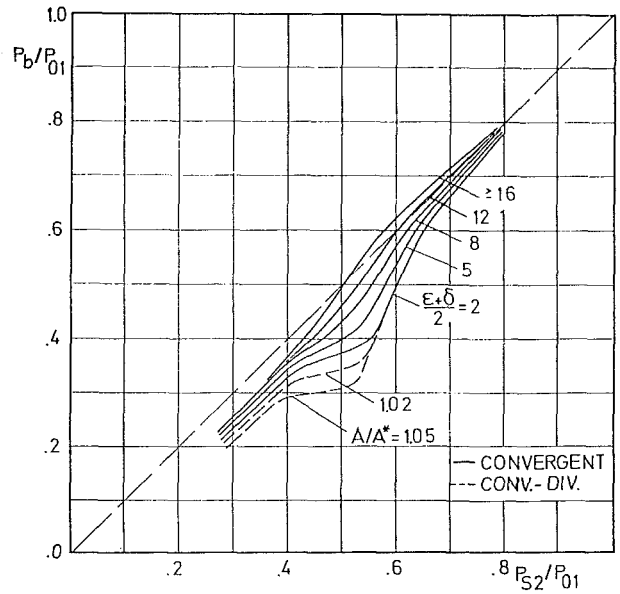


Fig. 27 Sieverding's base pressure correlation for transonic turbine blades

is suggested that this value should be used in Eq. (26) to calculate the mixed out loss of subsonic two-dimensional cascades.

**7.3 Effect of Mach Number on the Two-Dimensional Loss.** The loss of both turbine and compressor blades increases rapidly as sonic conditions are approached. Figure 26 from Xu and Denton (1988), shows typical results for a family of turbine cascades with different trailing edge thicknesses. This figure shows the difference between the overall two-dimensional loss and the measured boundary layer loss, illustrating how much of the loss is arising from the trailing edge. Figure 24 showed a similar result.

For turbine cascades most of the increase can be attributed

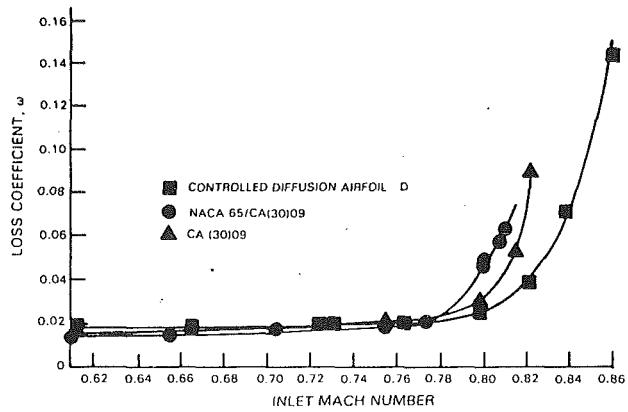


Fig. 28 Profile loss versus inlet Mach number for compressor blades (from Hobbs and Weingold, 1983)

to the trailing edge loss. Figure 10 shows that the base pressure required for zero loss increases rapidly as the exit Mach number approaches unity. The actual base pressure is even more difficult to predict accurately at high exit Mach numbers than it is in subsonic flow but the most widely used method is the correlation by Sieverding et al. (1983), which is shown in Fig. 27. The correlation predicts the base pressure as a function of the far downstream pressure, $P_{s2}$, the change in suction surface slope downstream of the throat $\delta$ and the trailing edge wedge angle $\epsilon$. Surprisingly it does not include any measure of trailing edge blockage. The correlation shows that the base pressure falls below the downstream pressure as the Mach number is increased. The loss will be proportional to the difference between the actual base pressure and the base pressure for zero loss illustrated in Fig. 10.

Chen (1987) presents a correlation for the variation of turbine profile loss with Mach number. This shows the loss rising rapidly as $M_2$ approaches unity but decreasing between $M_2 = 1.0$ and 1.2 before increasing again at higher Mach numbers ($M_2 > 1.2$). Surprisingly the correlation does not include any measure of trailing edge thickness and so it must be assumed to be for blades with thin trailing edges. There is little published experimental evidence for the decrease of loss at high Mach numbers although Denton and Xu (1990) predict the result theoretically and explain it as being due to the expansion from sonic conditions at the throat to the supersonic far downstream flow being matched to the increase in flow area at the trailing edge. A similar result is obtained for blades with converging-diverging passages, which only work well at high supersonic exit Mach numbers.

Figure 28, from Hobbs and Weingold (1984) shows the variation of loss with inlet Mach number for a compressor cascade. The increase of loss in this case is due to a completely different mechanism to that for turbine blades. For conventional compressor blades the peak suction surface velocity is well above the inlet velocity and will reach sonic conditions when $M_1$ is about 0.7. Further increase of $M_1$ causes the peak Mach number and hence the ratio $V_{max}/V_1$ to rise extremely rapidly. In general the sonic region is terminated by a normal shock. Thus the increase in $M_1$ causes shock loss, high suction surface entropy generation (Eq. (41)), and possibly boundary layer separation, all of which contribute to the rapid rise in loss.

Compressor blades specially designed for supersonic inflow delay this loss increase by being very thin and having low or reverse suction surface camber so that the peak suction surface Mach number is not much greater than the inlet Mach number. The lift is obtained from a low velocity on the pressure surface rather than a high one on the suction surface so the boundary layer loss is comparatively low. This, coupled with the high blade loading, means that the shock loss, illustrated in Fig. 13, can be tolerated at least up to the point at which the shock

separates the suction surface boundary layer. This is likely when $M_1$ is greater than about 1.4 (Atkin and Squire, 1992).

There has been much discussion about the relative importance of shock loss and boundary layer loss in supersonic compressor blading and it is sometimes claimed that the shock loss is small relative to the loss in the shock-induced boundary layer thickening and possibly separation. The author's view, based mainly on numerical predictions, is that the magnitudes of the two components are comparable at inlet Mach numbers around 1.4, but that the shock loss becomes dominant at higher Mach numbers. The success of Freeman and Cumpsty's method also supports the idea that the shock loss is dominant. Although, in principle, the shock loss could be greatly reduced by splitting the pressure rise between two shocks (section 5), this does not seem to occur in practical compressor blades.

## 8 Tip Leakage Losses

**8.1 Effect on Blade Lift and Work.** The loss of performance due to leakage of flow over blade tips has been intensively studied for many years. Early methods tended to work in terms of the induced drag on the blades, analogous to the induced drag on an aircraft wing. However, this drag is an inviscid effect. In the case of the wing it produces extra kinetic energy of the surrounding atmosphere but it does not create entropy. Hence, from the point of view of a turbomachine it does not cause loss. More recent studies have concentrated on measuring the tip leakage flow in great detail, e.g., Bindon (1989) for turbines and Storer (1991) for compressors. As a result the flow and loss mechanisms are now well understood for unshrouded blades. Much less work has been done on leakage flow over shrouded blades.

The most obvious effect of flow leakage over the tips of both shrouded and unshrouded blades is a change in the mass flow through the blade passage. At first sight this would seem to lead to a reduction in work for both turbines and compressors. However, considering shrouded blades first because they are simpler, flow will leak upstream over the shroud of a compressor blade. Hence, for a fixed overall flow rate, the mass flow through the blade itself will be increased by the leakage, which will tend to increase the work input but reduce the pressure rise. There will be other factors affecting this, such as a change in deviation caused by the disturbance to the inlet flow when the leakage flow mixes with the mainstream, but the main effect is likely to be an increase in blade work proportional to the leakage flow. For shrouded turbine blades the leakage will be from upstream to downstream of the blade row and so, for a fixed total throughflow, both the blade work and the pressure drop will be reduced. These changes of blade work and pressure difference are independent of any entropy generation or change of efficiency. They would occur in a complete inviscid flow where they would manifest themselves as changes in the mass flow–pressure ratio characteristic of the machine rather than as changes in efficiency.

The situation for unshrouded blades is qualitatively the same, although the interaction between the leakage flow and the mainstream flow is much stronger. In a compressor blade the meridional velocity of the flow leaking over the tips is certain to be less than that of the mainstream flow and may even be directed upstream. Hence, the mass flow through the remainder of the blade must be increased. In a turbine the leakage flow has an increased meridional velocity and forms a strong leakage jet, so the flow through the remainder of the blade must be decreased.

The change in blade work must be reflected in a change of lift, which occurs partly in the immediate vicinity of the tip gap and partly over the whole span of the blade. For unshrouded blades there is always a loss of lift at the blade tip, which occurs both because the blade length is reduced and because the blade loading drops off toward the tip. Both experiments and calculations show that the latter is confined to a very small region not much greater than the tip gap. In fact simple theory, treating the leakage flow as flow through a two-dimensional orifice, shows that the *total* loss of lift at the tip, relative to a blade with no clearance, is given by

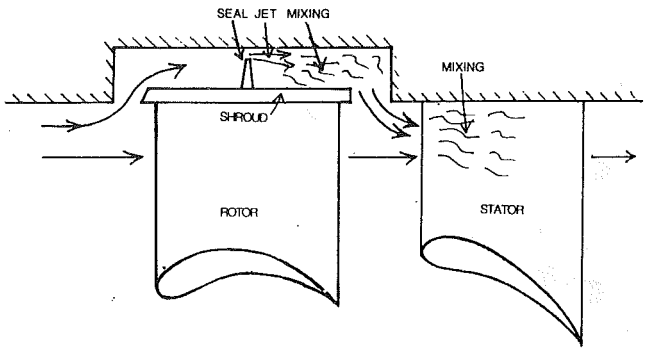


**Fig. 29 Flow over a shrouded tip seal**

$$\Delta L = L_{2d} g \left( \frac{2C_c^2}{1 - 2C_c + 2C_c^2} \right) \tag{49}$$

where $C_c$ is the tip jet contraction coefficient, $g$ is the tip gap, and $L_{2d}$ is the two-dimensional lift per unit span.

The change of lift due to the changed mass flow is, however, not confined to the tip region and numerical calculations show that it affects most of the span. For a turbine blade both these effects contribute to a loss of lift while for a compressor blade the increase in lift over the span is likely to outweigh the loss of lift near the tip. Again it should be emphasized that these changes in lift and work are primarily inviscid and are not necessarily associated with a loss of efficiency.

**8.2 Leakage Loss of Shrouded Blades.** Entropy creation due to tip leakage flows is primarily associated with the mixing processes that take place between the leakage flow and the mainstream. Considering first shrouded blades, the flow over the shrouded turbine blade with a single tip seal is illustrated in Fig. 29. The leaking flow contracts to a jet as it passes through the seal with the area of the jet being lower than the seal clearance by a contraction coefficient whose value is typically about 0.6. If there is no significant restriction upstream of the seal the flow up to the throat of the jet can be considered to be isentropic and so the amount of leakage flow is determined by the seal clearance, the contraction coefficient, the upstream stagnation pressure based on meridional velocity and by the static pressure in the jet. The latter will be influenced to some extent by the method of injecting the leakage flow back into the main flow; however, if there is no further restriction downstream of the seal, this pressure is not likely to be greatly different from the static pressure downstream of the blade row.

The jet mixes out in the clearance space and this mixing process is irreversible, creating entropy. In most practical cases the height of the clearance space is much larger than the leakage jet and so virtually all the kinetic energy associated with the *meridional velocity* of the jet is dissipated. However, measurements by Denton and Johnson (1976) show that the swirl velocity of the leakage flow is not greatly changed during this process and remains roughly the same as that of the flow approaching the blade row.

The leakage flow must now be re-injected into the main flow where the differences in both the meridional velocity and the swirl velocity of the two flows will generate further mixing loss. It can be verified by performing mixing calculations for a flow injected into a vortex that the theory of Appendix 4 for the mixing of a coolant jet can be applied independently to the meridional and swirl components of velocity. Equation (22) shows that the result depends on the angle at which the

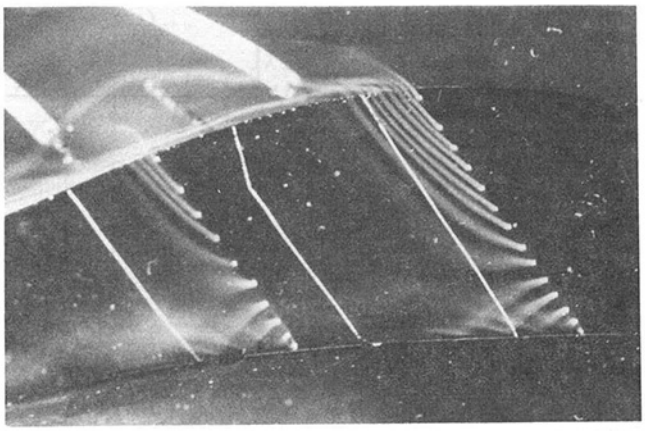

A) Smoke introduced through the blade tip showing reversed flow in the separation bubble

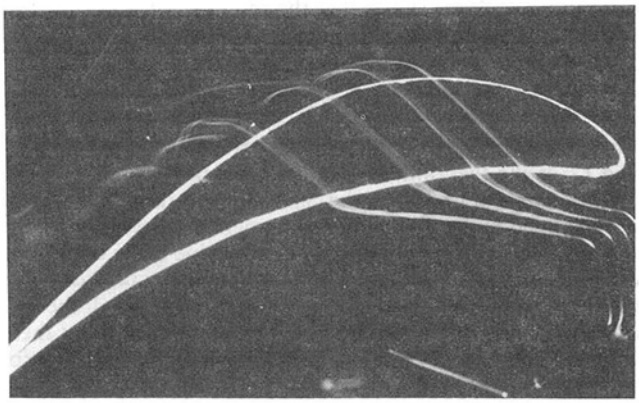

B) Smoke introduced on the pressure surface and passing over the blade tip to form the tip leakage vortex

Fig. 30 Smoke visualization of the flow in the tip gap of a turbine cascade

leakage flow is injected into the mainstream and that the difference in meridional velocity of the mainstream and the injected flow should be as small as possible. However, in most cases the difference in swirl velocity of the two flows is likely to be dominant and this does not depend on the angle of injection. If the leakage flow suffers no change in swirl velocity in the clearance space the difference in swirl velocity will be the same as the change in swirl velocity across the blade row.

A theory for the leakage flow and loss of a shrouded turbine blade, based on the above model, is presented in Appendix 5. The analysis is for incompressible flow but is easily extended to compressible flow by numerical calculations. This theory is based on simplification of an extremely complex flow; however, its predictions have been reasonably well verified by measurements of the flow over a model of a turbine shroud by Denton and Johnson (1976). The predicted rate of change of stage efficiency with tip clearance is also realistic with $d\eta/d(g/h)$ in the range 1.5–2.5, increasing with stage loading and with reaction. It is interesting to note that the theory predicts that any loss of swirl velocity of the leaking flow before it mixes with the mainstream flow, e.g., by friction on the casing, acts to reduce the overall loss. It is also interesting that the overall entropy rise per percent of leakage flow is determined almost entirely by the mixing process downstream of the blade row while the flow processes over the shroud mainly affect the leakage flow rate.

There are few other methods available for estimating the loss of shrouded turbine blades. Came (1969) suggests using the same formula as he recommends for unshrouded blades (a modified form of Ainley and Mathieson's method) but multiplying the result by about 0.9. For shrouded blades with multiple seals the blade pressure drop should be roughly equally

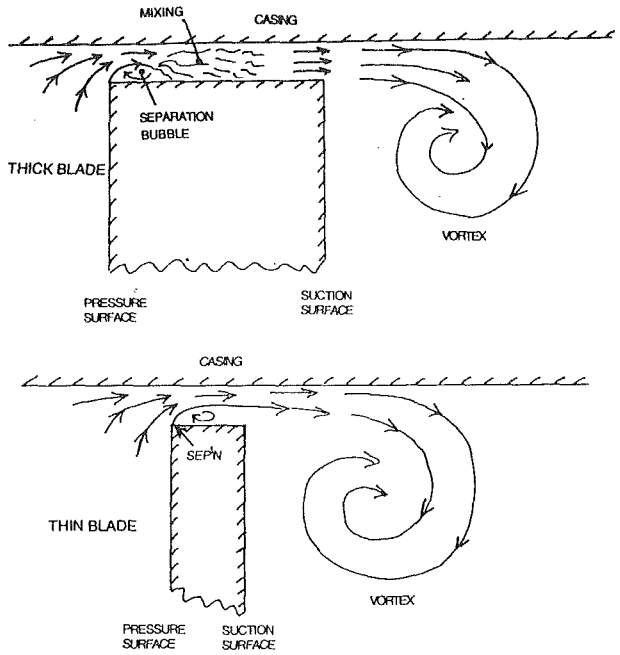


Fig. 31 Flow over the tip gap for an unshrouded blade

divided between the seals (provided that they have the same clearance) and so, for incompressible flow, the resultant leakage and loss should vary inversely as the square root of the number of seals. Came quotes unpublished data suggesting that the loss varies as the number of seals to the power $-0.42$.

There is no known work on the detailed flow processes over shrouded compressor blades. The flow through the seal and clearance space can be assumed to be similar to that described above but the disturbance caused when the leakage flow reenters the main flow upstream of the blade row through which it is leaking is likely to be much more important. This flow will have substantial negative incidence relative to the blade inlet angle and this could cause increased losses in the flow through the blade tip region. However, the disturbance to the flow entering the next downstream blade row should be reduced by the bleeding off endwall fluid to leak upstream over the shroud.

**8.3 Tip Leakage Loss of Unshrouded Blades.** The leakage flow over unshrouded blades has been much more intensively studied than that over shrouded blades. For turbine blades detailed measurements are reported by Bindon (1989), Moore and Tilton (1988), Heyes and Hodson (1993), and Yaras and Sjolander (1992). Bindon's smoke visualization of the flow over the tip using smoke is shown in Fig. 30 and the flow in the tip gap is sketched in more detail in Fig. 31. The flow entering the tip gap from the pressure side of the blade separates from the blade tip and contracts to a jet, with a contraction coefficient of about 0.6. The exact value of the contraction coefficient depends on the radius of the pressure surface corner. The flow up to the throat of the jet is almost isentropic and is not greatly influenced by the component of velocity along the chord of the blade, i.e., out of the paper in Fig. 31. This chordwise velocity may be significant within the separation bubble and convects low-energy fluid to the point of minimum pressure above the tip. However, because the area of the bubble is so small, the mass flow involved is unlikely to be significant.

If the blade thickness is more than about four times the tip gap (Fig. 31*a*), as is usually the case for turbines, the jet mixes out above the blade tip with a consequent increase in static pressure and in entropy. The chordwise component of velocity is substantially conserved during this mixing. The static pressure after the mixing is usually assumed to be the same as that

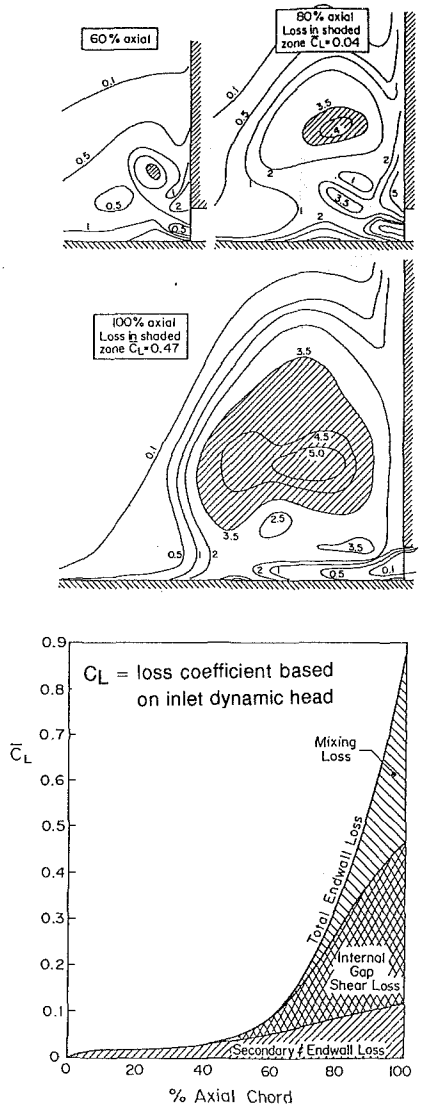


**Fig. 32 The growth of tip leakage loss through a turbine blade passage, from Bindon (1988)**

on the suction surface of the blade. However, some measurements (e.g., Bindon, 1989; Yaras and Sjolander, 1992) show this is significantly lower than the two-dimensional pressure because of the blockage effect of the tip leakage vortex. If the pressure after mixing is known the leakage flow rate and the entropy generation in the tip gap can be obtained by treating the flow as a two-dimensional orifice with a known contraction coefficient (Moore and Tilton, 1988).

The mixing of the leakage flow and the mainstream flow on the suction surface side of the tip gap is another example of the type of mixing process described in section 4 of this paper in which the overall loss can be obtained by applying the global conservation equations. Since the two flows have different velocities, in both magnitude and direction, there is a vortex sheet at their interface, Fig. 30, and this rolls up into a concentrated vortex as the leakage flow moves downstream along the suction surface-endwall corner. However, the overall entropy production in the mixing process is not dependent on the details of this vortex. Equation (22), for the mixing of a jet with a mainstream, can be applied directly and shows that the entropy generation is proportional to the difference in the streamwise velocity of the two flows. If the jet mixes out close to the suction surface, this is effectively the same as the difference between the surface velocities on the suction side and pressure sides of the blade. Figure 32, from Bindon (1989), shows stagnation pressure contours and loss growth through a turbine cascade with tip clearance and illustrates that most of the mixing takes place near the suction surface but that it is not complete at the trailing edge. In a machine mixing will continue through the next blade row and this makes it difficult to make accurate predictions of the overall loss.

The leakage flow over unshrouded compressor blades is not different in principle from that described above for turbines. The main difference arises because the thickness of the blades relative to the tip gap is likely to be much less than for turbines. As a result the leakage jet is unlikely to reattach to the blade tip within the gap, as shown in Fig. 31(*b*). Storer (1991) finds that the jet does not reattach within the gap if the latter is more than about 40 percent of the blade thickness. This means that there is no pressure recovery in the clearance gap and so the discharge coefficient relating the leakage flow rate to the tip gap and pressure difference will be less than for a turbine. Storer finds a typical value of 0.8 for this discharge coefficient.

Equation (22) shows that the *total* entropy production in the mixing process depends on the leakage flow rate and on the difference in the streamwise velocity of the mainstream (suction side) flow and the leakage flow. This velocity difference will be closely the same as the difference in blade surface velocities and so it can be argued that it is not affected by whether the mixing takes place above the blade tip or with the mainstream near the suction surface. Much of the mixing takes place near the suction surface of the blade and for compressor blades this will be a region of decelerating flow, hence the entropy production will be greater than that calculated for mixing at constant area. However, Storer finds that most of the entropy generation takes place near the point of leakage and so this effect may not be dominant.

A simple theory for the tip leakage loss of unshrouded blades based upon the above model is reproduced in Appendix 6. The model is equally applicable to compressors and turbines. It is developed for incompressible flow but is easily extended to compressible flow. The method assumes that the surface pressure distribution is known but for cases where it is not simple approximations to estimate the pressure distribution in terms of the inlet and outlet flow angles and blade solidity are suggested. These approximations take no account of the lowering of the suction surface pressure near the tip by the blockage effect of the leakage vortex.

The only empiricism contained in the theory is a value (usually 0.6) for the contraction coefficient of the leakage jet. Despite this it gives realistic predictions of the rate of change of efficiency with tip clearance. For both turbines and compressors the value of $d\eta/d(g/h)$ is predicted to lie in the range 2.0–3.0, increasing with increased stage loading and with reduced flow coefficient. This is typical of the values quoted by Roelke (1973) for turbines and by Moyle (1988) for compressors.

**8.4 Effect of Relative Motion Between the Blade Tip and Casing.** All known theories for leakage loss neglect the relative motion between the blade tip and the endwall. In a compressor this relative motion is such as to increase the leakage flow and in a turbine it acts to reduce it. The motion may also affect the pressure difference across the blade tip by forming a scraping vortex on the leading surface of the blade. The importance of the relative motion has been investigated by Morphis and Bindon (1988) and by Yaras and Sjolander (1992) all of whom worked on turbine blades. Both found that the general flow pattern over the tip was not greatly affected by the relative motion and that the relative motion increases the pressure on the suction side of the clearance gap. The latter effect acts to reduce the leakage and loss. Yaras and Sjolander found that the discharge coefficient was approximately halved by this effect at full tip speed. This reduction in leakage flow appeared to be caused by the change in the tip pressure dif-

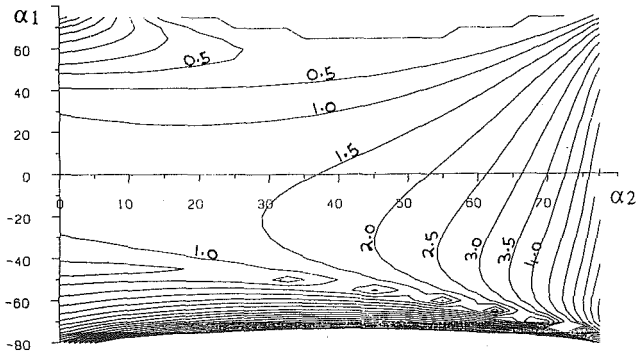


**Fig. 33 The tip leakage loss coefficient of shrouded blades: contours in percent exit dynamic head per 1 percent clearance/height**

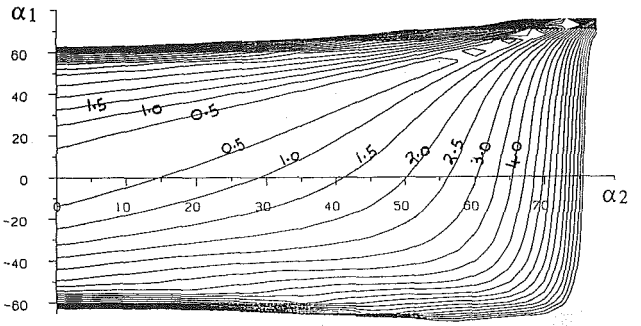


**Fig. 34 The tip leakage loss coefficient of unshrouded blades: contours in percent exist dynamic head per 1 percent clearance/height**

ference rather than a change in the velocity profile within the tip gap. In particular the boundary layer on the endwall within the gap appeared to be *extremely* thin. This implies that theories such as that of Appendix 6 can still be used either with a modified surface pressure distribution or with an empirical modification to the discharge coefficient.

The main weakness of all these methods is the assumption that the mixing between the main flow and the leakage flow takes place immediately after they meet. Equation (23) suggests that most of the mixing takes place very quickly and this is supported by Storer's findings for compressor blades. However, Bindon's results for turbine blades, Fig. 32, show that some of the mixing continues well downstream of the point of leakage. Hence, in practice diffusion during mixing may increase the mixing loss, for both compressors and turbines.

**8.5 Comparison of Shrouded and Unshrouded Blades.** It is of interest to compare the tip leakage loss of shrouded and unshrouded blades. Results from the theories of Appendices 5 and 6 are presented in Figs. 33 and 34. The loss coefficients plotted are those obtained at a tip clearance of 1 percent of blade height and are defined in terms of the blade exit dynamic head, even when the blade represents a compressor. Figure 34 for unshrouded blades is applicable to both turbines and compressors, but Fig. 33 is only really applicable to shrouded turbines. For unshrouded blades the pressure difference driving the leakage flow is that between the pressure and suction surfaces of the blades, while for shrouded blades it is the overall pressure change over the blade tip. For most blade rows these two pressure differences are similar and so, for the same tip clearance, the leakage flow rates will be similar for shrouded and unshrouded blades. However, for low-reaction rotor blades, the pressure drop over the blade row becomes much less than that between the blade surfaces and so shrouded blades will have a lower leakage flow rate.

The leakage flow coefficient depends both on the proportional leakage flow and on the magnitude of the velocity difference between the leaking flow and the mainstream flow with which it mixes. This is the suction side to pressure surface velocity difference for unshrouded blades and the change in swirl velocity across the whole row for shrouded blades. Again these two velocity differences will be comparable for most blade rows but for low-reaction shrouded blades, which have high turning, the overall change in swirl velocity will be larger than the suction to pressure side surface velocity difference.

Hence we may conclude that for most blade rows there is little to choose between unshrouded blades and shrouded blades *with a single tip seal.* For low-reaction blades the situation is less clear since shrouded blades will have a lower leakage flow rate but a greater loss per unit leakage. Only for impulse blades, where the leakage flow drops to zero, do shrouded blades have a decided advantage. This is confirmed by Figs. 33 and 34, which predict that shrouded blades have a slightly lower loss coefficient for most combinations of flow angle but a significantly lower one for near impulse conditions. For most blade rows the real advantage of using shrouded blades comes from the ability to use more than one tip seal.

## 9 Endwall Loss

The term "endwall loss" will be used in preference to "secondary loss" to describe all the loss arising on the annulus walls both within and outside of the blade passage. This is the most difficult loss component to understand and to predict and virtually all prediction methods are still based on correlations of empirical data, often with very little underlying physics. The flow patterns near the endwalls are determined by the secondary flow whose strength depends mainly on the thickness of the upstream boundary layer and on the amount of turning in the blade row. They can be predicted approximately by classical secondary flow theory, or nowadays, more accurately, by numerical calculations. It is important to realize that the secondary flow is an inviscid phenomenon that does not by itself give rise to any entropy generation. Conversely, secondary flow is caused by streamwise vorticity, which is itself a direct result of viscous shear on the endwalls.

For turbines, endwall loss is a major source of lost efficiency, contributing typically 1/3 of the total loss. It is generally accepted that in order to explain observed turbine efficiencies the entropy generation per unit surface area of the endwall must be considerably greater than that on the blade surfaces.

For compressors it is more difficult to separate endwall loss from tip leakage loss and from losses due to flow separation, and some prediction methods make no distinction between the two. The reduced turning of compressor blades tends to reduce the strength of the secondary flows but the thicker endwall boundary layers increase the amount of fluid involved. The fact that the flow is being decelerated makes fluid near the endwalls of compressors prone to separate with consequent major effects on the blockage factor and the stalling point of the blade rows. Overall, the effects of endwall flow and losses in compressors are probably even more important than in turbines. Because of the major differences between them the endwall loss of turbines and compressors will be considered separately.

**9.1 Endwall Loss in Turbines.** Dunham (1970) reviewed the available correlations for turbines and compared them with cascade data. He found very large discrepancies both between the correlations themselves and between the correlations and the data. Based on this survey Dunham and Came (1970) suggested an improved correlation for use in turbines where, in order to predict the correct overall efficiency, they found that it was necessary to use an endwall loss several times greater than measured in cascades. This correlation is still widely used; however, it contains little physics and in fact predicts that the loss is independent of blade solidity while simple physical arguments would suggest that this is one of the most important factors influencing endwall loss. More recent correlations have

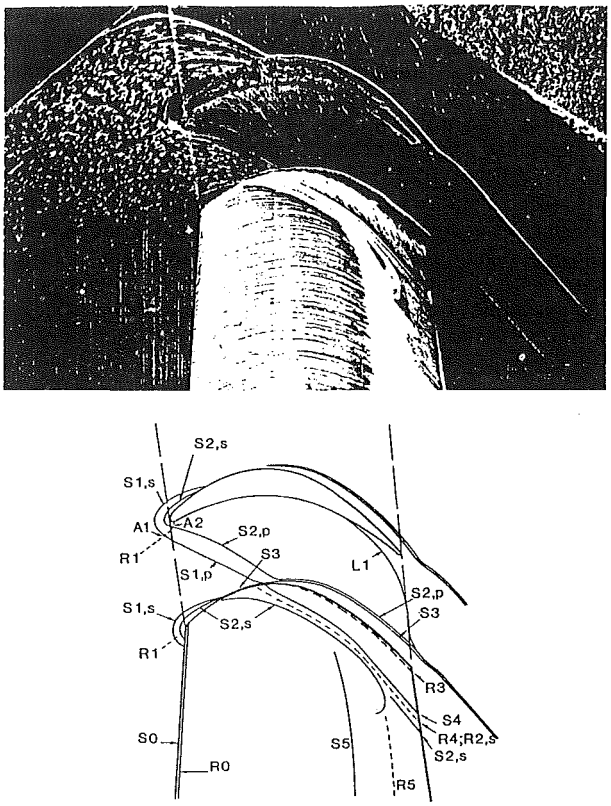


**Fig. 35 Flow visualization on the endwall and suction surface of a turbine cascade from Hodson and Dominy (1985)**

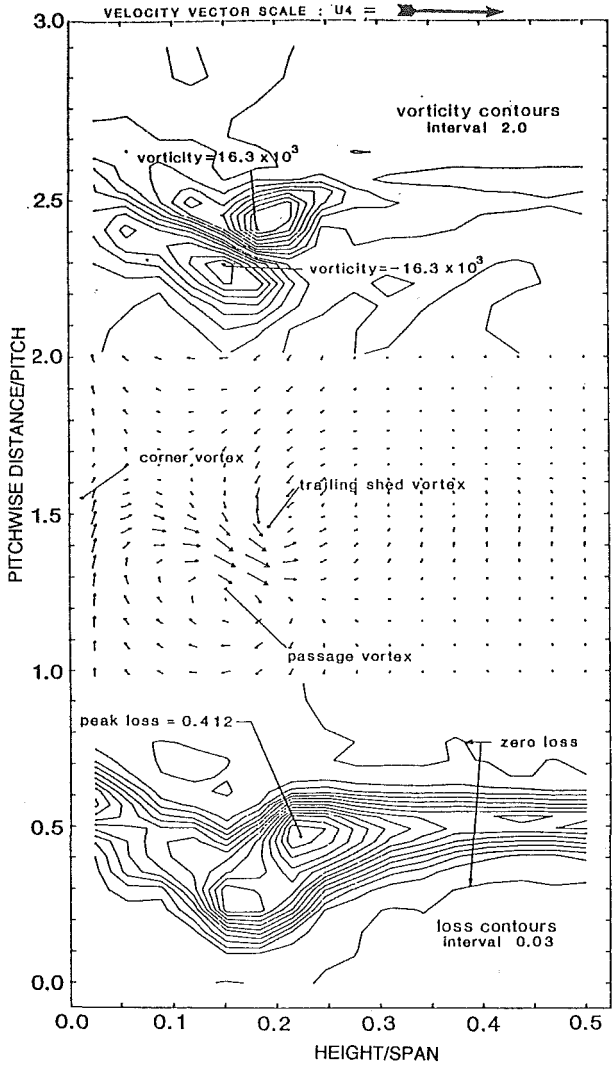


**Fig. 36 Loss coefficient and vorticity contours and secondary velocity vectors downstream of the cascade of Fig. 35**

been produced by Sharma and Butler (1987) and by Gregory-Smith (1982). Both of these include some simple physical modeling of the flow processes and both base their loss predictions partly on simplified endwall boundary layer calculations. Sharma and Butler suggest that the skin friction on the endwall needs to be increased considerably above two-dimensional values (in fact by a factor of about 5) to explain the observed loss, while Gregory-Smith uses a conventional two-dimensional turbulent boundary layer calculation, with no increase in skin friction, and includes an estimate of the secondary kinetic energy as a loss.

The flow processes near the endwall of turbine cascades have been intensively studied and there is an enormous literature on the subject. The first detailed measurements of the secondary flow processes in a turbine cascade were given by Langston et al. (1977) and more recently Sieverding (1985) presented a comprehensive review of the flow processes in cascades. Very detailed measurements of the endwall flow within turbine cascade passages have recently been published by Walsh and Gregory-Smith (1990) and by Harrison (1989). As a result of this and much other work the flow processes near the endwalls of turbine cascades are well understood. Figure 35, from Hodson and Dominy (1987) illustrates some aspects of this complex flow and a brief description of it is necessary if we are to consider the loss-producing mechanisms.

The endwall boundary layer undergoes a three-dimensional separation as it approaches the leading edge stagnation point, giving rise to the well-known horseshoe vortex. The boundary layer fluid is funneled between the two lift-off lines of this separation (e.g., lines $S1,s$ and $S1,p$ in Fig. 35) and is driven toward the suction surface of the blade by the cross-passage pressure gradient. The greater the blade turning and loading the sooner the endwall boundary layer fluid moves onto the suction surface. Once on the suction surface this fluid is driven up it (between lines $S2,s$ and $S4$) by the secondary flow and convected along it by the mainstream flow so that at the trailing edge it appears as a region of high-entropy fluid above the suction surface–endwall corner.

A new endwall boundary layer must grow downstream of the separation lines. Initially this is extremely thin and probably laminar. It is subject to a strong cross-stream pressure gradient and to the "scouring effect" of the secondary flow, both of which make the boundary layer highly three dimensional and try to sweep it toward the suction surface. As a result fluid is continually being removed from this boundary layer and swept onto the suction surface so that the new endwall boundary layer itself stays thin. Harrison (1989) gives detailed measurements of the development of this boundary layer and finds that it remains laminar over much of the endwall. The strong crossflow in the new boundary layer induces a small corner vortex, rotating in the opposite sense to the main passage vortex, in the endwall–suction surface corner. Figure 36 shows results from traverses behind the cascade of Fig. 35 illustrating the loss concentration and the secondary flow vortex.

Downstream of the trailing edge the high-entropy fluid from the upstream boundary layer and the blade wake are both distorted and convected by the passage vortex and gradually mix out with the mainstream flow. In a turbine this mixing is unlikely to be complete before the next blade row. The endwall boundary layer is still very thin at the trailing edge. In a cascade, it continues to grow relatively undisturbed downstream of the blade row and becomes more two dimensional as the passage vortex and the cross stream pressure gradient decay. In a tur-

bine the boundary layer will have to cross the gap separating the stationary and rotating parts of the endwall and will then find itself adjacent to a surface moving with a different velocity before it enters the next blade row. As a result of this change of frame of reference the endwall boundary layers entering all except the first blade row in a turbine will be skewed relative to the mainstream flow. Hence cascade tests, which usually have a comparatively thick collateral endwall boundary layer, may not be representative of conditions in a turbine.

The direction of the boundary layer skew in a turbine is such as to induce negative incidence onto the blade row and so the direction of the relative inlet flow in the boundary layer reinforces the secondary flow. This can also be thought of as being due to the increased streamwise vorticity resulting from the skew. Unless the inlet boundary layer is very thick, the effects of the skew on blade loading are not large and so the local negative incidence does not significantly reduce the cross-passage pressure gradient driving the secondary flow.

The effects of skewing of the inlet boundary layer on the flow and loss have been examined by Bindon (1979), Boletis et al. (1983), and by Walsh and Gregory-Smith (1990). All of them used cascades with moving endwalls and found that the skewing had a large effect on the secondary flow and loss. The latter in particular found that skewing in the direction found in a turbine greatly increased the magnitude of the secondary flow and increased the loss by about 50 percent while skewing in the opposite sense reduced both. The effects of skew clearly need to be included in a realistic turbine prediction method but this is seldom done.

We can now consider the effects of this complex flow on the entropy generation in turbines. The first question that comes to mind is whether the entropy generation per unit surface area of the endwalls can be estimated in the same way as that on the blade surfaces by using a simple approximation to the dissipation factor, $C_d$. As far as is known there are no published results for the dissipation in a boundary layer with strong crossflow. Equation (A1.6) includes the dissipation due to crossflow but it cannot be integrated until the variation of the transverse shear stress through the boundary layer is known. Harrison (1989) makes an estimate of the effects of skew on the dissipation. By using his measured velocity profiles, which have up to 50 deg of skew, and assuming that the distribution of turbulent viscosity is unchanged, he concludes that the skew changes the dissipation by at most 10 percent. This is only a tentative conclusion, but it suggests that the dissipation rate on the endwalls is unlikely to be greatly different from that in a collateral boundary layer with the same $\mathrm{Re}_\theta$. However, the state of the endwall boundary layer is a major unknown and will have a very large effect on the dissipation coefficient. The boundary layer entering the blade row is almost certain to be turbulent but that after the separation line is likely to be laminar with a very low value of $\mathrm{Re}_\theta$. Harrison found that it remained laminar over most of the region near the pressure surface but became turbulent in the higher velocity region near to the suction surface.

If we make the gross assumption that the dissipation coefficient is constant over the whole endwall and obtain the relative velocity from blade to blade calculations, we can integrate Eq. (39) to calculate the entropy production rate. Harrison obtained an average dissipation coefficient of 0.0014 on the endwall of his cascade in this way, i.e., rather less than the value of 0.002 suggested in section 3 for use on the blade surfaces. This is to be expected given that the boundary layer was partly laminar.

A rough idea of the magnitude of the dissipation on the endwalls can be obtained by assuming that the relative velocity varies linearly across the pitch from the suction surface to the pressure surface. If the endwall is not moving relative to the blades the entropy production rate can then be integrated across the pitch to give

$$\dot{S} = 0.25 \int_0^{C_x} \frac{C_d}{T} \frac{(V_s^4 - V_p^4)}{(V_s - V_p)} \rho\, w\, dx \tag{50}$$

where $x$ is the axial distance and $w$ is the local suction to pressure surface gap.

Denton (1990) gives estimates of this integral obtained in a similar manner to the estimates of blade surface loss presented in Fig. 20. However, comparison of Eqs. (50) and (41) shows that for the same value of $C_d$ the average loss per unit surface area on the endwall is predicted to be only about one quarter of that on the blade surfaces. This is because the dissipation varies as the cube of the velocity and only a small area of the endwalls, adjacent to the suction surface, is subject to high velocity levels similar to those on the suction surface. The ratio of the surface area of *both* endwalls to that of the blade suction surface is approximately

$$\frac{A_{\text{wall}}}{A_{\text{suct}}} = \frac{2}{A_r} \frac{C_x}{C} \frac{p}{C} \tag{51}$$

where $A_r$ is the blade aspect ratio based on the true chord. both $C_x/C$ and $p/C$ are likely to be about 0.75 and so the ratio of areas is of the same order as the reciprocal of the aspect ratio. Hence Eqs. (41) and (50) predict that at an aspect ratio of unity the entropy generation on the endwalls within the blade row would be only about 1/4 of that on the blade surfaces. In fact at this aspect ratio the total endwall loss is usually considered to be comparable to the blade surface loss. Hence, even allowing for a slightly increased value of $C_d$ due to the skewing and low $\mathrm{Re}_\theta$ it seems unlikely that entropy generation in the boundary layer within the blade row can explain the observed magnitude of turbine endwall loss.

The endwalls downstream of a turbine blade are subject to the full blade exit velocity and so their entropy generation rate per unit area will be comparable to the maximum value on the suction surface. In a turbine these downstream endwalls typically extend about 1/4 of an axial chord behind the blades before the relative velocity between the flow and the wall is reduced by the change from stationary to rotating walls, or vice versa. Thus the entropy generation in this region is comparable to that on the endwall within the blade row. This is a significant loss component, which can only be reduced by minimizing the area of endwall exposed to the full blade exit flow velocity.

The endwalls upstream of a turbine blade are subject to the relative inlet velocity, which is usually significant less than the exit velocity. The axial extent of these walls is unlikely to be more than about 1/4 of an axial chord and so the entropy generated in the inlet boundary layers is usually much less than that on the downstream endwalls. Hence it seems that the total entropy generation in the endwall boundary layers, upstream of, within, and downstream of the blade row can only explain about 2/3 of the observed endwall loss.

There is a good deal of evidence, summarized by Sharma and Butler (1987), that the endwall loss generated within the blade row, i.e., the total loss minus the loss present in the inlet boundary layer, remains almost constant as the thickness of the inlet boundary layer is changed. This implies that the loss generated by the mixing out of the inlet boundary layer within the blade row is small. On a one-dimensional basis this mixing takes place in an accelerating flow so the mixing loss should be reduced. However, secondary flow and inlet skew produce streamwise vorticity and streamwise acceleration amplifies this and increases the kinetic energy associated with it. This is often called secondary kinetic energy (s.k.e.).

Kinetic energy is a relative quantity and so care is needed in defining exactly what is meant by s.k.e. It is usually taken to be the kinetic energy associated with the velocity component perpendicular to some primary flow direction, but exactly how this direction is defined is arbitrary. The production of s.k.e. by secondary flow is an inviscid process and so is not initially

a loss. Classical secondary flow theory (Hawthorne, 1955) predicts that there is a value of the ratio of inlet boundary layer thickness to blade pitch that maximizes the s.k.e., but it is not known how well this applies to real flows with large disturbances. The s.k.e. also increases with blade turning and with inlet boundary layer skew. Some of the s.k.e. arises from the inviscid secondary flow induced by the inlet boundary layer and some of it comes from the secondary flow induced by the new endwall boundary layer. Comparison of results from viscous and inviscid calculations suggests that most of the secondary flow is generated by the inlet boundary layer and in fact viscous effects within the blade row appear to reduce its strength slightly.

When the mean flow is accelerated, the s.k.e. of a streamwise vortex increases and it can be shown that in inviscid flow the s.k.e. is proportional to the square of the length of the vortex. It is known that dissipation within a vortex core is very high and so the subsequent decay of this s.k.e. leads to an increase in entropy. Hence vortex stretching provides a mechanism for the generation of high endwall losses in highly accelerating blade rows. Some of the dissipation within the vortex core occurs within the blade row and will be measured as a loss at the trailing edge. However, the dissipation continues downstream of the blade row and it is often assumed that all the s.k.e. of the vortex at the trailing edge is lost. Gregory-Smith's method of estimating the loss assumes this. The magnitude of the s.k.e. in cascades has been measured by many workers. Its value is typically in the range 0.2–0.50 of the endwall loss present at the trailing edge.

The flow downstream of a trailing edge has been studied in detail by Moore and Adhye (1985) who found that the decay of s.k.e. as the flow progressed downstream from the trailing edge closely matched the increase in entropy. The mixing loss downstream of a trailing edge can of course be calculated by applying the conservation equations between the trailing edge flow and a completely uniform mixed out downstream flow. This is often done in presenting cascade results. However, a completely uniform mixed out flow is not representative of what happens in a machine where spanwise variations in the circumferentially averaged flow decay slowly and will certainly remain at entry to the next blade row. They will be seen by this row as a spanwise variation in average inlet angle, which will be reflected in the blade work. Hence they are not a loss, and cascade measurements based on a completely uniform mixed out downstream flow will overestimate the endwall loss. The pitchwise variations in flow decay more rapidly than the spanwise variations (as found by Moore and Adhye) and it is not obvious whether they can be used by a following blade row.

The interaction between a secondary flow vortex (or a tip leakage vortex) and a downstream blade row is an extremely difficult problem that has not been widely researched. Some results are available from Sharma et al. (1992) and from Binder (1985). These illustrate the complexity of the unsteady flow but they tell us little about loss. The possibility of the highly dissipative process known as vortex breakdown occurring in turbomachines deserves investigation.

To summarize the loss-producing mechanisms associated with a turbine endwall we may say that the total loss is a combination of many factors. About 2/3 of it comes from entropy generation in the annulus wall boundary layers within, upstream of, and downstream of the blade row. When turned into a loss coefficient, this will vary inversely with aspect ratio as illustrated by Eq. (51). A further part comes from mixing loss of the inlet boundary layer, which is amplified by the secondary flow and will give a loss coefficient proportional to the ratio of inlet boundary layer thickness to span but which is an unknown function of blade load and turning. A third component is the loss associated with the s.k.e., which is of the order of 1/4 of the total endwall loss. This proportion will depend on inlet boundary layer thickness and skew and on blade turning and blade loading but there are no simple theories relating the loss to any of these factors. The proportion of the s.k.e. that is lost is also not yet predictable. Other contributions to endwall loss may come from local flow separations and from thickening and premature transition of the blade surface boundary layers as a result of the secondary flow. In all the situation is too complex and too dependent on details of the flow and geometry for simple quantitative predictions to be made. The main hope in the near future is that the loss can be quantified by three-dimensional Navier–Stokes solutions, which already give good qualitative predictions of the flow.

**9.2 Endwall Loss in Compressors.** The endwall flow in a compressor cascade has been less intensively studied than that in a turbine, possibly because the flow in a cascade is less relevant to that in a real machine than is the case for a turbine. The major differences between the endwall flows in compressors and turbines are that the blade turning is much less, the endwall boundary layers are much thicker relative to the blade chord, and the boundary layers are being decelerated. The first two of these factors tend to make the secondary flow less intense but the last tends to amplify it. The endwall losses are, if anything, more important in compressors than in turbines and Howell's (1945) well-known graph of the breakdown of losses in a typical axial compressor shows about 2/3 of the loss due to "annulus loss" and "secondary loss" at design conditions.

Cumpsty (1989) points out clearly that the endwall boundary layers cannot be considered as conventional boundary layers during their interaction with a blade row. The overall thickness of the endwall boundary layer in a multistage compressor is typically half the blade chord, hence the pressure changes take place in a few boundary layer thicknesses, which is very much more rapid than those considered by conventional boundary layer theory. This means that viscous forces play relatively little part in the flow behavior, which is likely to be more like that of an inviscid shear layer than a boundary layer. If we assume that a compressor blade has a collateral endwall boundary layer with a free-stream inlet velocity $V_1$ and an exit velocity $V_2$, then on a one-dimensional, incompressible and inviscid basis, all the fluid in the inlet boundary layer with a velocity less than

$$V_{sep} = V_1\sqrt{1-(V_2/V_1)^2} \tag{52}$$

must separate within the blade row. At a typical value of $V_2 = 0.7\,V_1$ this implies that all fluid with velocity less than about 30 percent of the inlet free-stream velocity would separate. In practice this fluid does not separate in the conventional two-dimensional sense. As it decelerates, it becomes more susceptible to the cross-passage pressure gradient, which is driving the secondary flow, so that before its meridional velocity becomes zero it has acquired a component of velocity toward the suction surface. On reaching the suction surface–endwall corner this high entropy fluid accumulates and is further decelerated by the overall pressure rise to form the large corner separation that is almost invariably seen in compressor cascades. This separation is responsible for much of the blockage observed in compressor blade rows. Its effects may not be localized and it can interact with the suction surface boundary layers to cause separation over much of the blade span. Figure 37 (zero tip clearance case) shows an example of such a separation in a compressor cascade.

The above behavior applies directly to cascade flows with collateral inlet boundary layers; however, in an actual compressor the picture is altered by the effects of skewing and tip leakage. In a compressor the lower meridional velocity in the annulus boundary layer causes positive incidence onto the blades and so directs the relative velocity of the boundary layer fluid toward the pressure surface. In unshrouded blade rows

the relative motion of the endwall within the blade passage enhances this effect. The increase in *relative* tangential velocity within the skewed boundary layer may be greater than the deficit in meridional velocity so that the endwall fluid can have higher *relative* stagnation pressure than the mainstream flow. Both these factors act to oppose the conventional secondary flow. For rotor tip sections, where the blade turning is low, the effect of skewing is likely to dominate and drive the endwall fluid toward the blade pressure surface. Here it will enter a region of favorable pressure gradient and so may cause less harm than if there were no skew. For rotor hub and stator tip sections the blade turning is greater and so the effects of secondary flow usually dominate those of skew and the endwall boundary layer fluid ends up on the suction surface–endwall corner where it is likely to cause separation.

The interaction between tip clearance and the endwall flow can have a dominant influence in compressors with unshrouded blade tips. The tip leakage flow directs a jet of high-velocity fluid from the pressure surface into the suction surface–endwall corner where the high-entropy inlet boundary layer fluid tends to concentrate. This may succeed in re-energizing the boundary layer fluid sufficiently to prevent the corner separation with a consequent reduction of loss. This interaction accounts for the observation that in some compressors there is an optimum tip clearance that gives higher efficiency than either zero clearance or larger clearances. This corresponds to the leakage flow being just sufficient to prevent the corner separation but not sufficient to generate a large tip leakage loss. This phenomenon has been studied in detail in cascade by Storer (1991), some of whose results are shown in Fig. 37.

If compressor endwall boundary layers remain attached the entropy generation per unit surface area of the endwalls can be estimated from Eq. (50). In fact, because the $\mathrm{Re}_\theta$ of the endwall boundary layer is so large it is possible that the dissipation per unit surface area may be somewhat less than on the blades. Storer measured an endwall loss of about the same magnitude as the profile loss on his compressor cascade with no tip clearance and infers a similar level when tip clearance is present. However, if this were always the case compressors would be much more efficient than they are in practice.

The effects of endwall flow on the loss of compressor blades are believed to be dominated by mixing and by the promotion or suppression of separations. The mixing loss in the endwall boundary layer will be increased because of the diffusing flow and the very large increases of mixing loss, shown by Fig. 11 at typical levels of compressor blade diffusion, would correspond to the endwall boundary layer separating. As described above this separation will be highly three-dimensional and so cannot be predicted by the usual diffusion factor arguments. Once a separation occurs it will mix out partly within the blade passage and partly downstream. Storer's results, Fig. 37, show that the mixing is far from complete half a blade chord behind his cascade.

The interblade row gap is so small in most axial compressors that it is likely that much of the mixing takes place in the unsteady environment of the downstream blade row. Even for mixing within and immediately downstream of the blade row there is no satisfactory theory to calculate the entropy generated by the mixing out of a separation. When mixing occurs in the downstream blade row the situation is even less predictable.

There are comparatively few published methods for predicting endwall losses in axial compressors. Howell (1945) distinguished between annulus loss and secondary loss and predicted each of them in terms of a drag coefficient. However, the expression for annulus loss does not include the surface area of the annulus and the secondary loss is based on the induced drag of a wing tip vortex, which, as previously noted, is an inviscid phenomenon. Hence, although Howell's method has been widely used for many years, it cannot be said to be

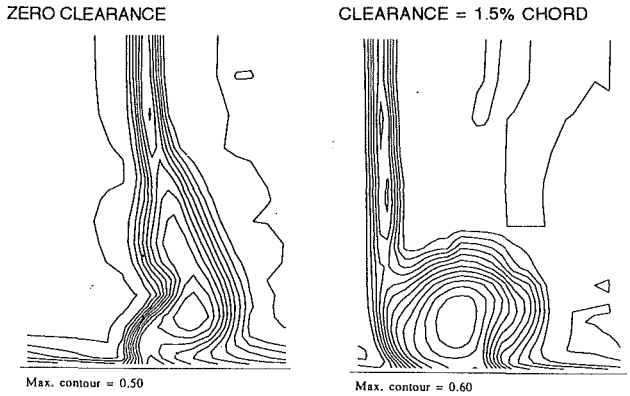


**Fig. 37 Loss contours near the endwall of a compressor cascade with and without tip clearance**

related to the physics of the flow. Koch and Smith (1976) use a method that is described in more detail by Smith (1970). Their method is based on the concept of a repeating stage for which one can use the definition of efficiency in the form

$$\frac{\Delta\eta}{\eta} = \frac{\Delta m}{m} - \frac{\Delta T_q}{T_q} \tag{53}$$

where $T_q$ is the blade row torque, to relate changes of efficiency relative to a stage with no endwall loss to changes of mass flow and to changes of blade tangential force. The change of flow is found from the endwall boundary layer displacement thickness, which is correlated against the ratio of tip clearance to staggered gap, and the pressure rise as a fraction of maximum pressure rise. The change of torque is found from the tangential force defect in the tip region, which is correlated as a function of the displacement thickness and pressure rise. Equation (53) is thereby effectively a vehicle for correlating the annulus boundary layer displacement thickness and tangential force deficit thickness. The method is useful in including the effects of tip clearance, endwall loss, and blockage in a single method and it includes some of the physics of the endwall flow. However, it cannot pretend to allow for the complexities of the real flow and so can only be used reliably when experimental data on similar designs are available.

Several methods that calculate the annulus boundary layer displacement thickness via a two-dimensional boundary layer calculation along the whole endwall of a compressor have been published (e.g., de Ruyck and Hirsch, 1983). These use conventional boundary layer theory and in view of what has been said about endwall boundary layer behavior in compressors this must be regarded as dubious. However, they also include considerable empiricism, including correlations for the tangential force defect, and so are able to give reasonable predictions.

Despite these criticisms of current compressor endwall loss prediction methods the author cannot offer any alternatives that will be generally valid. The flows are so complex and depend so much on the details of the geometry and of the incoming boundary layers that it is hard to believe that anything other than three-dimensional Navier–Stokes calculations can give general results. It is hoped that an understanding of the loss mechanisms will bring about improvements in design but at present these can only be quantified by experiment.

## 10 Application to Radial Flow Machines

Most of discussion so far has been in the context of axial flow turbomachines. Many of the ideas presented are directly applicable to radial flow turbines and compressors but there are significant differences in the relative importance of the various loss mechanisms. These will be discussed in this section.

Both radial inflow turbines and centrifugal compressors typically have a stage loading coefficient, $\Delta h_o / U_{\mathrm{tip}}^2$ around unity,

where $U_{tip}$ is the maximum blade speed. This means that for both types of machine the change in $V_\theta$ is comparable to $U_{tip}$. The major difference from axial flow machines arises because the blade speed $U$ varies considerably through the rotor. This causes the change of *relative* velocity through the rotor to be less than that in an axial flow machine with the same $U_{tip}$ and $\Delta h_o$. Hence, in a centrifugal compressor we can produce the same enthalpy rise with less diffusion of the relative flow in the rotor, and in a radial inflow turbine we can produce the same enthalpy drop with less acceleration, than in a comparable axial machine. However, in both cases the change in absolute velocity through the stators is comparable to that in an axial flow machine with the same enthalpy change.

The lower change in relative velocity through the rotor is particularly advantageous for compressors since it is the diffusion of the *relative* velocity that brings about boundary layer growth and separation. Hence centrifugal compressors can obtain much higher pressure ratios for the same rotor diffusion factor than can axial compressors. In effect most of the pressure rise is being balanced by the centrifugal force field rather than by deceleration of the relative velocity. In radial inflow turbines the reduced change in relative velocity means that higher pressure ratios can be obtained before choking, and without the losses associated with transonic flow, than is possible in axial turbines.

As regards entropy generation: In both types of machine, the average relative velocity through the rotor will be less than that in an axial flow machine with the same $U_{tip}$ and $\Delta h_o$ while that through the stator will be comparable to that in the axial flow machine. On this basis one would expect radial flow machines to be more efficient than comparable axial flow machines while in practice they are generally accepted to be slightly less efficient. The discrepancy is probably due to the more complex geometry inherent in the change of flow direction from axial to radial and vice versa. This involves a 90 deg bend, which causes stronger secondary flows than in most axial machines and also a decrease of blade span with radius, which means that radial flow machines are usually of relatively low effective aspect ratio. In comparing them with axial machines we should choose machines of comparable aspect ratio (or specific speed) and on this basis their efficiency is not obviously lower.

**10.1 Radial Inflow Turbines.** Radial inflow turbines usually have stator blades located in a flow where the meridional velocity is radially inward, although in small turbochargers a vaneless volute may be used to accelerate the flow. The flow through the stator blades is highly accelerating and, because of the decrease in radius the blade throat is close to, or even behind, the trailing edge. Hence blades can be designed with little or no suction surface diffusion. This means that the boundary layers on the stator may be largely, or even completely, laminar and so very low levels of loss can be achieved. In fact most of the two-dimensional loss may arise from the trailing edge, which should therefore be kept thin relative to the blade throat. The endwall loss per unit surface area should also be small but the aspect ratio is usually low and so the total endwall loss may be significant. Huntsman (1993) measured a profile loss coefficient of 1.2 percent and an overall loss coefficient of 3.3 percent for his stator blade. Both of these are very low relative to comparable values for an axial flow turbine.

The annulus boundaries in the gap between stator and rotor are subject to the highest relative velocity in the machine and so this gap should be kept as small as is possible, subject to mechanical constraints. The velocity *relative* to the rotor is low at entry, but if the rotor is unshrouded, that relative to the casing continues to be high until well into the rotor passage. This will generate large amounts of entropy on the casing, which will be transported toward the casing–suction surface corner by both the relative motion of the casing and by the secondary flow. Shrouded rotors should generate less loss in this region. Farther into the blade passage the curvature of the radial-axial bend generates low pressures on the casing that drive the blade surface boundary layers toward the casing. Hence most of the high-entropy fluid ends up in the suction surface–casing (or shroud) corner where, in unshrouded rotors, it mixes with the tip leakage flow.

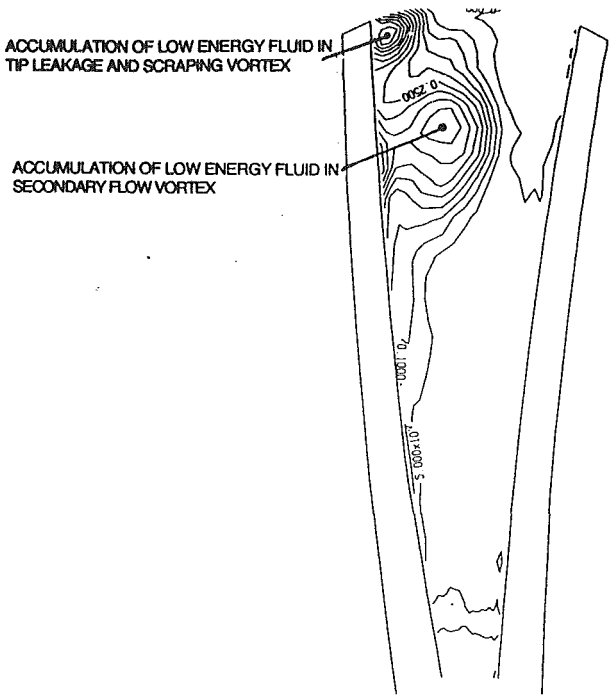


**Fig. 38 Contours of relative stagnation pressure at exit from a radial inflow turbine (from Huntsman, 1993)**

The entropy generation on the blade surfaces will increase rapidly as the relative velocity increases toward the blade exit. For a shrouded blade the loss on the shroud will increase similarly but for an unshrouded blade the casing loss will decrease as the velocity of the flow relative to the casing reduces. Hence, from the point of view of efficiency, it would be most beneficial to have a partly shrouded blade with a shroud only over the upstream part of the bladed passage.

For unshrouded blades tip leakage loss is likely to be more important than in an comparable axial flow machine because the low aspect ratio means that the ratio of leakage flow area to blade throat area is large. However, the relative motion of the thick casing boundary layer and blade tip will generate a scraping effect that will oppose the leakage. For shrouded blades the leakage should be very small because of the radial pressure gradient set up in the swirling leakage flow. In this case the windage loss of the shroud may be more significant than the loss due to tip leakage.

Trailing edge loss will be significant for many radial flow turbines, which, because of stressing problems, tend to have very thick trailing edges, especially near the hub where the blockage may approach 50 percent. Thus, although the rotor relative exit velocity is lower than in a comparable axial machine, the trailing edge loss may be greater. The spanwise pressure gradient resulting from the meridional curvature of the streamlines at the trailing edge is likely to produce considerable spanwise flow in the base region. The effect of this on the base pressure and trailing edge loss is not known.

Figure 38 shows contours of relative stagnation pressure measured downstream of the rotor of Huntsman's unshrouded radial inflow turbine. The accumulation of high-entropy (low-energy) fluid on the blade suction surface toward the tip can be seen, as can that in the tip leakage/scraping vortex. This

turbine, which was designed using three-dimensional calculation methods, has an efficiency of about 93 percent, comparable to that of a good axial flow machine.

**10.2 Centrifugal Compressors.** Centrifugal compressors usually have axial inlet flow and radial outflow. The velocity of flow relative to the rotor is greatest near the tip at inlet, where it may be supersonic for high-pressure-ratio machines. Because the blade turning is much larger than in transonic axial compressors supersonic inflow can lead to very high Mach numbers and strong shocks within the inducer if it is not designed very carefully. The relative velocity decreases through the rotor and is usually comparatively modest at rotor exit. High-pressure-ratio compressors produce a large increase in density within the impeller so the meridional flow area must decrease, and the blade height decrease even more, to accommodate this. The effective aspect ratio, i.e., the mean blade height divided by the meridional chord, is of order 1/3 for many centrifugal impellers, this is much lower than in most axial flow compressors, and this should be borne in mind when comparing the two.

The flow within the impeller is now well understood, and is always highly three dimensional. The axial to radial bend induces strong secondary flows convecting the blade surface boundary layers toward the casing. Similarly the blade loading induces secondary flows convecting the hub and casing boundary layers toward the suction surface. In unshrouded impellers the latter is opposed by the relative motion of the casing. The net result is usually that a large concentration of high-entropy fluid collects in the vicinity of the casing-suction surface corner and it is this that forms the well-known jet-wake structure at the exit of the impeller. Figure 39 shows results from a numerical calculation predicting the growth of this wake through a shrouded impeller.

In unshrouded impellers the velocity of the flow relative to the casing is comparatively low at inlet and increases toward impeller exit where it becomes larger than the maximum blade surface relative velocity. Consequently the entropy generation on the casing of unshrouded blades is large while that on the rotating hub is much less. For shrouded blades the velocity relative to the shroud is always comparable to that relative to the blade surfaces and so decreases toward impeller exit. Hence, from the point of view of efficiency it would be preferable to have a shroud over the rear part of the impeller but to leave it unshrouded at inlet.

Despite these regions of high loss, the efficiency of the impeller alone is usually very high because the relative velocities are low compared to the enthalpy rise. Moore and Moore (1980) quote an impeller efficiency of 95.4 percent for Eckardt's low-pressure-ratio centrifugal impeller. The overall machine efficiency is much less than this because most of the entropy increase takes place downstream of the impeller.

Immediately downstream of the impeller there is usually a short vaneless space. The wake from the impeller starts to mix out in this space and the associated mixing loss can be calculated by applying the conservation equations, provided that the size and depth of the wake at the impeller exit are known. These may be obtained from either correlations or from numerical calculations. The methods available for this mixing calculation are reviewed by Cumpsty (1989) who concludes that the effect of the mixing loss on the overall efficiency is usually small. Since the swirl component of velocity leaving the impeller is much greater than the radial component most of the mixing loss arises from the difference in swirl velocity between the wake and the main flow. In practice it is unlikely that the mixing is complete before the flow enters the diffuser blades thus making the flow into them highly unsteady.

The flow leaving the impeller has a high velocity relative to both the hub and the casing; in fact this is the highest relative velocity anywhere in the machine and entropy generation on

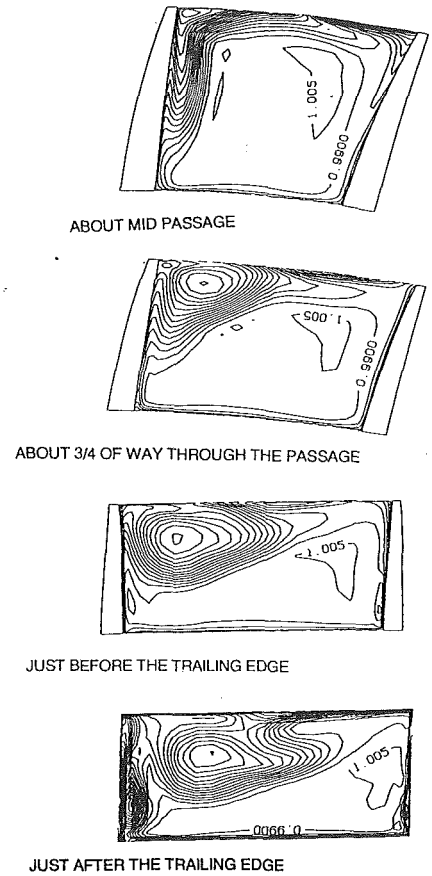


**Fig. 39 Growth of the wake through the impeller of a centrifugal compressor; contours of entropy**

the walls of the vaneless space will be extremely high. Moore and Moore (1980) found that more than half the entropy rise in Eckardt's compressor occurred in the vaneless diffuser. Figure 40 shows numerical predictions of entropy growth on and downstream of a shrouded impeller illustrating the high loss on the shroud at rotor inlet and especially on the walls of the vaneless space. This result implies that for machines with vaned diffusers the length of the vaneless space should be kept as short as possible and there is a strong case for having rotating walls in this region if practicable.

There is a large radial pressure gradient in the vaneless space that arises mainly from the centripetal acceleration of the highly swirling flow. Because the meridional velocity is much less than the swirl velocity (the swirl angle is typically 70 deg), this pressure gradient has a disproportional effect on the radial velocity, tending to make it reverse near the endwalls. Numerical calculations predict this separation to be very prevalent (e.g., Krain and Hoffman, 1989) but although it has been measured (Inoue and Cumpsty, 1984) the effect does not seem to be as common as predicted. This must be because the mixing processes are more intense than are predicted by numerical solutions, which implies enhanced dissipation in the vaneless space. This effect is especially important for machines with vaneless diffusers.

The concept of entropy generation per unit surface area provides a particularly simple method for estimating the losses in the vaneless space. Simple analysis gives a loss coefficient, based on local velocity, of

$$\zeta = \frac{4\, C_d\, \Delta r}{h \cos \alpha} \tag{54}$$

where $h$ is the passage height, $\Delta r$ is the radius change, and $\alpha$ is the swirl angle. This is the same result as obtained from the conventional analysis using skin friction if $C_d = 0.5\ C_f$. Equa-

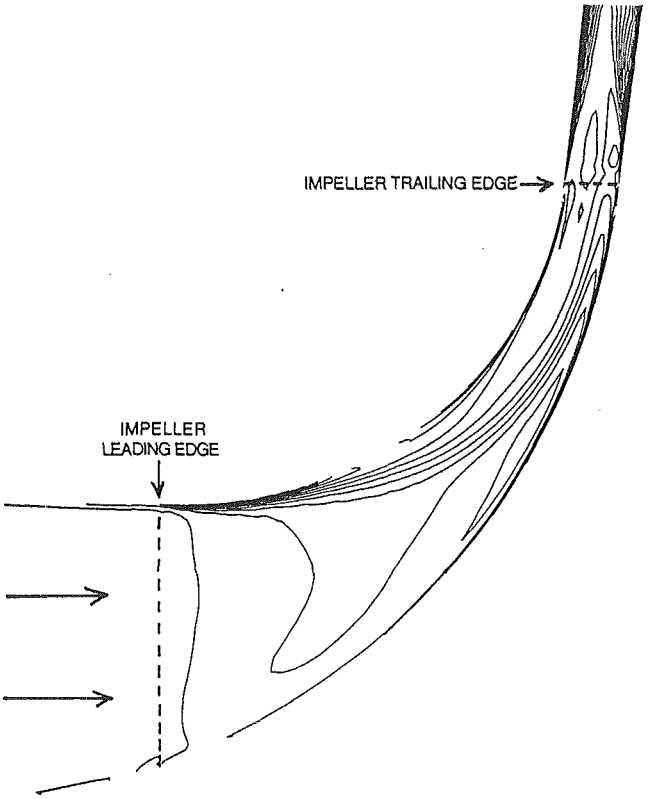


Fig. 40 Calculated loss generation in a centrifugal compressor; contours of pitchwise-averaged entropy

tion (54) explains why the loss increases with the swirl angle as observed in practice. They value of $C_d$ must be found experimentally and is likely to be larger than is usual in two-dimensional boundary layers because of the highly three-dimensional nature of the flow.

The stator or diffuser blades have the most difficult task in a centrifugal compressor. The pressure rise in the impeller can be produced without excessive diffusion but the diffuser blades must produce a comparable pressure rise by diffusion alone. This is made more difficult by the fact that the flow entering them is nonuniform, unsteady, and possibly transonic. Some of the pressure rise occurs in the semivaneless space before the throat of the diffuser and the entropy generation here must be a continuation of the high level in the vaneless space itself.

The leading edge of the diffuser blades is invariably thin and this makes the effects of incidence very important. The velocity at the throat of the diffuser can be estimated from the mass flow rate and the stagnation conditions at its entry. At low flow rates this velocity will be much less than the flow velocity approaching the diffuser; the flow must then separate at the leading edge so that the resulting separation partly blocks the throat and increases the throat velocity. This is a separation in a relatively high-speed part of the flow and will create a large mixing loss. In transonic flow there will also be shock losses in this region. Morishita (1982) found that intense turbulent viscous dissipation occurred in the vicinity of his subsonic leading edge but that once inside the diffuser passage the flow was comparatively well ordered. He estimated that, even at design conditions, the entropy generation around the diffuser leading edge was the major cause of lost efficiency in the whole machine. Conversely, at high flow rates the flow must accelerate into the diffuser throat, possibly causing choking but certainly increasing the losses in the diffusion downstream of the throat.

The flow downstream of the diffuser throat is like that in a conventional two-dimensional diffuser with entropy generation in the boundary layers being greatest in the high-velocity region near the throat. However, the major source of entropy is likely to come from separation and the subsequent mixing of the boundary layers toward the exit of the diffuser. If the separation does not have time to mix out within the diffuser passage it will increase the kinetic energy of the flow leaving the diffuser. This kinetic energy may be either dissipated by discharging directly into a plenum or it may be partly recovered in a volute.

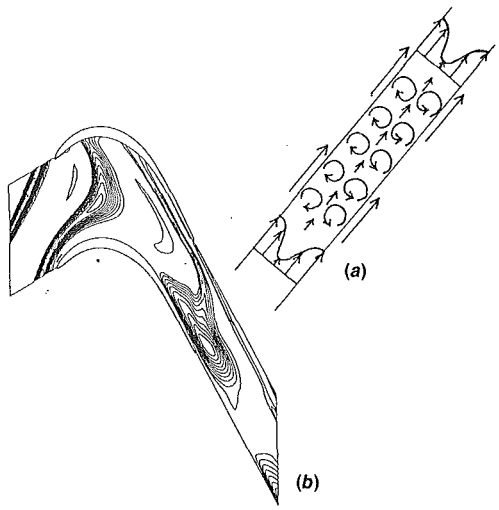


Fig. 41 (*a*) The wake as a vortex sheet; (*b*) the convection of a wake through a blade row; contours of entropy

## 11 Other Sources of Loss

There are numerous other sources of loss in turbomachines; most of them are small in most applications but can become significant in special cases. The most important of these will be discussed briefly in this section. More details of all but those due to unsteady effects can be found in Chap. 8 of Glassman (1973).

**11.1 Loss Due to Unsteady Flow.** The fact that wakes, vortices, and separations from one blade row often mix out in the downstream blade row has been mentioned several times in this paper. As they convect through the downstream row their pressure and velocity change continually so that they mix in an unsteady environment, quite different from that modeled in cascade tests. For a wake the effect of this on the dissipation can be thought of qualitatively in terms of the effect on the velocity difference between the center of the wake and the mainstream.

A two-dimensional wake can be thought of as being contained between two vortex sheets (Smith, 1966); this is illustrated in Fig. 41(*a*). The velocity difference between the center of the wake and the mainstream determines the strength of the sheets. Neglecting viscosity, as the wake convects the circulation in the vortex sheets bounding a fixed quantity of fluid must remain constant (by Kelvin's theorem) and so if the wake is stretched the velocity difference between its centerline and the mainstream is decreased. Conversely, the velocity difference is amplified if the wake is compressed. This is compatible with the results presented in section 4 for the effect of acceleration and deceleration on wake mixing loss. The convection of a wake through a blade row can now be calculated and typical results are shown in Fig. 41(*b*) (He, 1992). These show that the wake becomes highly distorted and stretched because the part adjacent to the suction surface convects more rapidly than that adjacent to the pressure surface. The velocity deficit of the center of the wake is reduced by this inviscid effect as it also is by viscous effects. The implication is that the dissipation in the wake will be reduced by mixing in a downstream

blade row relative to that when mixing in a uniform flow. Since the mixing loss of a wake is comparatively small and most of the mixing takes place very close to the trailing edge this is probably not a very important effect. The same argument can be applied to a flow separation, which is in effect only a large wake; however, the mixing loss of a separation can be large and so any reduction may be significant.

A vortex from one blade row will be convected through a downstream blade row very much like a wake but the implications for loss are very different. Kelvin's theorem tells us that the circulation around a stream tube remains constant and so if the diameter of the tube is reduced by stretching the streamwise vorticity is amplified. When a vortex is stretched or compressed longitudinally it can be shown that its secondary kinetic energy will vary as the square of its length. Hence stretching a vortex will greatly amplify its secondary kinetic energy and when this is subsequently dissipated by viscous effects it will increase the loss. The magnitude of this effect is not known but if, as discussed in section 9.1, the kinetic energy of secondary flow vortices is significant, it could have important implications. Tip leakage vortices will be similarly affected.

Because the entropy increase in a shock wave is such a nonlinear function of the preshock Mach number, Eq. (31), any periodic motion of the shock will generate increased loss. Effectively the increase in entropy generation when the shock is moving forward will be greater than the reduction when it is moving backward. Ng and Epstein (1984) found evidence of high-frequency fluctuations in the loss of two transonic compressors and attributed it to oscillation of the shock position. They found that only a very small motion of the shock (0.3 mm) was needed to explain their results but the resulting loss of compressor efficiency was only 0.15 percent. It is not known how general this result is, but larger shock amplitudes with consequently larger increases in loss appear quite plausible. Similar mechanisms certainly occur in turbines when the trailing edge shock system from a stator interacts with the downstream rotor but no estimates of their magnitude are known.

Other means in which unsteady flow can affect entropy generation are through dissipation of the spanwise vorticity shed from a trailing edge as a result of changes in blade circulation, i.e., changing lift, and the presence of unsteady velocity profiles in the boundary layer due to wake passage. Both of these mechanisms have been examined by Fritsch and Giles (1992) who found that both have only a small effect on loss. The former was estimated to give at most 0.3 percent loss of efficiency for a turbine stage while the latter caused only a 0.09 percent loss.

The effects of unsteady boundary layer transition on the loss can be important, especially if the Reynolds number is in the transitional range. The large body of work on this topic is discussed by Mayle (1992).

**11.2 Partial Admission Loss.** Partial admission is used mainly in steam turbines as a means of varying the mass flow and hence the power output. Flow is only admitted to a segment of the first stator blades and leaves them as a jet occupying only part of the annulus. However, the full annulus area is available to the flow through the following rotor. Traditionally the first stage is of impulse design so that there is little circumferential pressure gradient after the stators and so little tendency for the jet leaving them to expand in the circumferential direction. The rotor blade passages well within this jet should behave as in a full annulus but the passages entering and leaving the jet are in an unsteady flow and will suffer additional losses. In both cases this may be regarded as a mixing loss between the jet and the surrounding stagnant fluid, similar to the mixing of a wake discussed in the previous section. However, in this case the "wake" is no longer small and will have a considerable effect on the blade loading and hence on the distortion of the interface between the jet and the nearly stagnant fluid. The flow pattern and losses can only really be predicted by an unsteady viscous calculation. What little is known about the magnitude of this effect is reviewed by Roelke (1973).

If the partial admission stage is followed by other full admission stages there must be a rapid circumferential redistribution of flow as its enters the second stator row. This is because there is a substantial pressure drop across stator passages that pass the full flow but little pressure drop across passages with low flow. Hence, if the static pressure is uniform at the second stator exit, there must be a strong circumferential pressure gradient at its entry. This can only be produced by a large curvature of the jet boundary in the blade to blade plane. The changes in flow direction near the jet boundary will lead to large circumferential variations of incidence onto the second stator and so will certainly induce additional losses. The author knows of no published information on this effect nor on how many such stages are needed for the flow to become circumferentially uniform.

In addition to the mixing loss at the boundaries of the jet there will be extra windage loss as the rotor blades move through the region with no throughflow. Here they will behave rather like the blades of a centrifugal compressor and will set up a complex recirculating flow, which will certainly generate significant amounts of entropy and will directly reduce the shaft torque. Results quoted by Roelke suggest that this pumping loss exceeds the mixing loss at small arcs of admission.

**11.3 Windage Loss and Disk Cooling Flows.** This is the loss due to viscous friction on all parts of the machine other than the blade and annulus boundaries, where it has already been accounted for. It is usually considered only in terms of the viscous torque on rotating disks and hence is often called disk friction loss. However, the idea of entropy creation shows that entropy is produced wherever fluid is moving relative to a solid boundary and this entropy must find its way into the flow and be present at machine exit. The views of the effect of windage in terms of lost torque and of entropy creation are entirely compatible since the lost power due to frictional torque is given by

$$\Delta W = \Omega \int \tau r \, dA \tag{55}$$

where the integral is over all rotating surfaces.

The total entropy creation is

$$\dot{S} = \int \frac{\tau \Delta V}{T} dA \tag{56}$$

where $\Delta V$ is the velocity difference across which the shear stress $\tau$ acts. In the case of the gap between stationary and rotating faces $\Delta V = \Omega r$ and so the two expressions predict the same loss of output. However, the entropy creation concept shows that loss does not only occur on rotating surfaces but on any surface exposed to the flow. It also shows that there is some reheat effect on the windage loss since the loss of machine output is given by

$$\Delta W = T_{\text{out}} \dot{S} = T_{\text{out}} \int \frac{\tau \Delta V}{T} dA \tag{57}$$

so that the lost work is reduced if the windage takes place at high temperatures. Physically this can be thought of as the frictional effects generating heat, which re-enters the flow and so increases the work output or input of any downstream stages. The view of windage loss in terms of lost torque does not account for this reheat effect.

Formulae for estimating the windage loss are given by Roelke (1973). These are effectively obtained by applying a skin friction factor to all rotating surfaces with the coefficient being a function of Reynolds number as shown in Fig. 42. The

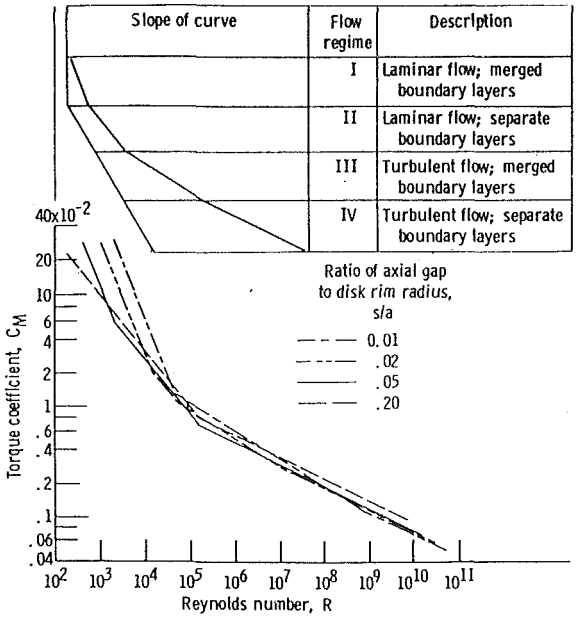


**Fig. 42 Moment coefficient for frictional torque on rotating disks from Roelke (1973)**

coefficient plotted in Fig. 42 is the moment coefficient $C_m$, which is related to the skin friction factor $C_f$ by $C_f = 0.398\ C_m$. However, these friction factors were generally obtained from tests on smooth disks rotating in smooth chambers. They can be considerably increased by surface protuberances such as bolts or webs. The entropy generation concept shows that these are equally undesirable on stationary and rotating surfaces.

A simple estimate of the ratio of the power lost by windage to useful power, assuming an axial flow machine with a two-sided disk, is given by

$$\frac{\Delta W}{W} = 0.1 \frac{C_f}{\phi\psi} \frac{D_d}{h_b} \frac{1}{1 + 4h_b/D_d} \tag{58}$$

where $C_f$ is the skin friction factor, $D_d$ is the hub diameter of the disk, $h_b$ is the height of the blades, and $\phi$ and $\psi$ are the stage flow and loading coefficients based on the mean blade speed. Figure 42 shows that the value of $C_f$ ($= 0.398\ C_m$) is of order 0.002. Hence Eq. (58) shows that the fraction of lost power is very small for most machines, being most significant for those with short blades and low flow and loading coefficients. It should be emphasized that this is a minimum estimate and the loss can be much greater if the disks are not smooth.

In some gas turbines cooling flows are introduced into the disk cavity to cool the disk. These flows subsequently enter the mainstream through the slot in the hub separating stator and rotor. Roelke states that such cooling flows enter the mainstream with a swirl velocity about 0.45 times the rotational speed of the hub and suggests that the extra torque needed to provide this angular momentum is simply added to the windage torque with no flow. This simple approach assumes that the cooling flow only affects the shear stress and entropy generation within the cavity sufficiently to provide its own change of angular momentum. This seems unlikely to be true; with no flow the shear stress must extend across the whole gap while a cooling flow is likely to make the shear layers behave more like boundary layers, which will be thinner and have higher rates of entropy generation. Chew and Vaughan (1988) present numerical predictions of the effect of cooling flows on the windage torque, which show agreement with Roelke's approach at low flow rates but show the torque becoming constant at about 1.7 times the zero flow value at high cooling flow rates.

The above discussion considers the effect of disk cooling flows on loss solely in terms of the entropy generation within the disk cavity. However, extra loss will occur when the cooling flow is injected into the main stream. Here the mixing process will be exactly like that of the leakage flow over a shroud, as discussed in section 8 and in Appendix 5. Most of the entropy generation will be due to the difference in swirl velocity between the flow leaving the cavity and the main flow. This velocity difference should be minimized by preswirling the cooling flow when possible.

**11.4 Lacing Wires and Part-Span Shrouds.** These are used in both turbines and compressors to control the vibration of long blades. In their simplest form they consist of a circular rod (a lacing wire) joining adjacent blades while more sophisticated versions replace the rod by an aerofoil section, which may be aligned to the local meridional flow direction. For convenience both types will be referred to as struts.

The flow over such a strut is complex. Because of the blade loading there will be a gradient of static pressure along its span and this will generate secondary flows on the strut very much like those on the endwalls. Traverses behind such struts show secondary vortices and loss concentrations near the intersection with the blade suction surface. If the strut has a blunt trailing edge, like a lacing wire, then the separated flow in its wake is also subject to this pressure gradient and the low-energy fluid in the wake will move onto the blade suction surface where it will merge with the loss in the secondary vortex. Hence, the drag and entropy generation will not be the same as for the same cross section of strut in a uniform flow. In fact the entropy generation is likely to be increased in the same way as that on endwalls was found to be greater than on blade surfaces.

The loss of such struts is usually obtained in terms of their drag, which, in a uniform flow, can be turned into an entropy rise by using Eq. (7) in the form

$$T\Delta s = \frac{D}{\rho A_f} \tag{59}$$

where $D$ is the total drag force acting in the direction of the streamlines and $A_f$ is the total flow area projected in that direction. However, the actual strut is not in a uniform flow, the local velocity varies considerably from suction surface to pressure surface and from its leading edge to trailing edge. There will also generally be a pitchwise component of velocity making the strut analogous to a swept wing. Hence neither estimation of the drag nor application of Eq. (59) is straightforward.

If $C_d$ is the drag coefficient of the strut based on its frontal area $A_s$ *projected in the relative flow direction* and on an average relative flow velocity $V_{\text{avg}}$, then the loss coefficient based on $V_{\text{avg}}$ is

$$\zeta = \frac{T\Delta s}{0.5\ V_{\text{avg}}^2} = \frac{C_d A_s}{A_f} = \frac{C_d A_{ms}}{A_{mf}} \tag{60}$$

where $A_{ms}$ and $A_{mf}$ are the *meridional* projections of the areas. Given that $C_d$ is of order unity for circular wires and of order 0.1 for aerofoils, the advantage of using streamlined struts is apparent.

Koch and Smith (1976) present a method for compressor blades based on this concept. The drag of the strut is estimated by treating it as a swept airfoil at the average relative Mach number and by also including a term for the interference drag generated at the junction of the strut and the blade surfaces. They find that the drag must be increased by a factor of 1.8 above the value calculated for an aerofoil to obtain agreement with the measured loss of struts on compressor blades.

The entropy generation concept provides an alternative method of estimating the loss due to the boundary layers on streamlined struts. The strut surface velocity distribution can only be obtained accurately from a three-dimensional calculation but it may be estimated from the blade surface velocity

distribution and used in Eq. (41) to estimate the total entropy generation. This approach shows the importance of locating the strut in a region where its relative velocity is as low as possible, i.e., toward the trailing edge of compressor blades or toward the leading edge of turbine blades. If the strut is not streamlined and so has a large separated region behind the trailing edge, then the base pressure term in Eq. (26) is likely to be the dominant source of entropy. The base pressure coefficient will be particularly difficult to estimate because of the nonuniform flow.

## 12 Conclusions

It must be clear be now that there are many details of loss generation in turbomachines where our understanding is still very weak. The author believes that our understanding will be improved by thinking the loss in terms of entropy generation and one of the objectives of this paper has been to encourage this way of thinking.

There are a few sources of loss where we can say that we understand the mechanism clearly and can accurately quantify the rate of entropy generation. Flow is attached, two-dimensional, fully turbulent or fully laminar boundary layers, where numerical calculation methods should be very accurate, is an example of this. However, even for the straightforward problem of calculating the loss of a two-dimensional cascade the author maintains that an *a priori* prediction, using the best available methods, is unlikely to be accurate to better than about $\pm 20$ percent. Twenty years ago (Denton, 1973) he gave an estimate of $\pm 10$ percent! This is because he now realizes the difficulty of predicting boundary layer transition, separation bubbles, and base pressure coefficients.

For other sources of loss we understand the mechanism but cannot accurately quantify the entropy production without making considerable use of empirical data. Tip leakage loss, subsonic trailing edge loss, and loss due to blade surface separations all fall into this category. In such cases we may be able to identify good and bad features of the flow and modify our designs accordingly even though we cannot quantify the improvement before testing them. In this situation the ability to test modifications quickly and cheaply, and to relate the results to the physics of the flow, is very important.

There are still some major loss sources for which we do not yet fully understand the mechanisms. Endwall loss, transonic trailing edge loss, and loss due to mixing in a downstream blade row all fall into this category. In such cases predictions must use empirical correlations, which may not even be based on the correct physics. It is important that when using these correlations we recognize their limitations and do not develop a false sense of security if they happen to give the correct answer. This is especially dangerous when correlations are "verified" against the same data that were used to generate their empirical constants. For this type of loss we must strive to obtain a better understanding of the mechanism involved so that we can at least make qualitative improvements to our designs.

In computing flows through turbomachines the author has continually been struck by the ability of soundly based but grossly oversimplified models to give realistic predictions of the flow pattern and loss. The reason for this is that many flows are dominated by the conservation of mass, energy, and momentum and not by detailed viscous effects. The power of the conservation equations should never be underestimated and flow models that do not satisfy these equations are doomed to failure.

Finally, we should never be afraid to admit our lack of understanding of complex entropy generating mechanisms or to address fundamental questions. We are most likely to make progress when we know our limitations and continually strive to reduce them.


## Acknowledgments

As will be obvious to many readers, this paper is largely based on work performed at the Whittle laboratory over the last 20 years. The authors is greatly indebted to all past and present staff and students of the laboratory for the stimulating environment that they provide. Thanks are also due to the colleagues who have read early drafts of this paper and commented constructively on them. Above all thanks are due to the IGTI Gas Turbine Scholar program for providing the opportunity for me to collect and present my thoughts on this fascinating topic.


## References


Adamcyzk, J. J., Celestina, M. L., and Greitzer, E. M., 1993, "The Role of Tip Clearance in High Speed Fan Stall," ASME JOURNAL OF TURBOMACHINERY, Vol. 115, No. 1, pp. 28–39.

Ainley, D. G., and Mathieson, G. C. R., 1951, "An Examination of the Flow and Pressure Losses in Blade Rows of Axial Flow Turbines," ARC, R&M 2891.

Atkin, C. J., and Squire, L. C., 1992, "A Study of the Interaction of a Normal Shock Wave With a Turbulent Boundary Layer at Mach Numbers Between 1.3 and 1.55," *Eur. J. Mechanics B/Fluids*, Vol. 11, No. 1.

Binder, A., 1985, "Turbulence Production Due to Secondary Vortex Cutting in a Turbine Rotor," ASME *Journal of Engineering for Gas Turbine and Power*, Vol. 107, pp. 1039–1046.

Bindon, J. P., 1979, "The Effect of Hub Inlet Boundary Layer Skewing on the Endwall Shear Flow in an Annular Turbine Cascade," ASME Paper No. 79-GT-13.

Bindon, J. P., 1989, "The Measurement and Formation of Tip Clearance Loss," ASME JOURNAL OF TURBOMACHINERY, Vol. 111, pp. 257–263.

Boletis, E., Sieverding, C. H., and Van Hove, W., 1983, "Effects of a Skewed Inlet Boundary Layer on the 3D Flow Field in an Annular Turbine Cascade," *Viscous Effects in Turbomachines*, AGARD CP 351.

Brown, L. E., 1972, "Axial Flow Compressor and Turbine Loss Coefficients: A Comparison of Several Parameters," ASME Paper No. 72-GT-18.

Came, P. M., 1969, "Tip Clearance Losses in Turbines—A Review of Experimental Data and Prediction Methods," NGTE report NT.754.

Carter, A. D. S., 1948, "Three-Dimensional Flow Theories for Axial Compressors and Turbines," *Proc. IMechE*, Vol. 159.

Cebeci, T., and Carr, L. W., 1978, "A Computer Program for Calculating Laminar and Turbulent Boundary Layers for Two-Dimensional Time-Dependent Flows," NASA TM 78470.

Chen, S., 1987, "A Loss Model for the Transonic Flow Low Pressure Steam Turbine Blades," IMechE Paper No. C269/87.

Chew, J. W., and Vaughan, C. M., 1988, "Numerical Predictions of the Flow Induced by an Enclosed Rotating Disc," ASME Paper No. 88-GT-127.

Cumpsty, N. A., 1989, *Compressor Aerodynamics*, Longman.

Dawes, W. N., 1990, "A Comparison of Zero and One Equation Turbulence Models for Turbomachinery Calculations," ASME Paper No. 90-GT-303.

de Ruyck, J., and Hirsch, Ch., 1983, "Endwall Boundary Layer Calculations in Multistage Axial Compressors," *Viscous Effects in Turbomachines*, AGARD CP 351.

Denton, J. D., and Hoadley, D., 1972, "Calculation of the Effect of Surface Roughness on the Profile Loss of Turbine Blades," GEGB report R/M/N630.

Denton, J. D., 1973, "A Survey and Comparison of Methods of Predicting the Profile Loss of Turbine Blades," IMechE Paper No. C76/73.

Denton, J. D., and Johnson, C. G., 1976, "Tip Leakage Loss of Shrouded Turbine Blades," CEGB report R/M/N848.

Denton, J. D., and Cumpsty, N. A., 1987, "Loss Mechanisms in Turbomachines," IMechE Paper No. C260/87.

Denton, J. D., and Xu, L., 1990, "The Trailing Edge Loss of Transonic Turbine Blades," ASME JOURNAL OF TURBOMACHINERY, Vol. 112, pp. 277–285.

Denton, J. D., 1990, "Entropy Generation in Turbomachinery Flows," SAE SP-846.

Dunham, J., 1970, "A Review of Cascade Data on Secondary Losses in Turbines," *IMechE J. Mech. Eng. Sci.*, Vol. 12, No. 1.

Dunham, J., and Came, P. M., 1970, "Improvements to the Ainley–Mathieson Method of Turbine Performance Prediction," ASME *Journal of Engineering for Power*, Vol. 92.

Freeman, C., and Cumpsty, N. A., 1989, "A Method for the Prediction of Supersonic Compressor Blade Performance," ASME Paper No. 89-GT-326.

Fritsch, G., and Giles, M., 1992, "Second-Order Effects of Unsteadiness on the Performance of Turbomachines," ASME Paper No. 92-GT-389.

Glassman, A. J., "Turbine Design and Application," Vols. 1–3, NASA SP-290.

Gregory-Smith, D. G., 1982, "Secondary Flows and Losses in Axial Flow Turbines," ASME *Journal of Engineering for Power*, Vol. 104, pp. 819–822.

Gregory-Smith, D. G., Graves, C. P., and Walsh, J. A., 1988, "Growth of Secondary Losses and Vorticity in an Axial Turbine Cascade," ASME JOURNAL OF TURBOMACHINERY, Vol. 110, pp. 1–8.

Harrison, S., 1989, "The Influence of Blade Stacking on Turbine Losses," Ph.D. thesis, Cambridge University, United Kingdom.

Harrison, S., 1990, "Secondary Loss Generation in a Linear Cascade of High-

Turning Turbine Blades," ASME JOURNAL OF TURBOMACHINERY, Vol. 112, pp. 618–624.

Hart, M., Hall, D. M., and Singh, G., 1991, "Computational Methods for the Aerodynamic Development of Large Steam Turbines," IMechE Paper No. C423/009.

Hartsel, J. E., 1972, "Prediction of Effects of Mass-Transfer Cooling on the Blade-Row Efficiency of Turbine Aerofoils," AIAA Paper No. 72-11.

Hawthorne, W. R., 1955, "Some Formulae for the Calculation of Secondary Flow in Cascades," Cambridge Univ. Engineering Dept. Report.

He, L., 1992, Whittle Lab., Cambridge, United Kingdom, personal communication.

Heyes, F. J. G., and Hodson, H. P., 1993, "Measurement and Prediction of Tip Clearance Flow in Linear Turbine Cascades," ASME JOURNAL OF TURBOMACHINERY, Vol. 115, pp. 376–382.

Hobbs, D. E., and Weingold, H. D., 1984, "Development of Controlled Diffusion Aerofoils for Multistage Compressor Application," ASME *Journal of Engineering for Gas Turbines and Power*, Vol. 106, pp. 271–278.

Hodson, H. P., and Dominy, R. G., 1989, "Three-Dimensional Flow in a Low-Pressure Turbine Cascade at Its Design Condition," ASME JOURNAL OF TURBOMACHINERY, Vol. 109, pp. 177–185.

Horlock, J. H., 1958, *Axial Flow Compressors*, Butterworths, United Kingdom.

Howell, A. R., 1945, "The Design of Axial Flow Compressors," *Proc. IMechE*, Vol. 153.

Huntsman, I., Hodson, H. P., and Hill, S. H., 1992, "The Design and Testing of a Radial Flow Turbine for Aerodynamic Research," ASME JOURNAL OF TURBOMACHINERY, Vol. 114, pp. 411–418.

Huntsman, I., 1993, "An Investigation of Radial Inflow Turbine Aerodynamics," Ph.D. Thesis, Cambridge University, United Kingdom.

Inoue, M., and Cumpsty, N. A., 1984, "Experimental Study of Centrifugal Compressor Discharge Flow in Vaneless and Vaned Diffusers," ASME *Journal of Engineering for Gas Turbines and Power*, Vol. 106, pp. 455–467.

Koch, C. C., and Smith, L. H., 1976, "Loss Sources and Magnitudes in Axial Flow Compressors," ASME *Journal of Engineering for Power*, Vol. 98, No. 3.

Krain, H., and Hoffman, W., 1989, "Verification of an Impeller Design by Laser Measurements and 3D Viscous Flow Calculations," ASME Paper No. 89-GT-159.

Langston, L. S., Nice, M. L. and Hooper, R. M., 1977, "Three-Dimensional Flow in a Turbine Cascade Passage," ASME *Journal of Engineering for Power*, Vol. 99, No. 1.

Mayle, R. E., 1991, "The Role of Laminar-Turbulent Transition in Gas Turbine Engines," First IGTI Gas Turbine Scholar Lecture," ASME JOURNAL OF TURBOMACHINERY, Vol. 113, pp. 509–537.

Mee, D. J., Baines, N. C., Oldfield, M. L. G., and Dickens, T. E., 1992, "An Examination of the Contributions to Loss on a Transonic Turbine Blade in Cascade," ASME JOURNAL OF TURBOMACHINERY, Vol. 114, pp. 155–162.

Moore, J., and Moore, J. G., 1980, "Three Dimensional Viscous Calculations for Assessing the Thermodynamic Performance of Centrifugal Compressors—Study of the Eckardt Compressor," AGARD CP 282.

Moore, J., and Moore, J. G., 1983, "Entropy Production Rates From Viscous Flow Calculations. Part 1—A Turbulent Boundary Layer," ASME Paper No. 83-GT-70.

Moore, J., and Adhye, R. Y., 1985, "Secondary Flows and Losses Downstream of a Turbine Cascade," ASME *Journal of Engineering for Gas Turbines and Power*, Vol. 107, pp. 961–968.

Moore, J., Shaffer, D. M., and Moore, J. G., 1987, "Reynolds Stresses and Dissipation Mechanisms Downstream of a Turbine Cascade," ASME JOURNAL OF TURBOMACHINERY, Vol. 109, pp. 258–267.

Moore, J., and Tilton, J. S., 1988, "Tip Leakage Flow in a Linear Turbine Cascade," ASME JOURNAL OF TURBOMACHINERY, Vol. 110, pp. 18–26.

Morishita, E., 1982, "Centrifugal Compressor Diffusers," M Sc. Thesis, Cambridge University, United Kingdom.

Morphis, G., and Bindon, J. P., 1988, "The Effects of Relative Motion, Blade Edge Radius and Gap Size on the Blade Tip Pressure Distribution in an Annular Turbine Cascade With Clearance," ASME Paper No. 88-GT-256.

Moyle, I. N., 1988, "Analysis of Efficiency Sensitivity Associated with Tip Clearance in Axial Compressors," ASME Paper No. 88-GT-216; "A Note on Efficiency Sensitivity to Tip Clearance Changes in Axial Flow Compressors," JOURNAL OF TURBOMACHINERY, Vol. 112, 1990, pp. 795–796.

Ng, W. F., and Epstein, A. H., 1984, "Unsteady Losses in Transonic Compressors," ASME Paper No. 84-GT-183.

Okan, M. B., and Gregory-Smith, D. G., 1992, "A Simple Method for Estimating Secondary Losses in Turbines at the Preliminary Design Stage," ASME Paper No. 92-GT-294.

Pierzga, M. J., and Wood, J. R., 1985, "Investigation of the Three Dimensional Flow Field Within a Transonic Fan Rotor," ASME *Journal of Engineering for Power*, Vol. 107, pp. 436–439.

Prato, J., and Lakshimarayana, B., 1993, "Investigation of Compressor Rotor Wake Structure at Peak Pressure Rise Coefficient and Effects of Loading," ASME JOURNAL OF TURBOMACHINERY, Vol. 115, pp. 487–500.

Roberts, Q., 1992, "The Trailing Edge Loss of a Simulated Turbine Blade," Final Year Project, Cambridge University Eng. Dept., United Kingdom.

Roelke, R. J., 1973, *Turbine Design and Application*, NASA SP-290, A. J. Glassman, ed., Vol. 2, Chap. 8.

Schlichting, H., 1966, *Boundary Layer Theory*, 6th ed., McGraw-Hill, New York.

Schlichting, H., 1978, *Boundary Layer Theory*, 7th ed., McGraw-Hill, New York.

Shapiro, A. H., 1953, *The Dynamics and Thermodynamics of Compressible Fluid Flow*, Wiley, New York.

Sharma, O. P., and Butler, T. L., 1987, "Predictions of Endwall Losses and Secondary Flows in Axial Flow Turbine Cascades," ASME JOURNAL OF TURBOMACHINERY, Vol. 109, pp. 229–236.

Sharma, O. P., Pickett, G. F., and Ni, R. H., 1992, "Assessment of Unsteady Flows in Turbines," ASME JOURNAL OF TURBOMACHINERY, Vol. 114, pp. 79–90.

Sieverding, C. H., Stanislas, M., and Snoek, J., 1983, "The Base Pressure Problem in Transonic Cascades," ASME Paper No. 83-GT-50.

Sieverding, C. H., 1985, "Recent Progress in the Understanding of Basic Aspects of Secondary Flows in Turbine Blade Passages," ASME *Journal of Engineering for Gas Turbines and Power*, Vol. 107, pp. 248–257.

Smith, L. H., 1966, "Wake Dispersion in Turbomachines," ASME *Journal of Basic Engineering*, Vol. 88.

Smith, L. H., 1970, "Casing Boundary Layers in Multistage Axial Flow Compressors," in: *Flow Research on Blading*, L. S. Dzung, ed., Elsevier.

Stewart, W. L., 1955, "Analysis of Two Dimensional Compressible Flow Loss Characteristics Downstream of Turbomachine Blade Rows in Terms of Basic Boundary Layer Characteristics," NACA TN 3515.

Stewart, W. L., Whitney, W. J., and Wong, R. J., 1960, "A Study of Boundary Layer Characteristics of Turbomachine Blade Rows and Their Relation to Overall Blade Loss," ASME *Journal of Basic Engineering*, pp. 588–592.

Storer, J. A., 1991, "Tip Clearance Flow in Axial Compressors," Ph D thesis, Cambridge University, United Kingdom.

Sutton, A., 1990, "The Trailing Edge Loss of Subsonic Turbine Blades," M Sc Thesis, Cambridge University, United Kingdom.

Truckenbrodt, E., 1952, "A Method of Quadrature for the Calculation of Laminar and Turbulent Boundary Layers in Plane and Rotational Symmetric Flow," *Ingenieur-Archiv*, Vol. 20; translated as NACA TM 1379.

Walsh, J. A., and Gregory-Smith, D. G., 1990, "Inlet Skew and the Growth of Secondary Losses and Vorticity in a Turbine Cascade," ASME JOURNAL OF TURBOMACHINERY, Vol. 112, pp. 633–642.

Wennerstrom, A. J., and Puterbaugh, S. L., 1984, "A Three-Dimensional Model for the Prediction of Shock Losses in Compressor Blade Rows," ASME *Journal of Engineering for Gas Turbines and Power*, Vol. 106, pp. 295–299.

Yaras, M. I., and Sjolander, S. A., 1992, "Effects of Simulated Rotation on Tip Leakage in a Planar Cascade of Turbine Blades. Parts 1 and 2," ASME JOURNAL OF TURBOMACHINERY, Vol. 114, pp. 652–667.

Xu, L., and Denton, J. D., 1988, "The Base Pressure and Loss of a Family of Four Turbine Blades," ASME JOURNAL OF TURBOMACHINERY, Vol. 110, pp. 9–17.

## APPENDIX 1

### Entropy Production in a Boundary Layer

Consider the flow along a stream tube in the boundary layer with the $x$ direction aligned with the stream tube and the $y$ direction being perpendicular to it. Hence $V_y$ and $V_z$ are both zero at the location considered.

For thin boundary layers the stream tube can be assumed to be very closely aligned with the surface so the $x$ and $y$ directions are effectively perpendicular and parallel to the surface respectively.

The second law applied along the stream tube gives

$$T\frac{ds}{dx}=\frac{dh}{dx}-\frac{1}{\rho}\frac{dP}{dx}=\frac{dh_o}{dx}-V_x\frac{dV_x}{dx}-\frac{1}{\rho}\frac{dP}{dx} \qquad \text{(A1.1)}$$

Let $F_x$ be the viscous force acting per unit mass of fluid in the $x$ direction. The momentum equation in the $x$ direction is then

$$F_x-\frac{1}{\rho}\frac{dP}{dx}=V_x\frac{dV_x}{dx} \qquad \text{(A1.2)}$$

Combining (A1.1) and (A1.2) gives

$$T\frac{ds}{dx}=\frac{dh_o}{dx}-F_x \qquad \text{(A1.3)}$$

This is a well-known result, which shows that if $h_o$ is constant, as it often is in adiabatic flow, entropy is created by any frictional force acting along the streamline in the direction opposing the flow.

Now consider unit mass of fluid moving along the streamline from a Lagrangian point of view. The energy equation for the unit mass is:

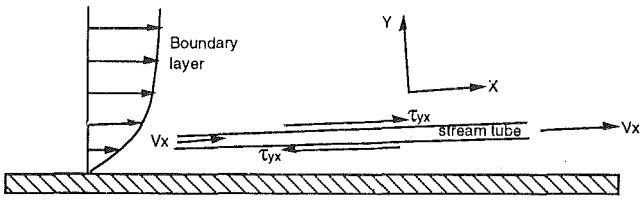


Fig. A1.1

$$\frac{D}{Dt}\left(e+\frac{1}{2}V^2\right) = -P\frac{D}{Dt}\left(\frac{1}{\rho}\right) + V_x\left(F_x - \frac{1}{\rho}\frac{\partial P}{\partial x}\right) + \frac{1}{\rho}\left(\tau_{yx}\frac{\partial V_x}{\partial y} + \tau_{yz}\frac{\partial V_z}{\partial y}\right) - \frac{1}{\rho}\frac{\partial q}{\partial y} \quad \text{(A1.4)}$$

where $e$ is the specific internal energy ($e = C_v T$), $q$ is the heat flow per unit area in the $y$ direction and $\tau_{yx}$ and $\tau_{yz}$ are the viscous shear stresses. Viscous normal stresses and heat flow in the $x$ and $z$ direction are ignored.

For steady flow

$$\frac{D}{Dt} = V_x\frac{\partial}{\partial x}$$

and so Eq. (A1.4) becomes

$$V_x\frac{\partial h_o}{\partial x} = F_x V_x + \frac{1}{\rho}\left(\tau_{yx}\frac{\partial V_x}{\partial y} + \tau_{yx}\frac{\partial V_z}{\partial y}\right) - \frac{1}{\rho}\frac{\partial q}{\partial y} \quad \text{(A1.5)}$$

Combining Eqs. (A1.3) and (A1.5) to eliminate $h_o$ leads to

$$V_x T\frac{\partial s}{\partial x} = \frac{1}{\rho}\left(\tau_{yx}\frac{\partial V_x}{\partial y} + \tau_{yz}\frac{\partial V_z}{\partial y}\right) - \frac{1}{\rho}\frac{\partial q}{\partial y}$$

If $\Delta A$ is the cross-sectional area of the stream tube $\rho V_x \Delta A =$ constant along it, so

$$T\frac{\partial}{\partial x}(\rho V_x s \Delta A) = \Delta A\left(\tau_{yx}\frac{\partial V_x}{\partial y} + \tau_{yz}\frac{\partial V_z}{\partial y} - \frac{\partial q}{\partial y}\right)$$

If we consider unit depth in the $z$ direction, $\Delta A = dy$ and so integrating through the boundary layer, thickness $\delta$, gives

$$\int_0^\delta \frac{\partial}{\partial x}(\rho V_x s)dy = \int_0^\delta \frac{1}{T}(\tau_{yx}dV_x + \tau_{yz}dV_z - dq)$$

If we now assume an adiabatic surface $q = 0$ both at the surface and at the edge of the boundary layer, where the entropy is $s_\delta$, we end up with

$$\frac{d}{dx}\int_0^\delta (\rho V_x(s - s_\delta)dy) = \int_0^\delta \frac{1}{T}(\tau_{yx}dV_x + \tau_{yz}dV_z) \quad \text{(A1.6)}$$

for the rate of change of entropy flux of the flow per unit depth in the $z$ direction.

For a two-dimensional boundary layer $\tau_{yz}$ is zero (no skew) and so the result simplifies to

$$\frac{d}{dx}\int_0^\delta (\rho V_x(s - s_\delta))dy) = \int_0^\delta \frac{1}{T}\tau dV \quad \text{(A1.7)}$$

The left-hand side of this equation is the rate of change of entropy flux per unit depth of the flow and so the right-hand side may be thought of as giving the rate of entropy creation per unit surface area by viscous effects within the boundary layer.

## APPENDIX 2

### Entropy Production Due to Mixing of Two Streams

Consider two streams of perfect gas mixing in a constant area duct as sketched in Fig. A2.1. The inlet stagnation pressure and stagnation temperature of both streams is supposed to be specified as are the areas $A_1$ and $A_2$ of the supply ducts. It is

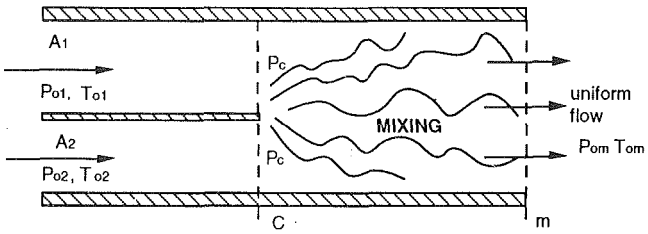


Fig. A2.1 Mixing of two streams in a constant area duct

assumed that the two streams meet at plane $C$ where they both have a common and uniform static pressure $P_c$. This assumption is almost universally made but is not exactly true because the mixing downstream of plane $C$ can induce streamline curvatures and hence cross-stream pressure gradients at plane $C$. The pressure $P_c$ may be varied at will by opening or closing a downstream throttle and so we can assume that it is specified and known. Downstream of plane $C$ the two streams mix with turbulence and probably unsteadiness, but with no friction on the walls, until at a downstream plane $m$ the flow has become completely uniform. The "no friction" assumption may be realized in practice by considering a periodic flow rather than one bounded by solid surfaces.

Knowing $P_{o1}$, $P_{o2}$, and $P_c$, the Mach number of streams 1 and 2 at $C$ may be calculated from standard compressible flow relationships:

$$\frac{P_c}{P_{o1}} = \left(1 + \frac{\gamma - 1}{2}\mathrm{M}_1^2\right)^{(\gamma/(1-\gamma))} \quad \text{(A2.1)}$$

Hence the mass flow rates $m_1$ and $m_2$ can be calculated as can the velocities $V_1$ and $V_2$. We can now evaluate the total momentum flux of the two streams at $C$ as

$$I_c = P_c(A_1 + A_2) + m_1 V_1 + m_2 V_1 \quad \text{(A2.2)}$$

Since the mixing takes place at constant area and we neglect wall friction this must equal the total momentum flux $I_m$ of the mixed out flow at $m$.

The energy equation applied between $C$ and $m$, assuming adiabatic flow, gives

$$T_{om} = \frac{(m_1 T_{o1} + m_2 T_{o2})}{(m_1 + m_2)} \quad \text{(A2.3)}$$

Hence we can evaluate the impulse function

$$F_m = \frac{I_m}{(m_1 + m_2)\sqrt{C_p T_{om}}} \quad \text{(A2.4)}$$

at plane $m$. This is a function of Mach number and $\gamma$, given by

$$F_m = \frac{\sqrt{\gamma - 1}}{\gamma \mathrm{M}_m}\frac{(1 + \gamma \mathrm{M}_m^2)}{\sqrt{\left(1 + \frac{\gamma - 1}{2}\mathrm{M}_m^2\right)}} \quad \text{(A2.5)}$$

and so knowing $F_m$ we can find the Mach number $\mathrm{M}_m$ of the mixed out flow. From the Mach number, stagnation temperature and area all the other properties of the downstream flow can easily be evaluated using standard compressible flow functions. In particular the increase in mass-weighted specific entropy can be calculated and turned into an entropy loss coefficient for the process.

We have obtained this loss coefficient without knowing any details of the mixing process, even whether it is laminar or turbulent, steady or unsteady. This illustrates the power of the control volume analysis, i.e., the ability to use the global conservation equations to obtain overall results without having to solve the Navier–Stokes equations. It is the author's view that this ability accounts for much of the success of Computational Fluid Dynamics applied to turbomachinery flows. In many

applications the overall result will be correct even when the turbulence model is grossly inadequate.

There are always two possible values of Mach number satisfying Eq. (A2.5), one subsonic and the other supersonic. If both the entering flows are subsonic then only the subsonic solution is possible since the supersonic solution would involve a decrease of mass averaged entropy. If one or both of the entering flows are supersonic then both subsonic and supersonic solutions may be physically possible.

Figure 6 shows the computed entropy loss coefficient for two flows, which initially occupy equal areas and mix at constant area as shown in Fig. A2.1. The static pressure at plane $C$ is held constant at a value that would produce a Mach number of 0.5 when both flows have the same stagnation pressure $P_{oavg}$ and stagnation temperature $T_{oavg}$. The stagnation pressure of one flow is set at $P_{oavg}+\Delta P$ and that of the other is $P_{oavg}-\Delta P$, while the stagnation temperatures are similarly $T_{oavg}+\Delta T$ and $T_{oavg}-\Delta T$. $\Delta P$ and $\Delta T$ are systematically varied and a loss coefficient defined as $\zeta = T_{oavg}\Delta s/0.5\, V^2_{avg}$ is calculated for the mixing process.

It can be seen that the loss coefficient contours are almost symmetric about both axes and this shows that the increase of entropy due to differences in stagnation pressure is almost independent of the difference in stagnation temperature and vice versa. The relation of this entropy increase to turbine performance is discussed in section 6 and in Appendix 4.

Further examples of the application of the global conservation equations to mixing problems are given in Appendices 3 and 4.

## APPENDIX 3

### Entropy Production Due to the Mixing Out of a Wake Behind a Trailing Edge

Consider the idealized model sketched below, which represents a trailing edge of thickness $t$ on a blade row with stagger angle $\alpha$ and pitch $(w/\cos\alpha)$. The flow is assumed uniform across the throat $AB$ and also far downstream of the trailing edge on $ED$. The displacement and momentum thickness of the combined boundary layers on the blade surface at $AB$ are $\delta^*$ and $\theta$. The average pressure acting on the base of the trailing edge, $AF$, is $P_b$ and that on the suction surface from $B$ to $C$ is $P_s$. For simplicity we assume incompressible flow but this restriction is easily removed in numerical solutions.

We will apply the equations for the conservation of mass and momentum to the dashed control volume $ABCDEF$. At inlet the mass flow rate is $m=\rho V_1(w-t-\delta^*)$ so the continuity equation is

$$m=\rho V_1(w-t-\delta^*)$$
$$=\rho V_2 w\cos(\alpha-\delta)/\cos\alpha\approx\rho V_2 w(1+\delta\tan\alpha) \quad \text{(A3.1)}$$

where the last term assumes that $\delta$ is small.

The deviation angle $\delta$ can be found from the momentum equation in the $y$ direction, which is

$$(P_s-P_2)w\tan\alpha=\rho V_1(w-t-\delta^*)V^2\sin\delta \quad \text{(A3.2)}$$

Combining this with the continuity equation and assuming that $\delta$ is small gives

$$\delta\approx\frac{(P_s-P_2)w^2\tan\alpha}{\rho V_1^2(w-t-\delta^*)^2} \quad \text{(A3.3)}$$

The value of the deviation angle $\delta$ is therefore largely determined by the value of the pressure coefficient $(P_s-P_2)/\rho V_1^2$. This must be input to the calculation.

The momentum equation in the $x$ direction gives

$$(w-t)P_1+tP_b+mV_1-\rho_1V_1^2\theta=wP_2+mV_2\cos\delta \quad \text{(A3.4)}$$

Assuming that $\delta$ is small, this becomes

$$\rho V_1^2(w-t-\delta^*-\theta)-\rho V_2^2 w(1+\delta\tan\alpha)=(P_1-P_b)t+(P_2-P_1)w$$

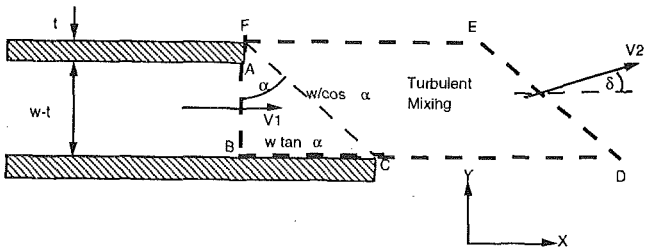


Fig. A3.1 · Control volume model for a thick trailing edge

so

$$(P_1-P_2)=-\rho V_1^2\left(1-\frac{t}{w}-\frac{\delta^*}{w}-\frac{\theta}{w}\right)$$
$$+\rho V_2^2(1+\delta\tan\alpha)+(P_1-P_b)\frac{t}{w} \quad \text{(A3.5)}$$

Rearranging this gives

$$(P_{01}-P_{02})=0.5\,\rho V_2^2(2\delta\tan\alpha+1)$$
$$-0.5\,\rho V_1^2\left(1+2\left(\frac{t+\delta^*+\theta}{w}\right)\right)+(P_1-P_b)\frac{t}{w}$$

so

$$\frac{P_{01}-P_{02}}{0.5\,\rho\,V_1^2}=\frac{V_2^2}{V_1^2}(2\,\delta\tan\alpha+1)-1$$
$$+2\left(\frac{t+\delta^*+\theta}{w}\right)-C_{pb}\frac{t}{w} \quad \text{(A3.6)}$$

This may be solved by using the continuity equation to eliminate $V_2/V_1$ but the algebra becomes complex unless we make the assumption that the deviation angle $\delta$ is zero. This assumption is discussed in section 4 where it is justified on the grounds that it makes the total entropy creation behind a trailing edge almost independent of the blade stagger. The trailing edge loss coefficient then becomes

$$\zeta=-\frac{C_{pb}t}{w}+\frac{2\theta}{w}+\left(\frac{\delta^*+t}{w}\right)^2 \quad \text{(A3.7)}$$

An alternative common assumption (e.g., Stewart, 1955) is that $P_s=P_1$ in which case the deviation is negative and the algebra becomes much more complex. In practice the suction surface pressure is likely to lie somewhere between these two assumptions.

The first term on the right-hand side of Eq. (A3.7) is the loss due to the low base pressure acting on the trailing edge; in general this must be obtained from empirical data. The second term is the mixed out loss of the boundary layers on the blade surface just before the trailing edge and the third term arises from the combined blockage of the trailing edge and the boundary layers.

## APPENDIX 4

### Thermodynamics of a Cooled Turbine

**(a) Cycle Analysis.** Figure A4.1 shows an idealized cooled gas turbine cycle. Coolant flow $m_c$ is assumed to be bled off at compressor delivery conditions and is gradually mixed with the turbine flow along the expansion from 3 to 4. Once added to the main flow the coolant flow subsequently expands with it and does useful work from its injection point to point 5. The efficiency of the cooled part of the turbine, 3–4, is assumed to be influenced by the mass flow rate of coolant while the efficiency of the uncooled part of the turbine from 4 to 5 is constant.

In a design situation we may imagine that the pressure ratio of the cycle and of the cooled turbine has been fixed and that the maximum temperature $T_3$ is being optimized by varying

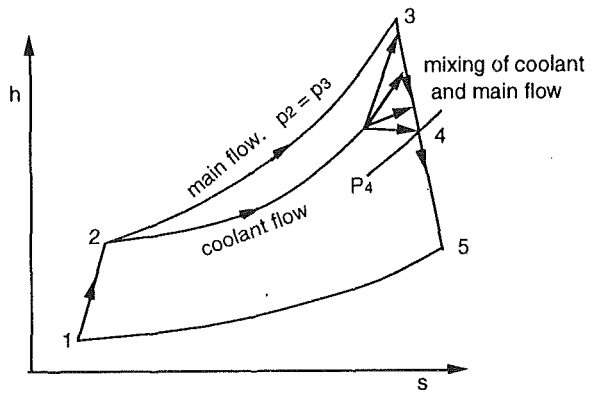


Fig. A4.1 Cycle for a cooled gas turbine

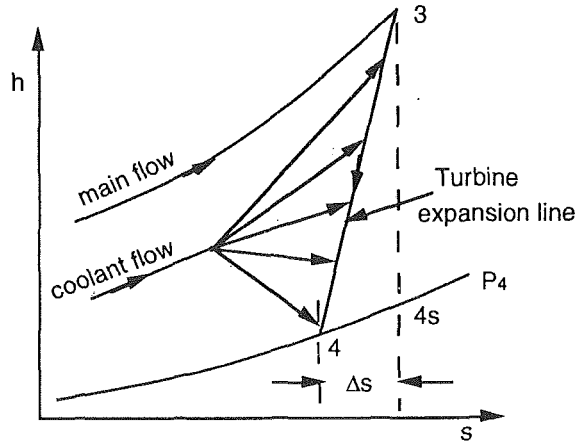


Fig. A4.2 The expansion through a cooled turbine

the proportion of cooling flow $m_{fc}$, where $m_{fc}$ is the ratio of coolant flow rate to compressor flow rate. The compressor efficiency is also considered fixed as is the efficiency of the uncooled part of the turbine 4–5. The efficiency of the cooled part of the turbine is $\eta_t$, which is a function of $m_{fc}$. The cycle efficiency will then be a function of $T_3$, $\eta_t$, and $m_{fc}$, so we can write

$$\Delta\eta_c = \frac{\partial\eta_c}{\partial T_3}\Delta T_3 + \frac{\partial\eta_c}{\partial m_{fc}}\Delta m_{fc} + \frac{\partial\eta_c}{\partial\eta_t}\Delta\eta_t \qquad \text{(A4.1)}$$

or, regarding $m_{fc}$ as the independent variable,

$$\Delta\eta_c = \left\{\frac{\partial\eta_c}{\partial T_3}\frac{dT_3}{dm_{fc}} + \left[\frac{\partial\eta_c}{\partial m_{fc}} + \frac{\partial\eta_c}{\partial\eta_t}\frac{d\eta_t}{dm_{fc}}\right]\right\}\Delta m_{fc} \qquad \text{(A4.2)}$$

It is only the last term that we will be concerned with in detail, i.e., the effect of coolant addition on the efficiency of the cooled part of the turbine. This efficiency is defined in terms of the change in properties of the main flow alone as will be described in section (b) of this appendix. The other terms in Eq. (A4.2) are equally important as regards cycle efficiency but cannot be considered as being the result of loss generation in the mainstream flow.

The values of the coefficients in Eq. (A4.2) can easily be calculated numerically for any specified cycle. For a typical civil aircraft engine cycle with overall pressure ratio 25, turbine entry temperature 1500 K and cooled turbine pressure ratio 4 we get

$$\frac{\partial\eta_c}{\partial T_3} = 1.035\,10^{-4}.\quad \frac{\partial\eta_c}{\partial m_{fc}} = -0.182.\quad \frac{\partial\eta_c}{\partial\eta_t} = 0.378.$$

**(b) Turbine Analysis.** Figure A4.2 illustrates the expansion through the cooled turbine where the expansion line 3–4 represents the state of main flow plus any cooling flow already added to it. We consider the main flow, flow rate $m_m$, which entered the turbine at 3 and the added coolant flow as two separate streams, which at any point in the turbine have identical properties. A total amount of heat $Q$ is transferred from the mainstream to the coolant stream. We consider the work done by the main flow only. The total work output from this flow is

$$W = m_m(h_3 - h_4) - Q \qquad \text{(A4.3)}$$

The isentropic work is

$$W_{is} = m_m(h_3 - h_4 + T_4\Delta s) = W + Q + m_m T_4\Delta s \qquad \text{(A4.4)}$$

and

$$m_m\Delta s = -\int dQ/T + m_m\Delta s_{\text{irrev}} \qquad \text{(A4.5)}$$

where $T$ is the temperature at which the heat transfer $dQ$ takes place and $\Delta s_{\text{irrev}}$ is the increase in specific entropy due to irreversibility in the flow. This is the entropy created by viscous effects arising from the differences in velocity between the mainstream and the coolant.

Hence,

$$W = W_{is} - \int (1 - T_4/T)\,dQ - m_m T_4\Delta s_{\text{irrev}} \qquad \text{(A4.6)}$$

The middle term of this equation represents the reduction in isentropic work because the heat removal from the mainstream flow causes the expansion to move to the left on the $h-s$ diagram, as shown in Fig. A4.2. This is a thermodynamic effect, which is not related to any irreversibility in the flow, and so it does not contribute to the last term of Eq. (A4.2). Its magnitude depends on where the heat transfer takes place and it will be greatest if all the heat removal takes place at the start of the expansion and zero if all heat removal is at the end. Numerical evaluation of the term for the case where the coolant is added continuously gives a value equal to about 0.14 $m_{fc}W$ for a typical cycle. Let the magnitude of this term be $\Delta\eta_q W_{is}$, then the overall isentropic efficiency of the expansion is

$$\eta_t = \frac{W}{W_{is}} \approx \eta_o - \Delta\eta_q - \frac{T_4\Delta s_{\text{irrev}}}{W_{is}} = \eta_o - \Delta\eta_q - \Delta\eta_{\text{irrev}} \qquad \text{(A4.7)}$$

where $\eta_o$ is the efficiency of the uncooled turbine and $\Delta\eta_{\text{irrev}}$ is the loss of efficiency due to irreversible mixing of the coolant flow and mainstream flow. It is only this term that we are concerned with in this paper.

The losses undergone by the coolant flow due to throttling within its supply ducts and passages affect the middle term of Eq. (A4.2). They depend mainly on the difference between the coolant supply pressure and the pressure at which it mixes with the mainstream flow. The value of $\partial\eta_c/\partial m_{fc}$ quoted above assumes that coolant is added continuously along the expansion with the amount added being proportional to the temperature change.

The last term $\Delta\eta_{\text{irrev}}$ in Eq. (A4.7), is the only one that contributes to the last term in Eq. (A4.2). It is exactly the same as the expression for the efficiency of an uncooled turbine but in the case of a cooled turbine some of the entropy creation occurs as a result of the addition of the cooling flow. This may be evaluated as follows.

Shapiro (1953) shows that the effects of *small amounts* of heat transfer and mass addition on the specific entropy of a perfect gas can be calculated from

$$\Delta s = C_p\left(1 + \frac{\gamma-1}{2}\mathrm{M}^2\right)\frac{\Delta T_o}{T_o} + C_p(\gamma-1)\mathrm{M}_2\left(1 - \frac{V_c\cos\alpha}{V_m}\right)m_{fc} \qquad \text{(A4.8)}$$

where $\Delta T_o$ is the change of stagnation temperature due to heat transfer and the coolant is injected with velocity $V_c$ at an angle

$\alpha$ to the main flow, which has velocity $V_m$ and Mach number M.

The first term can be written as $\Delta Q/T$ and so represents the entropy change due to heat transfer alone. The second term must therefore represent the entropy creation due to irreversibility. Using Eq. (3) to express $\Delta s$ in terms of $\Delta T_o/T_o$ and $\Delta P_o/P_o$ gives

$$\Delta s_{\text{irrev}} = C_p(\gamma-1)\mathrm{M}^2\left(1-\frac{V_c\cos\alpha}{V_m}\right)m_{fc}$$

$$= -R\frac{\Delta P_o}{P_o} - C_p\frac{\gamma-1}{2}\mathrm{M}^2\frac{\Delta T_o}{T_o} \qquad \text{(A4.9)}$$

This equation shows that the irreversibility depends not only on the loss of stagnation pressure but also on the change of stagnation temperature. The last term is a result of the well-known effect of heat transfer on the stagnation pressure of a high-speed flow. Any heat removal from the mainstream flow will tend to increase its stagnation pressure while viscous dissipation due to the difference in velocity between the mainstream and the injected flow will always tend to decrease it. Hence, when heat is being removed from a flow, the net loss of stagnation pressure is always less than that due to viscous dissipation.

Substituting the above expression for $\Delta s_{\text{irrev}}$ into Eq. (A4.7) gives for the change of cooled turbine efficiency

$$\Delta\eta_t = -\frac{T_4\Delta s_{\text{irrev}}}{C_p\Delta T_{ois}} = -\frac{T_4}{\Delta T_{ois}}(\gamma-1)\mathrm{M}^2\left(1-\frac{V_c\cos\alpha}{V_m}\right)m_{fc} \qquad \text{(A4.10)}$$

where $\Delta T_{ois}$ is the isentropic temperature drop from 3 to 4.

It is significant that the loss of turbine efficiency does not explicitly involve the coolant temperature. This is because $\Delta s_{\text{irrev}}$ is due solely to viscous effects, which depend on gradients of velocity and not on differences of temperature. It implies that experiments to determine the loss of efficiency due to cooling can be conducted without cooling the injected gas as long as the ratio of the velocity of injection to the main flow velocity is correct.

These results are for coolant addition through holes or slots in the blade or endwall surface and do not apply to coolant ejection through the trailing edge where the change of flow area and base pressure must also be included in the analysis. In fact coolant ejection through the trailing edge can increase the base pressure and so may be beneficial (see Denton and Xu, 1990).

## APPENDIX 5

### A Simple Theory for Tip Leakage Loss of Shrouded Blades

We consider the flow over a single tip seal as illustrated in Fig. (A5.1). We assume that the leakage flow suffers no loss before it reaches the throat of the leakage jet and that no tangential force acts on it so that it suffers no change of swirl velocity before it mixes with the main flow. It is also assumed that there is no significant restriction to the flow anywhere except at the seal and so the static pressure in the clearance space downstream of the seal is the same as the static pressure at exit from the blade row. The flow is viewed in a frame moving with the blade row and all quantities are measured relative to the row. If there is negligible change of radius the relative stagnation enthalpy of leakage flow and main flow is the same and remains constant.

For simplicity we will calculate the leakage flow rate assuming incompressible flow but this restriction can easily be relaxed at the expense of extra algebra.

At the throat of the leakage jet

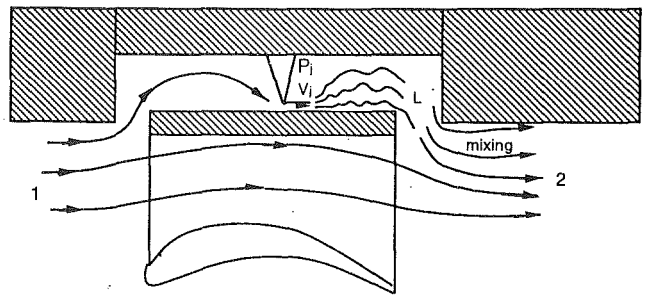


Fig. A5.1 Flow over a shrouded turbine tip seal

$$P_o = P_{o1} = P_j + 0.5\,\rho\,V_j^2 + 0.5\,\rho\,V_{\theta1}^2 = P_2 + 0.5\,\rho\,V_2^2 \qquad \text{(A5.1)}$$

where $V_j$ is the axial velocity of the leakage jet.

But we assume that $P_j = P_2$ so

$$V_j = \sqrt{V_2^2 - V_{\theta1}^2} \qquad \text{(A5.2)}$$

The leakage mass flow is therefore

$$m_L = \rho g C_c\sqrt{V_2^2 - V_{\theta1}^2} \qquad \text{(A5.3)}$$

where $C_c$ is the jet contraction coefficient. The fractional leakage is therefore

$$\frac{m_L}{m_m} = \frac{gC_c\sqrt{V_2^2 - V_{\theta1}^2}}{hV_2\cos\alpha_2} \qquad \text{(A5.4)}$$

where $h$ is the blade span.

If $V_x$ is constant through the blade row this can be written in terms of the flow angles as

$$\frac{m_L}{m_m} = \frac{gC_c}{h}\sqrt{\sec^2\alpha_2 - \tan^2\alpha_1} \qquad \text{(A5.5)}$$

Entropy increase of the mainstream flow only occurs when it mixes with the leakage flow. If the leakage flow re-enters the main flow with axial velocity $V_{XL}$ and swirl velocity $V_L$ it can be shown by applying the conservation equations to a swirling jet entering a vortex that Eq. (20) can be applied independently to the axial and tangential flow leading to

$$T\Delta s = \frac{m_L}{m_m}\left[V_{\theta2}^2\left(1-\frac{V_{\theta L}}{V_{\theta2}}\right) + V_{x2}^2\left(1-\frac{V_{xL}}{V_{x2}}\right)\right] \qquad \text{(A5.6)}$$

which is valid for compressible flow.

$V_{xL}$ cannot be calculated without knowing the geometry of the re-entry slot but in most cases it is likely to be negligible both because the slot is comparatively wide and because the leakage flow is directed almost radially inward. Hence, neglecting $V_{xL}$ we get

$$T\Delta s = \frac{m_L}{m_m}V_2^2\left(1-\frac{V_{\theta L}}{V_{\theta2}}\sin^2\alpha_2\right) \qquad \text{(A5.7)}$$

By assuming constant axial velocity through the blade row this can be further simplified to

$$\frac{T\Delta s}{0.5\,V_2^2} = 2\frac{m_L}{m_m}\left(1-\frac{\tan\alpha_1}{\tan\alpha_2}\sin^2\alpha_2\right) \qquad \text{(A5.8)}$$

This result is valid for compressible flow if $m_L/m_m$ has been calculated appropriately. Predictions from this theory are shown in Fig. 34.

## APPENDIX 6

### A Simple Theory for Tip Leakage Loss of Unshrouded Blades

We consider a model of tip leakage flow as illustrated in Figs. 31 and A6.1. The leakage flow passes over the blade tip with no change in its chordwise velocity component, which

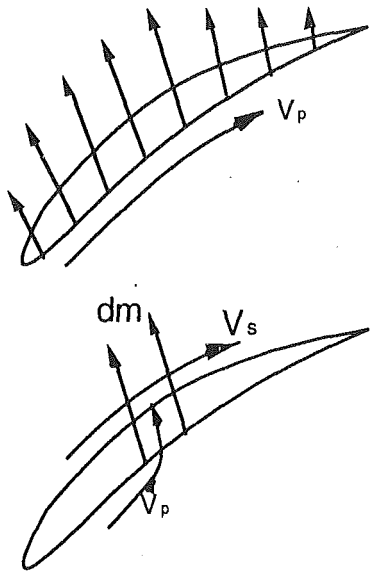


**Fig. A6.1 Tip leakage viewed as a jet in a crossflow**

remains equal to the surface velocity on the pressure side of the blade, $V_p$. The local rate of leakage flow is determined by the static pressure difference across the blade tip and by a discharge coefficient $C_d$, which may be either calculated theoretically assuming two-dimensional flow (Moore and Tilton, 1988) or determined empirically. The leakage flow therefore arrives at the suction side of the blade with a velocity component $V_p$ in the streamwise direction. It is then assumed to mix immediately with the surrounding flow, which has velocity $V_s$. The mixing may be treated by exactly the same theory as was used for a coolant jet in Appendix 4 but without any stagnation temperature difference.

Applying Eq. (A4.9) to the leakage over a small part of the blade chord gives

$$\Delta s_{\text{irrev}} = C_p(\gamma - 1)\mathrm{M}^2\left(1 - \frac{V_p}{V_s}\right)\frac{dm}{m_m} \qquad \text{(A6.1)}$$

where $dm$ is the mass flow rate of the leakage flow and $m_m$ is that of the mainstream. The Mach number at which the mixing takes place is taken as that of the mainstream flow on the suction surface and so we can rewrite this as

$$T\Delta s_{\text{irrev}} = V_s^2\left(1 - \frac{V_p}{V_s}\right)\frac{dm}{m_m} \qquad \text{(A6.2)}$$

To obtain the total entropy created we must integrate Eq. (A6.2) along the chord of the blade, giving

$$T\Delta s_{\text{tot}} = \frac{1}{m_m}\int V_s^2\left(1 - \frac{V_p}{V_s}\right)dm \qquad \text{(A6.3)}$$

which is valid for compressible flow provided that temperature changes are small.

The local leakage flow rate $dm$ can be calculated by assuming two-dimensional flow and applying the momentum equation in the direction perpendicular to the blade chord. This is most easily done for incompressible flow but the theory can be extended to compressible flow in numerical calculations. For incompressible flow the leakage over a length $dz$ along the chord of the blade is given by

$$dm = C_d g\sqrt{2\Delta P\rho}\, dz \qquad \text{(A6.4)}$$

where $g$ is the tip clearance, $C_d$ is the discharge coefficient and $\Delta P$ is the pressure difference between the suction and pressure sides of the blade. A typical value of $C_d$ would be about 0.7–0.8. Substituting this into Eq. (A6.3) gives

$$T\Delta s_{\text{tot}} = \frac{C_d g C}{m_m}\int_0^1 V_s^2\left(1 - \frac{V_p}{V_s}\right)\sqrt{2\Delta P\rho}\,\frac{dz}{C} \qquad \text{(A6.5)}$$

Since we have now assumed incompressible flow $\Delta P$ can also be related to the blade surface velocities

$$\Delta P = 0.5\,\rho\,(V_s^2 - V_p^2)$$

and the total mass flow through one blade passage can be written as

$$m_m = \rho V_2 hp\cos\alpha_2$$

where $h$ is the blade span and $p$ is the blade pitch.

Hence, Eq. (A6.5) becomes

$$T\Delta s_{\text{tot}} = \frac{C_d g C}{V_2 hp\cos\alpha_2}\int_0^1 V_s^2\left(1 - \frac{V_p}{V_s}\right)\sqrt{(V_s^2 - V_p^2)}\,\frac{dz}{C} \qquad \text{(A6.6)}$$

Turning the overall entropy increase into a loss coefficient based on $0.5\,V_2^2$ gives

$$\zeta = \frac{2C_d g C}{hp\cos\alpha_2}\int_0^1 \left(\frac{V_s}{V_2}\right)^3\left(1 - \frac{V_p}{V_s}\right)\sqrt{\left(1 - \left(\frac{V_p}{V_s}\right)^2\right)}\,\frac{dz}{C} \qquad \text{(A6.7)}$$

The terms in the integral can be evaluated when the blade surface velocity is known. Since for turbine blades the average value of $V_s/V_2$ is about unity and $V_p/V_2$ is about 0.3, the magnitude of the integral will be of the order 0.65. Hence, taking $C_d$ to be about 0.8, the loss coefficient is of the same order as the ratio of leakage area, $gC$, to blade throat area, $hp\cos\alpha_2$. This ratio is sometimes used as a measure of tip leakage loss.

It is interesting to note the occurrence of the term $(V_s/V_2)^3$ in the expression for the loss coefficient. This means that, exactly as was the case for boundary layer loss, highly loaded blades with high suction surface velocities will have a large tip leakage loss.

The above theory applies equally to compressor blades and to turbine blades. Equation (A6.7) can be used for compressor blades if subscript 2 is replaced by subscript 1. We then obtain the loss coefficient based on inlet dynamic head. This will now be of order of the ratio of leakage area to inlet flow area and again it will increase rapidly for highly loaded blades.

In cases where the blade surface velocity distributions are not known we can *estimate* the average values of $V_s$ and $V_p$ *very approximately* by assuming the blade loading to be uniform. This gives from the blade circulation

$$V_s - V_p \approx \frac{p}{C}V_x(\tan\alpha_2 - \tan\alpha_1) \qquad \text{(A6.8)}$$

and from continuity, assuming that the blade thickness is small

$$V_s + V_p \approx \frac{2\,V_x}{\cos\alpha}. \qquad \text{(A6.9)}$$

The local value of $\cos\alpha$ may be reasonably estimated by assuming that $\tan\alpha$ varies linearly with $x$.

Equations (A6.8) to (A6.9) enable Eq. (A6.7) to be integrated numerically and so provide a general means of *estimating* the tip leakage loss coefficients of turbine and compressor blades. Results from this method are plotted in Fig. 33.